UNIVERSITAT POLITÈCNICA DE CATALUNYA
BARCELONATECH

MASTER THESIS

Aircraft dynamic loads generated in wake vortex encounters

Carles Suñer Perucho

SUPERVISED BY

Sebastián Claverías Ceacero

Adeline de Villardi de Montlaur

Universitat Politècnica de Catalunya
Master in Aerospace Science & Technology
June 2014

This Page Intentionally Left Blank

Aircraft dynamic loads generated in a wake vortex encounters

BY

Carles Suñer Perucho

DIPLOMA THESIS FOR DEGREE

Master in Aerospace Science and Technology

AT

Universitat Politècnica de Catalunya

SUPERVISED BY:

Sebastián Claverías Ceacero
Structural Dynamics and Aeroelasticitiy Department
Airbus Defence And Space, Military Aircraft Division (former Airbus Military)

Adeline de Villardi de Montlaur
Escola d'Enginyeria de Telecomunicacio i Aeroespacial de Castelldefels
Universitat Politècnica de Catalunya

This Page Intentionally Left Blank

ABSTRACT

The study illustrated in these pages was developed in the Structural Dynamics and Aeroelasticity Department of the Military Aircraft division of Airbus Defence and Space in Getafe, Madrid (Spain). That department is a multidisciplinary one involving several categories. Some of its competences are the analysis of impacts, acoustics and vibrations for the aircraft and all their systems. Also, the dynamic response of the aircraft to different events is part of the tasks for that department. It is in that field where this project is located. Wake vortex encounters are a dynamic phenomenon similar to other excitations faced by aircraft in its usual operation. That excitation will induce dynamic loads in the aircraft structures as it passes through the wake. Obtaining and analyzing those loads are the main aims of this study.

First, it is important to introduce the concept of aircraft wake. In order to achieve the goals of the study, it is necessary to start with the basics of the problem. This is the acknowledgement of the physics of aircraft wakes and how they are generated. Then, how those wakes act as an excitation for other aircraft as they perturb the velocity field of the air.

Once the aircraft wakes are introduced, the next step consists of explaining the corresponding aircraft that will face those encounters. In this case, the particular aircraft is an Airbus A400M because that was the one used by Airbus Defence and Space in the campaign of the wake vortex encounters. The following considerations involve the procedures of the Structural Dynamics department in the computation of the numerical simulation for that kind of event. Therefore, it is necessary to know what the tools available for the resolution of this problem are and which aspects face each one. Furthermore, the software and models used in this study have been validated with flight tests and they are an excellent representation of the aircraft and problem considered.

After the presentation of the problem, the aircraft considered and tools used, the wake model is the next aspect of study. This is one of the widest fields of aircraft wakes. Having a good wake model is necessary for the accuracy of the results and the main tasks are focused on the wake aging model. That is how the wake evolves and changes as times goes by.

With all that, the last aspect of this study is the computation of the dynamic loads induced in wake vortex encounters. As it is an event that is not considered in aircraft regulations, it was difficult to define a particular scenario that is representative of the problem. For that reason, a stochastic analysis of the problem has been chosen to obtain the aircraft loads generated in this kind of event. This analysis consists of scattering the input variables affecting the problem and executing a high number of simulations. In that way, it is possible to derive a statistical behavior of the load response and establish a probability of occurrence for the results obtained. Finally, comparing those results with the reference loads of the aircraft, it is feasible to predict whether wake vortex encounters could be a significant event for the aircraft structure during its operational life.

This Page Intentionally Left Blank

Table of Contents

List of Figures

This Page Intentionally Left Blank

List of tables

This Page Intentionally Left Blank

INTRODUCTION

These pages contain the work done within the Structural Dynamics and Aeroelasticity department of Airbus Defence and Space about aircraft wake vortex encounters and the dynamic responses induced in such events. The main purpose of this Master Thesis is to improve the existent knowledge of the physical characteristics of aircraft wakes and to provide a reliable approximation of the loads generated when aircraft fly through those wakes.

Wake vortex encounters are events that were already considered in the developments of the Structural Dynamics department. As a referent company as Airbus Defence and Space, it is usual to be working in all the newly scenarios that could be an issue for the safety operation of aircraft. These events are gaining importance in the increasingly congested aircraft where airports face more and more operations per minute and military aircraft are likely to fly in formation. For those reasons, the wake vortex encounters was a scenario worth analyzing and in that direction, Airbus Defence and Space started the corresponding campaign. Since it is not a defined issue by the Airworthiness Authorities and Regulations, the initial tasks consisted of trying to characterize the problem in terms of aircraft response. The main aspects to consider were to derive a representative model of the wake and then obtain a complete set of dynamic loads given in wake vortex encounters. The Structural Dynamics department has already started to develop new software tools and to adapt its existent ones to compute the simulations for such event. The objectives of this Master Thesis are the improvement of the understanding of wake vortex encounters, developing new wake models and apply the existent tools to derive a reliable base of dynamic loads generated in the considered scenario.

In order to present the work done, the first chapter of this Master Thesis introduces the motivation of this study and the aircraft wake formation. It explains how the air is perturbed and this velocity field acts as external excitation for the aircraft that fly through it. That chapter is also an introduction to the loads problem due to wake vortex encounters.

The second chapter is focused on the aircraft chosen to perform the analysis, which is an Airbus A400M. This is the aircraft used by Airbus Defence and Space in its campaign about wake vortex encounter. Its main characteristics are presented along with the necessary models for the computation of the numerical simulations.

Once the aircraft for the problem is presented, the third chapter treats the methodology used in the computations. It explains the flow chart of the numerical simulations, detailing each step and software. This chapter is the basis to understand how the wake vortex encounters are simulated, what are the main steps in the resolution and how are the results obtained.

After the chapters about the aircraft models and software tools, the following section talks about how those models and tools are validated through flight tests. There, the flight test campaign performed by Airbus Defence and Space is presented. Then, the

methodology of adjustment of the tools to fit flight test results with numerical simulations, showing the satisfactory agreement between both.

Entering now in the physics of the problem, the fifth chapter presents how the wake is modeled. The wake vortex model used in this analysis concerns the first section of the chapter. After that, the main issue is the wake aging, differentiating the mechanisms affecting the wake as the time elapses, which are the circulation decay and the vortex radius diffusion.

As a continuation of the wake aging model, the sixth chapter focuses on the development of a pure diffusion wake aging model. The initial approach of the Department was to consider only circulation decay and the possibility of include a aging model based only in vortex diffusion is the topic of this chapter. Also, this proposed aging model is compared to flight test results in the last sections in order to establish its validity.

The seventh chapter is the one that introduces the type of analysis used in the loads computations. Since there is not any regulation that allows to establish a characteristic problem, the approach followed was to perform an stochastic analysis. In this chapter it is presented the definition of the analysis, explaining the input variables that will be scattered, the outputs obtained and the methodology followed.

After that, the next chapter contains the output results of the stochastic analysis. These are based on the comparison of the loads obtained with the reference loads of the aircraft. The philosophy of the study consists of obtaining load results with a number of executions high enough to be representative of the normal operation of the aircraft. Therefore, the results of the analysis will have a probability of occurrence that should be compared with the reference values in order to apply safety factors given by Airworthiness Authorities. Then, the results of the wake vortex encounter analysis can be referenced to the certified load values of the aircraft and discern whether they are assumable by the aircraft structure limitations.

Finally, this Master Thesis ends with a chapter devoted to the conclusions of the study and the future steps to be done in the field.

Chapter 1

WAKE VORTEX ENCOUNTER LOADS PROBLEM

1.1. Motivation

In the present time, there are more and more flying devices due to technological improvements and society demands. This fact leads to a current airspace increasingly crowded. Apart from other considerations in terms of flight safety or collision avoidance, there is one important aspect of this issue that generates a relevant alert and that should be considered and understood deeply. That is the behavior response of an aircraft when it enters the region of perturbed air generated by another aircraft. In this sense, there are some restrictions in the separation time for landing and takeoff for consecutives aircraft. This attempts to establish a safety waiting time where the air near the airstrip is calmed enough to ensure the correct operation of the consecutive maneuver.

Aside from that regulation, there is not any other airworthiness requirement for other cases where an aircraft crosses the wake of another one or itself. Due to the increment of air traffic and aerial operations, there will be more possible scenarios where this event could be of a relevant importance. For instance, there could be cases where an aircraft in a surveillance operation goes near its own wake or another where a single component of a swarm of aircrafts in a specific mission faces the perturbation generated by one of its companions.

Considering those aspects, it could be necessary to deeply understand the physical characteristics of the aircraft wakes and how is the velocity field induced. Moreover, it would be useful to assess what are the implications in terms of the aircraft dynamic response when one of them addresses this issue.

1.2. Literature review

Wake vortex of aircraft is a prominent field of study, whose main developments have appeared in the recent years. Therefore, there is not an exhaustive variety of literature about that event. The main efforts have been developed in the physical model of the wake. In this sense, there are several examples of academic references that talk about the wake model. For instance, Liu in his Master Thesis (see [2]) presents different wake models and analyses the wake vortex encounters considering those models. Another relevant work is the one derived by Proctor (see [6]) about the study of wake vortex decay. Regarding more complex publications, there are collections of papers in the AGARD conference proceedings (see [7]) that are focused on the characterization of aircraft wakes and Proctor [1] also has publications about algorithms of wake predictions.

Focusing on the work done previously in the Structural Dynamics Department, the titles are based on the development of the software tools and the validation of those tools. As a recent and own software development, a tool has been programmed to obtain the excitation from the wake [23]. Then, they have been working on the validation of the corresponding tools [21] and on obtaining representative results of the wake vortex encounter problem [24].

1.3. Introduction to Wake Vortex

Flying aircrafts disturb the air which they are flying in. One of those perturbations is the one generated by the wing tip vortices. These vortices extend stream down and form what is known as a wake vortex. Another way of seeing the effect is as the wake generated by the aircraft as it is flying, causing a path of turbulence and disturbed air.

The wing tip vortices are a present phenomenon in all flying aircrafts that generate lift. Lift is created by the difference of pressure between the two sides of the wing. Low pressure is created in the upper wing while high pressure is present under the wing. This pressure differential creates lift but also causes the airflow to roll into a swirling mass at the wing tips that forms two counter-rotating vortices downstream. The separation distance of these trailing vortices is less than a wingspan. They tend to remain at that distance while the sinking rate decreases and their strength decay over time. It is important to distinguish between the concepts of ‘trailing wake’ and ‘vortex wake’. Trailing wakes form as a result of flow passing a body in a viscous medium and is caused by the body’s drag. The wakes considered in this study are vortex wakes, which are formed from the flow around a body in viscous flow but due to generation of lift and correspondingly, induced drag.

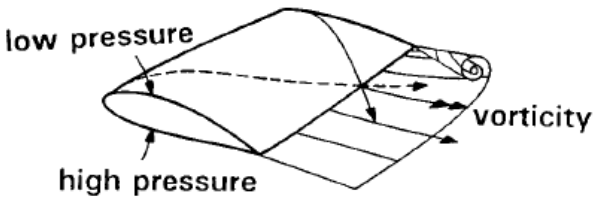

Figure 1.1 Vorticity created due to lift

A wake vortex encounter (WVE) occurs when an aircraft crosses the previous mentioned wake vortex generated by another aircraft or by itself. This event produces a dynamic phenomenon as the aircraft crosses through the vortex induced velocity field.

1.4. Wake Vortex Encounter Loads Problem

When a wake vortex encounter occurs, the aircraft crosses a velocity field that can induce a several effects on its performance. There is a momentary loss of controllability and a deterioration of handling qualities. Apart from these momentary aspects that are recovered after the crossing if there is enough altitude, there are also induced important dynamic loads that can affect the structure and that should be studied for the sake of safety.

The strength of vortex wakes is determined by the generating aircraft weight and speed. The strongest vortices are caused by large aircraft in heavy weight configurations and/or flying at slow speeds. This means that takeoff and landing procedures are especially hazardous for wake vortex encounters when there are low speeds and high weight (at takeoff). In both cases, the aircrafts are too close to the ground for the pilots to recover full control. For this reason, Air Traffic Management control sets a minimum separation distance between aircraft in order to allow for wake decay and dissipation, especially when a smaller aircraft operates after a larger one.

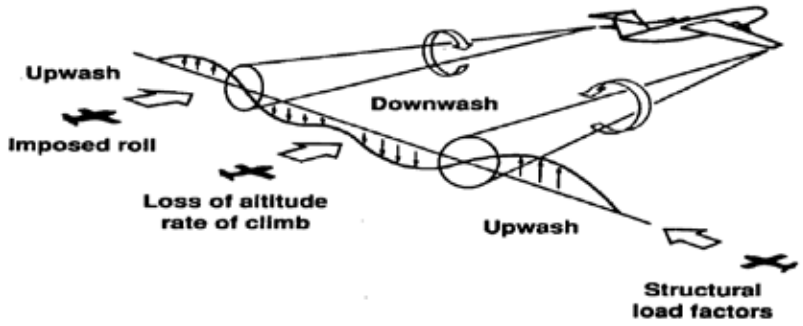

Figure 1.2 Outline of a wake vortex encounter

Focusing on the dynamic phenomenon of a wake vortex encounter, it has been said that crossing through such vortex velocity field induces dynamic loads that may represent a hazard to the aircraft in terms of structural damage. This case of dynamic loads due to wake vortex encounters is not reflected in any of the current airworthiness regulations, civil or military. Moreover, in the public available literature, there is not documented a detailed model of the excitation or a well-established procedure for evaluating those loads the wake yields in the follower aircraft. Due to the absence of works done in this issue, this project has a relevant importance. Specifically, the question is of special interest for military aircraft where the possibility of crossing its own wake or the wake of another aircraft increases with several mission profiles. For instance, there are surveillance missions where the aircraft has to repeat the same flight path over a target (mobile or not) in circles or similar, or operations where the aircrafts are close one to another such as formation flight or air refueling. These are good examples where wake vortex encounters may occur; therefore, it is an interesting phenomenon to study.

1.5. Wake structure

Vortex wakes are formed from the flow around a body in a viscous medium due to the generation of lift. This has as a consequence a formation, at a distance behind the body, of a pair of counter-rotating longitudinal vortices. The wake behind an aircraft is an unbounded flow that moves at a mean speed equals to the undisturbed flow speed. The total length of a vortex wake can be greater than 10 km and depends on several parameters such as the atmospheric conditions, the aerodynamic and high-lift devices configuration, the gross mass of the aircraft and the flight speed and altitude. The field of disturbance velocities, as well as the shape and spatial location of the tip vortices characterize the vortex wake. Looking at the total length of the vortex wake and its distribution, the following zones can be differentiated, as can be seen in figure 1.4 (see [12]):

- Wake formation zone
- Stable wake zone
- Unstable wake zone
- Wake breakdown zone

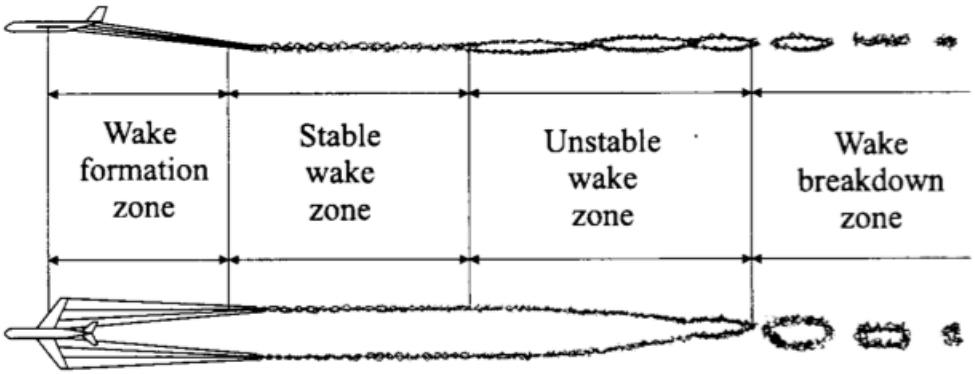

Figure 1.3 Vortex wake zones (ref [12])

In the wake formation zone, the roll-up takes place from the entire aircraft vortex structure into two vortex tubes. The boundary layer and exhaust gases induce an increase in temperature and velocity of the wing-tip vortices. It can be noted that the main contribution to the formation of the trailing wake behind the aircraft is made by the vortices shed from the wing, horizontal stabilizer and other lifting surfaces. As a result, immediately behind the trailing edge of the wing a turbulent vortex core of finite size is observed. This is the center around which the wing-tip vortex is formed. The wake formation zone ends with the formation of steady wing-tip vortices.

In the stable wake zone takes place the stable movement and sinking of wing-tip vortices with their gradual decay. The wing-tip vortices in this zone are stable structures rotating oppositely (rotation of the left wing's vortex is clockwise, the other vortex rotates counter-clockwise, from the pilot perspective). For the case of a symmetrically loaded wing, both vortices have the same intensity and the separation between them is around 0.8 times the wingspan. In the stable wake zone, the trailing

wake has a tendency to sinking. The sink of the wake is caused by the vortices' mutual interference and the sink rate is approximately equal to the velocity induced by one wing-tip vortex at the center of the other. The wake behavior follows the general laws of vortices' movement in the atmosphere. The velocity field in this zone is significantly non-uniform. The velocities of the disturbed field of air depend on the intensity of the wing-tip vortices and the wake age. The tangential velocity field generated downwash in the zone between vortices and upwash in the external region.

In the unsteady wake zone, the vortices begin to break down. The initiation of the breakdown is characterized by the natural decay due to vortex dissipation and diffusion and the instability of vortices associated to the atmospheric turbulence. The dominant factor of the breakdown will determine the intensity collapse of the wing-tip vortices and the spatial location relative to the vortex-generating aircraft. It is possible that the vortex system executes a symmetric and approximately harmonic motion. The vortex lines in each tube have a form of spiral wound around the axis of the tube. Atmospheric turbulence, wind gusts or others will influence the deformation of the vortex lines.

Finally, the wake breakdown zone contains a chain of isolated vortex rings. The flow in this zone is unstable and the instability of the vortices determines the process of the wake breakdown. This zone is significantly shorter than the unstable wake zone. It should be noted that wake breakdown is a process of changing the trailing wake state. This results in restructuring the flow pattern in the wing-tip vortex tubes, damping out disturbance velocities to the velocity fluctuations in the atmosphere, changing the spatial location of the wing-tip vortices and the associated alteration of the kinematic parameters of the flow.

Among all the zones of the wake vortex, the analysis and study performed in this project considers the aircraft wake as in the stable wake zone but with an infinite length. This means that the vortex tubes are stable, the circulation of the vortices and the wake age determines the velocity field and the rotation of each one is opposite.

Chapter 2

A400M AIRCRAFT AND DYNAMIC MODELS

2.1. Generalities

The aircraft used for this study of wake vortex encounters is an Airbus A400M. This model of aircraft has as main mission, to provide military transport capabilities to different zones and with different conditions, in times of peace, tension, emergencies or hostilities. The A400M is able to carry out missions such as normal military cargo, paratrooper role, heavy-load aerial delivery, passengers / troops transport and aero medical operations over long distance at high speed.

The main design characteristics of this aircraft are the following:

- Wide body compartment with a loadable rear ramp, sized to load critical high mass and high volume loads.
- Trapezoidal high wing.
- Conventional 'T-tail' configuration.
- Tricycle undercarriage and main gears retractable into the fuselage sponsons.
- Four under wing mounted single rotating turboprop engines.

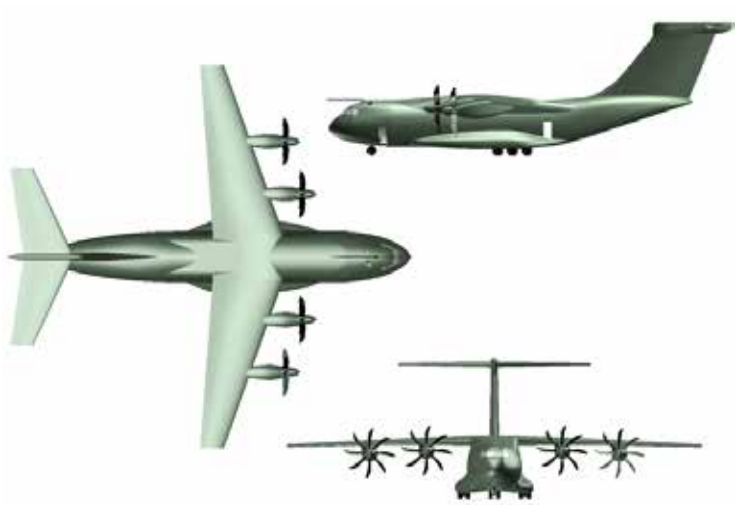

Figure 2.1 A400M layout

2.2. Coordinate system and units

Basic coordinate system used in this study has the following axis characteristics:

- X-axis: Along the fuselage reference line, positive direction from nose to tail.
- Y-axis: Perpendicular to the aircraft vertical plane of symmetry. Positive direction in the right wing from the pilot perspective.
- Z-axis: Perpendicular to the X and Y axes. Positive direction defined upwards.

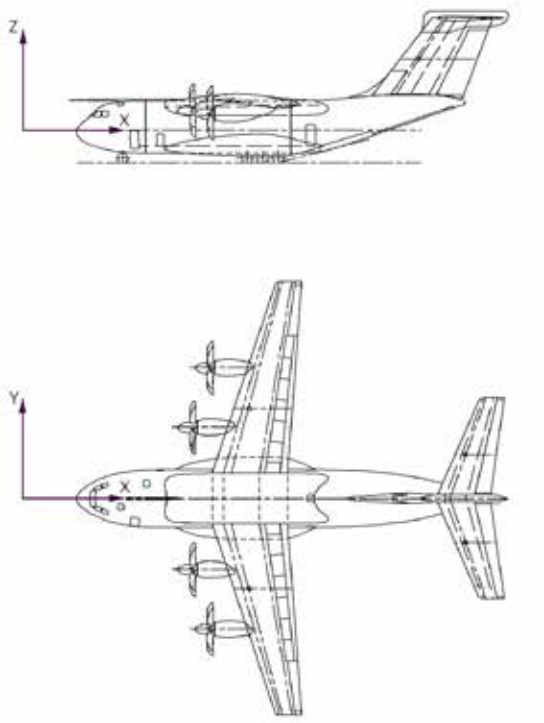

Figure 2.2 Basic coordinate system

The unit system will be the International System of Units (SI) or metric system:

Table 2.1 Units used in the project

Magnitude	Units	Symbol
Length	Meter	m
Mass	Kilogram	kg
Time	Second	s
Force	Newton	N

2.3. Geometrical Data

The following lines summarize the main geometrical aspects of the aircraft considered in this study. The aircraft dimensions in terms of length and height are presented and then, the following tables contain the geometrical data of the main parts of the aircraft. First, the relevant values for the three main surfaces of the A400M: wing, horizontal tail plane (HTP) and vertical tail plane (VTP) are shown in table 2.2. After that, dimensions for the fuselage are presented in table 2.3.

- **A400M Overall length**: 45.09 m
- **A400M Overall height**: 14.68 m

Table 2.2 Airbus A400M Geometrical data

Parameter	Wing	Horizontal tail plane (HTP)	Vertical tail plane (VTP)
Reference area - S_{ref}	221.5 m^2	67 m^2	46.4 m^2
Mean aerodynamic chord - $\bar{c}$	5.671 m	3.824 m	6.731 m
Span - b	42.357 m	18.844 m	6.898 m
Sweep - $\Lambda_{1/4}$	15º	32.5º	34.0º
Anhedral - Γ	4º	0º	-

Table 2.3 Airbus A400M Fuselage parameters

Parameter	Definition
Fuselage basic length	39.09 m
Fuselage maximum width	5.64 m
Fuselage maximum height	5.11 m
Useful length for payload	17.71 m
Cargo hold volume	340 m^3

2.4. A400M Dynamic Models

In order to solve the wake vortex encounter problem, different computational models of the aircraft were used for simplicity and reduction of the calculation. In this section, the main models necessary for the resolution of the problem will be shown. They will be presented in order of importance, starting with the structural and mass models, which form the basic mass and stiffness characteristics of the aircraft representation. After them, the aerodynamic model is the one in charge of capturing the aerodynamic related aspects of the problem. Last, some other models to consider other characteristics of the aircraft will be mentioned. With this collection of models, it is possible to get an idea of the characterization of the aircraft for this problem.

2.4.1. Structural model

First, the wake vortex encounter (WVE) problem is solved in modal coordinates based on the normal modes of the structure. This is not a symmetric problem because the aircraft can cross the wake at any angle. Thus, it is not feasible to use a model of half aircraft because there are not symmetry advantages. For that reason, a complete aircraft model is used.

The normal modes are obtained using the structural model shown in Figure 2.3. The structural model is a Finite Element Method (FEM) model and was created by Airbus Military. In order to save calculation time, Airbus Military has also condensed the initial model of 120000 grids to only 900 grids with negligible losses of accuracy for modes in the range of interest [0-50 Hz].

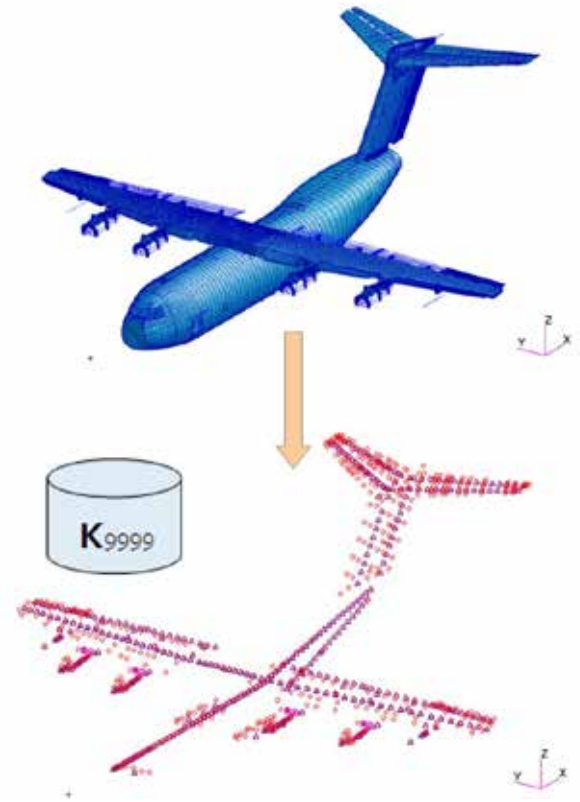

Figure 2.3 Structural model

The structural model reproduces adequately the load path of the structure and the stiffness characteristics of the different aircraft components. The masses have been represented as lumped masses loading the strong points of the structure to avoid local undesirable modes.

2.4.2. Mass model

The mass of the aircraft is modeled as concentrated masses associated to grid points. Those grid points are connected to the structural grids of the structural models. For instance, the mass of the fuselage is modeled as slices where the mass of each one is concentrated in the grid point located at the center. For other aircraft components such as wings or HTP and VTP, the modeling is similar.

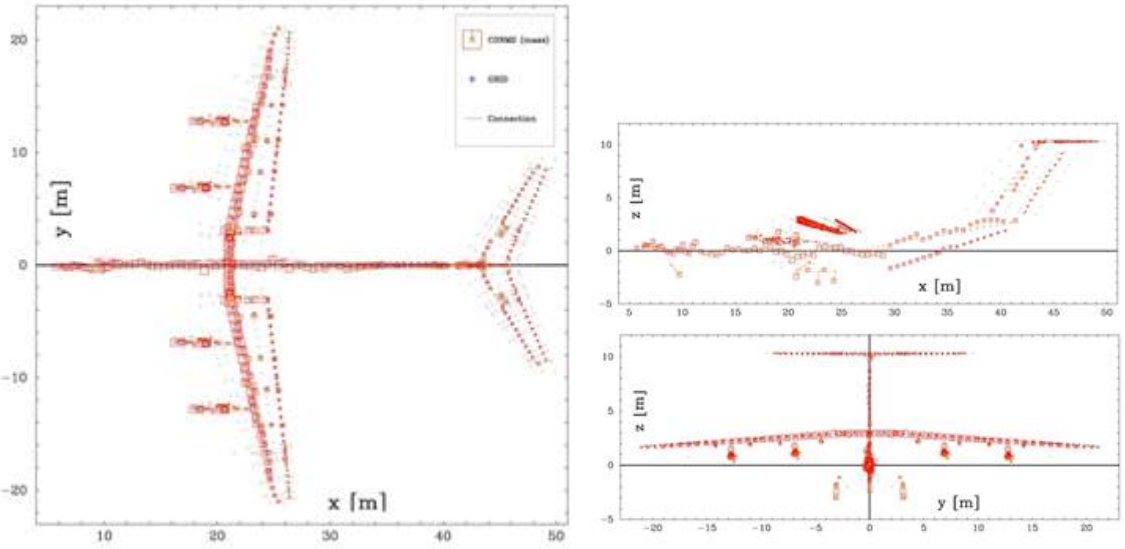

Figure 2.4 Overview of the mass model

2.4.3. Unsteady aerodynamic model

Apart from the structural and mass model, a model is also necessary in order to represent the aerodynamic behavior of the aircraft. For this purpose, an unsteady aerodynamic model created by Airbus Defence and Space was used to take into account the aerodynamic aspects of the problem.

Unsteady aerodynamics are computed using the Doublet Lattice Method (DLM) (see [10] and [11]). The Doublet Lattice model uses flat panels to model lifting surfaces (wings, HTP and VTP) and control surfaces (ailerons, elevator and rudder). The fuselage is modeled with a cross of panels and a flying ring plus pylon are included to model each engine (Figure 2.5). The interconnection between the structural and aerodynamic model is obtained by interpolation of structural grid displacements. This interpolation is made by means of surface splines. In order to maintain simplicity in the calculations, unsteady aerodynamics are computed for a range of reduced

frequencies that covers the significant aircraft response to the input excitation of this problem. Also, pressure correction factors are included in the model to fit aerodynamic derivatives to flight test data.

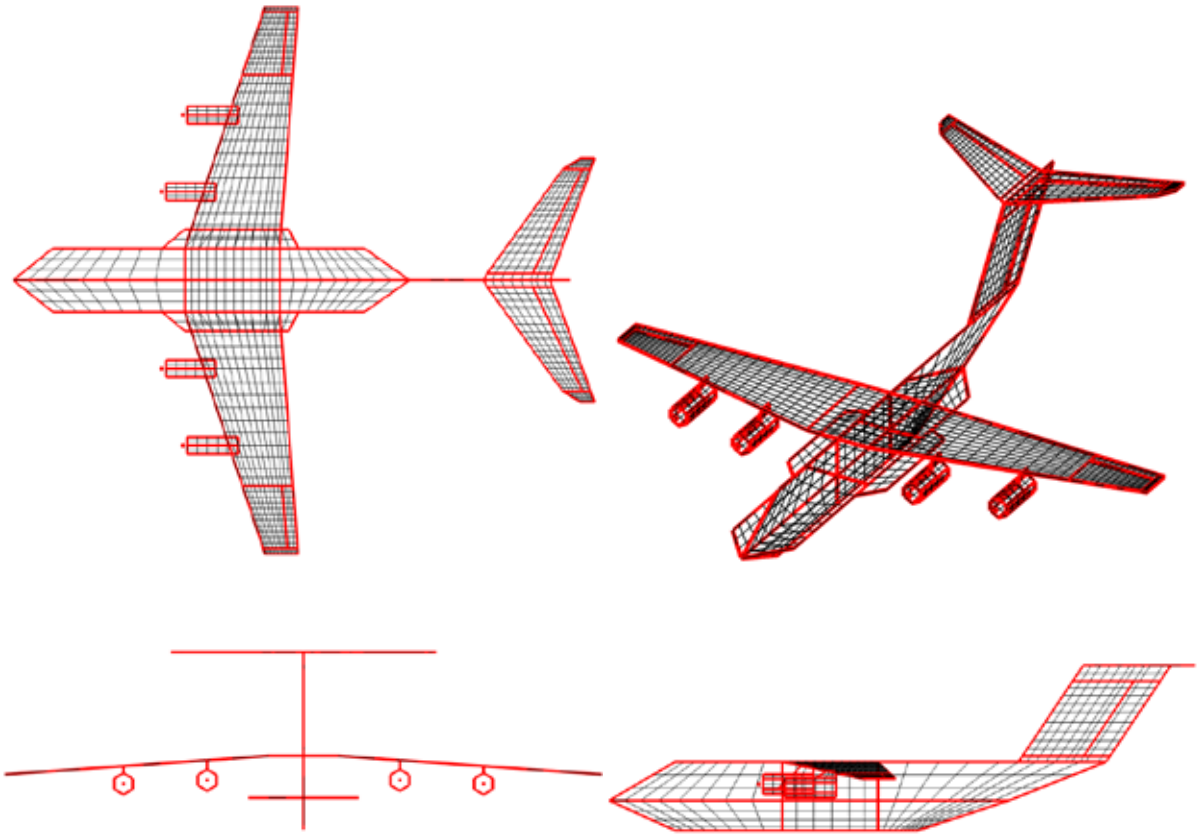

Figure 2.5 Unsteady aerodynamics model

2.4.4. Other models

There are also other models involved in the analysis that are included in this resolution and whose explanation is merely mentioned in this document. Those models are the damping behavior assumed for the model, the gyroscopic load model and the 1P loads model.

The damping law imposed is a constant viscous damping of 3% of the critical damping for all the frequency range. With the exception of an HTP yaw mode where the damping is increased at the corresponding frequency. That is due to the characteristics of the Doublet-Lattice model for the aerodynamics. The DLM is a flat plate model, thus, it cannot reproduce thickness effects. Therefore, this model does not precisely represent the drag of the HTP, and that drag is a relevant factor in HTP yaw mode that produces a more damped response in reality. So, it is necessary to increase the damping at HTP yaw mode frequency of the model.

Gyroscopic effects are induced by rotating bodies or structures (such as propellers) when the rotation axis moves out of his nominal position. When that occurs, it causes a reaction moment that could increase the structural loads in the near areas, in this case, the engine truss. The gyroscopic terms are formulated assuming the propeller as a rigid disk rotating with a constant angular velocity. Then, those terms are included in the dynamic equations by adding an incremental damping matrix to the generalized damping matrix of the problem.

The last remarkable effect considered is the one induced by the loads generated in the propeller due to the incidence of airflow with a specific angle of incidence (not perpendicular). When the airflow is perpendicular to the propeller plane, a force (thrust T) and a moment (propeller torque T) normal to the propeller plane are generated. An angle of incidence between the airflow and the normal to the propeller plane induces a force F1P and a moment M1P at the propeller blades, contained in the propeller plane. These loads change harmonically at the frequency of the rotation speed (figure 2.6), for that reason are called 1P.

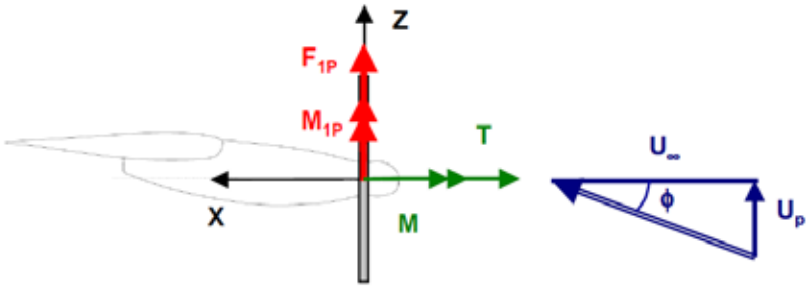

Figure 2.6 Propeller 1P loads

2.4.5. Aircraft models considerations

After the presentation of the several models of the aircraft, it is important to note that these models are the ones provided by Airbus Defence and Space and they are the ones used by them when they compute any load scenario. Therefore, they have been exhaustively validated through a comprehensive flight test campaign. They represent very precisely each relevant characteristic of the aircraft, basically mass and stiffness and steady aerodynamics. Hence, it is very satisfactory to know that the results obtained in this study will be greatly trusty due to the high confidence in these models.

Chapter 3

WAKE VORTEX ENCOUNTER NUMERICAL SIMULATIONS

3.1. Numerical solvers and software used

In a loads loop computation of a wake vortex encounter case, there are several solvers used in the process established by the Structural Dynamics department. One step is based on commercial software that is MSC.NASTRAN while the rest are self-developed or own codes. A wake vortex encounter solver process is divided into three main steps and a preliminary one in which the basic data is obtained.

The preliminary step is to generate the corresponding data matrices needed in the resolution of a typical dynamic loads computation. Data such as modal response, aerodynamic matrices and stiffness and damping matrices are obtained with the commercial software MSC.NASTRAN. Then, the first proper step is to compute the excitation input generated by the wake vortex. This is accomplished with an in-house code developed in the department of Structural Dynamics and Aeroelasticity, called WESDE (Wake Encounter Speed Distribution Evolution). Once the velocity profile of the excitation is computed, the second stepis the solver of the dynamic equations. That solver is an aeroservoelastic package called DYNRESP, developed by Karpel Dynamics in collaboration with the Structural Dynamics department. The last step is to obtain integrated loads for the whole aircraft using an in-house code of the department called DYNLOAD.

3.2. MSC. NASTRAN

MSC.NASTRAN is the software used as a preliminary step in order to obtain the corresponding files that will serve as inputs for the other codes. This is commercial software for several FEM structural analyses. In order to obtain the necessary data, an aeroelastic solution (SOL 146) with a dummy gust as excitation is run. A scheme of the typical flowchart for the NASTRAN solution is shown in figure 3.1. The FEM structural model, the corresponding damping model and the aerodynamic model of the aircraft are inputs of this previous step of the process. After the analysis, the necessary data matrices such as aerodynamic, stiffness and damping matrices as well as mass and modal shapes matrices are obtained along with the modal data of the specific aircraft configuration.

This could seem as an incoherent resolution because the solution is discarded (remember that the input excitation is a dummy gust), but it is carried out that way because MSC.NASTRAN does not have the possibility of introducing such excitation as the one produced in a wake vortex. Moreover, the solver to do so, WESDE, was developed for obtaining an output suitable for the dynamic equations solver, DYNRESP. Therefore, this NASTRAN analysis is performed only to obtain the

matrices of the dynamic equations of motion for further resolution, which will be presented in section 3.4.

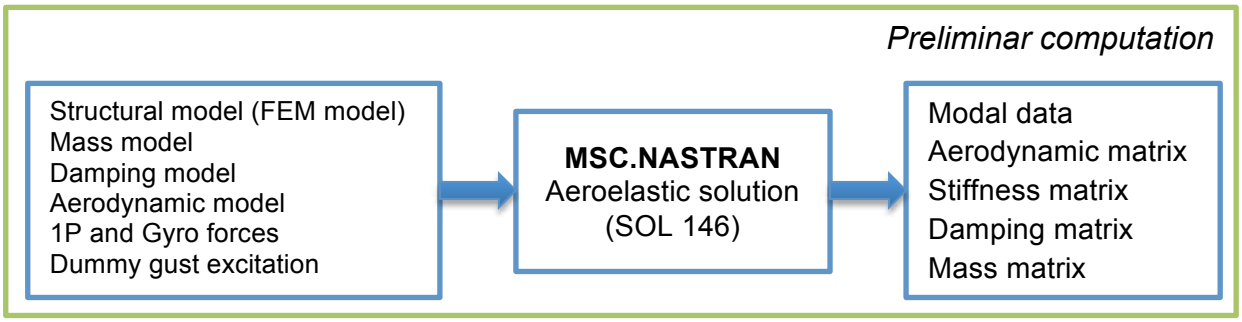

Figure 3.1 NASTRAN SOL146 flow chart

3.3. Obtain input excitation: WESDE

After the preliminary data of the problem is obtained, the first main step in the computation process of a wake vortex encounter is to obtain the velocity field generated by the wake in order to set it as the input excitation in the resolution of the dynamic equations of motion. In this problem, the wake vortex is modeled using a pair of counter-rotating vortices separated by a distance of a fraction of the wingspan. Once the parameters of that model, circulation of the vortices and vortex separation, have been set up, it is possible to obtain the velocity field induced by the wake at any point of space. The issue of determining the velocity profile seen by each point of the crossing aircraft is equivalent to obtaining the path of each point along the wake.

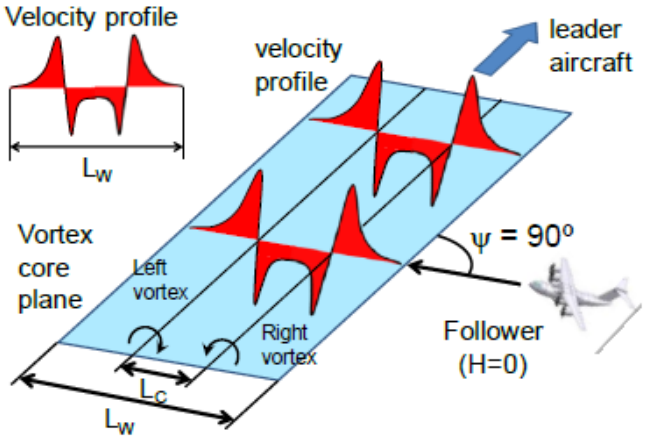

Figure 3.2 Wake encounter at ψ=90º and H=0

In order to understand the velocity field generated by the wake, several cases are presented sorted by complexity. The simplest case is the one where the reference surface of the follower aircraft crosses the wake at the same height that is generated, that is the vortex core plane, and with a perpendicular angle as it can be seen at figure 3.2. Here, the crossing aircraft will be subjected to a vertical velocity component only and due to the perpendicular angle, the same velocity profile is seen

by symmetric points of the aircraft at the same time. For the case where the reference aerodynamic surface of the follower aircraft enters the wake at the same height but with a non-perpendicular angle ($\psi \neq 90^o$), the velocity profile has again only a vertical component but now is longer than the perpendicular case. The scheme of this crossing is shown in figure 3.3. Another difference is that for this case, symmetric points of the aircraft do not see the same excitation at the same time. There is a delay in the excitation for symmetric points of the aircraft as it crosses the wake. The effects of that delay can be seen in figure 3.4.

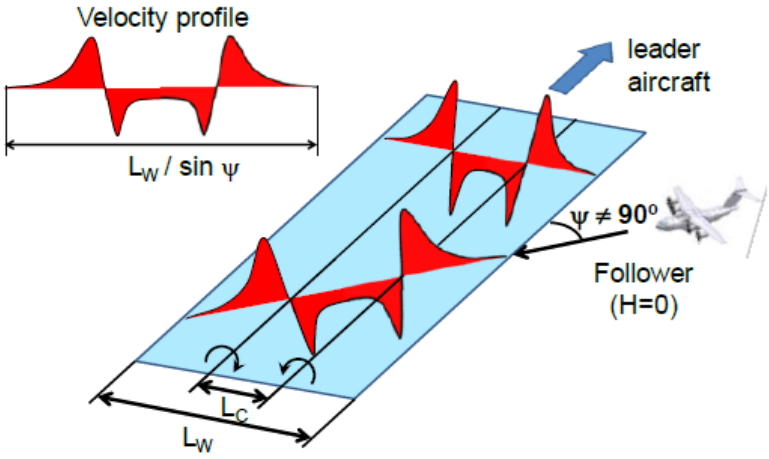

Figure 3.3 Wake encounter at $\psi \neq 90^o$ and H=0

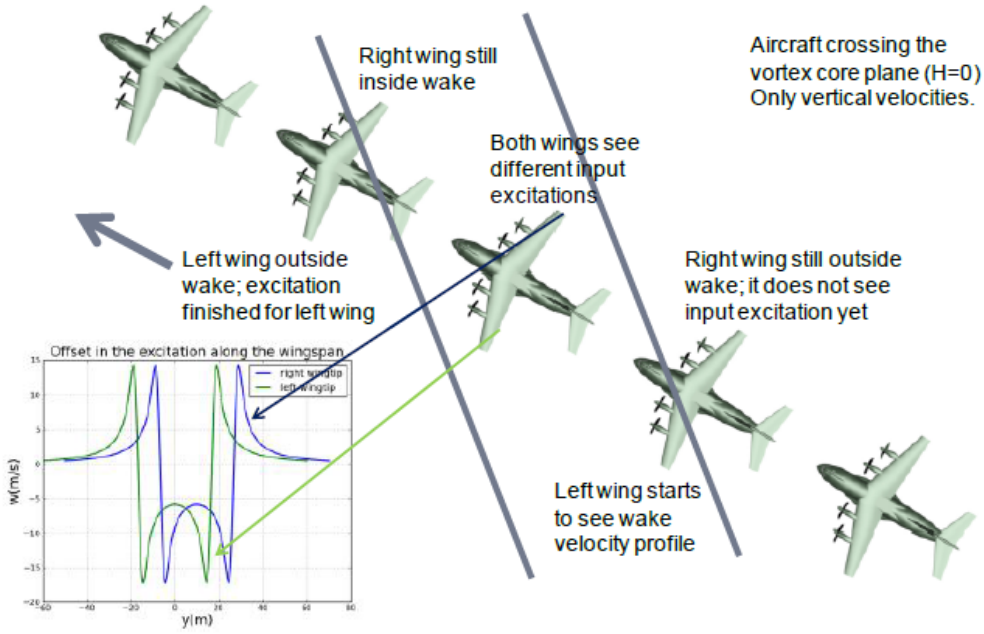

Figure 3.4 Delay in the velocity profile seen by right and left wings

The most generic case occurs when the reference surface of the follower aircraft crosses the wake at a different height from the vortex plane and at particular angle $\psi \neq 90^o$, which is presented in figure 3.5. Now, it appears a second component of the

velocity field. The excitation seen by each point of the aircraft has, for this case, a vertical velocity component as before and also a lateral velocity component.

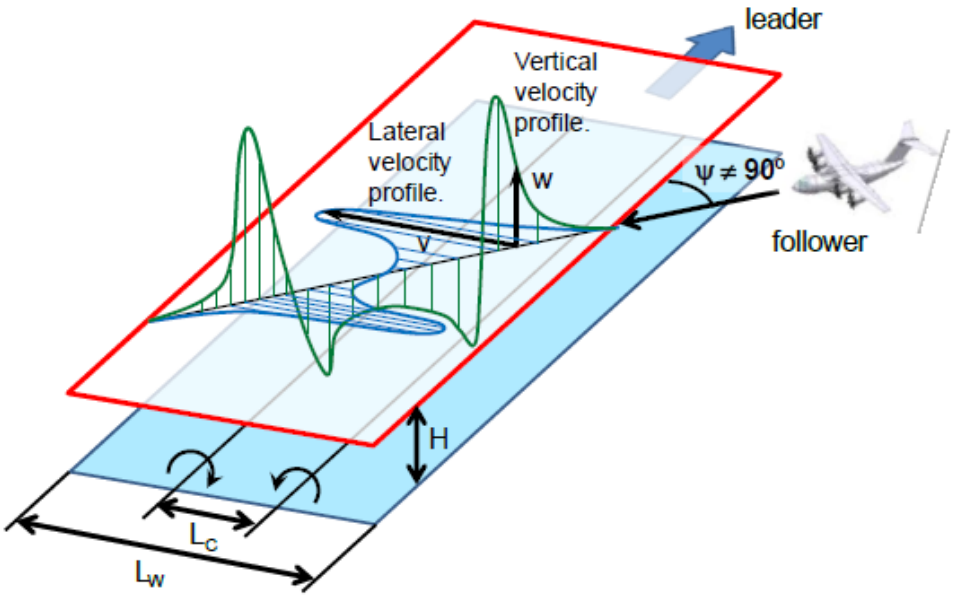

Figure 3.5 Generic cross at ψ≠90º and H≠0

After the understanding of these simple cases, it is possible to know how the excitation velocity is computed in a wake vortex. Once all the geometric parameters are known, the vortices are considered to lie in the same plane, the aircraft trajectory is the one that crosses at different distances from each vortex in order to model a generic crossing and the aircraft path is a rectilinear trajectory. The angle of attack, yaw angle and roll angle, which are all considered constant during the crossing, complete the encounter geometry definition. The definition of those parameters is presented in figure 3.6. It is important to remark that the software allows to establish different reference checkpoints from which the distance from both vortices are set, for instance, the wing root (nose impacts) or the HTP root (tail impacts). Finally, it is assumed that the aircraft crosses the wake without perturbing it, as if it was a 'ghost' flying through the wake.

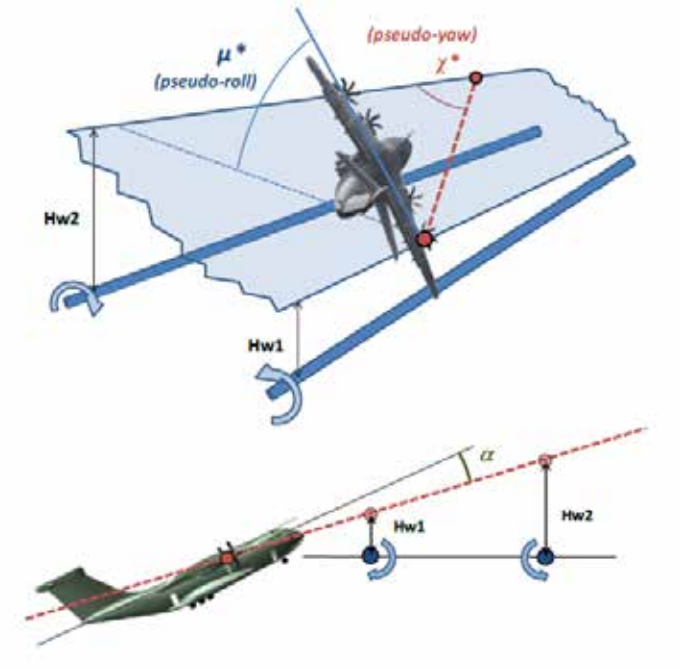

Figure 3.6 Attitude and trajectory parameters

Using all this information, the position of the aircraft is well defined at all times and, thus, the movement of each point in the aircraft with respect to the wake is also known. Therefore, the normal velocities, v_n, to the panels at each control point of the Doublet-Lattice model (aerodynamic model) are also known. These normal velocities constitute the input excitation for the dynamic equations of motion.

The excitation for this problem produced by the wake vortex depends on many geometrical parameters and environmental factors. Following those aspects, a dedicated tool has been developed within the company to provide the velocity field to the solver of the dynamic equations of motion. This tool has been named WESDE (Wake Encounter Speed Distribution Evolution) and is in charge of generating the adequate matrices with the evolution of the perpendicular velocity for each aerodynamic box of the Doublet-Lattice model along time. It takes as input parameters the following aspects:

- Geometry of the crossing (velocity, attitude and relative position of the aircraft with respect to the vortices, etc.)
- Parameters of the generator aircraft (velocity, span, weight and load factor).
- Wake model parameters (vortices separation, vortex core radius, and aging).

WESDE takes that data together with the aerodynamic model of the aircraft and computes time histories of velocities at the control point of each aerodynamic box. The main assumptions made at this step are:

- The crossing trajectory of the follower aircraft is rectilinear, at constant speed and constant attitude.
- The follower aircraft has not response to the wake encounter from the flight mechanics point of view. It does not change trajectory nor attitude angles.
- The input excitations are considered as the undisturbed wake velocities.

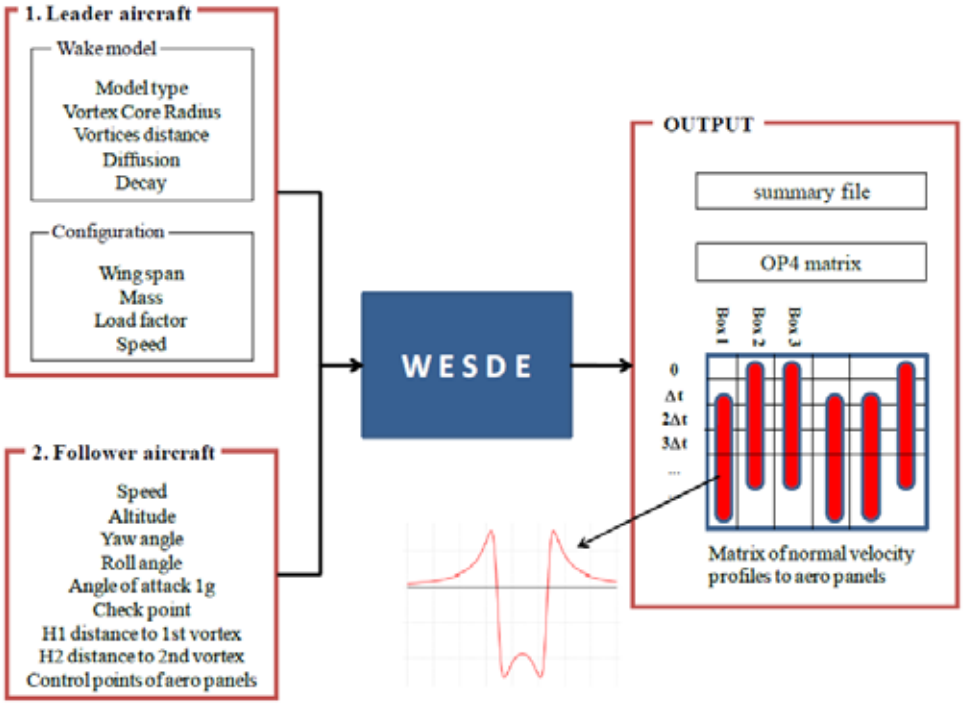

Figure 3.7 WESDE flowchart inputs and outputs

3.4. Solve dynamic equations: DYNRESP

Once the excitation for the wake encounter is computed, the next step it to solve the dynamic equations of motion in order to obtain the dynamic response of the aircraft. The solver used in Airbus Military for that is the DYNRESP aeroservoelastic package [15]. This is a tool developed by Karpel Dynamics Consulting, and it has the objective to obtain the dynamic response of an aircraft for different input excitations as discrete gusts, maneuvers commands and other direct forces. The figure 3.8 shows the general flow chart for DYNRESP. As it has the capabilities to compute discrete gust responses, the velocity profile for a wake vortex excitation is similar and, therefore, just little adjustments were necessary to adapt to the characteristics of this problem.

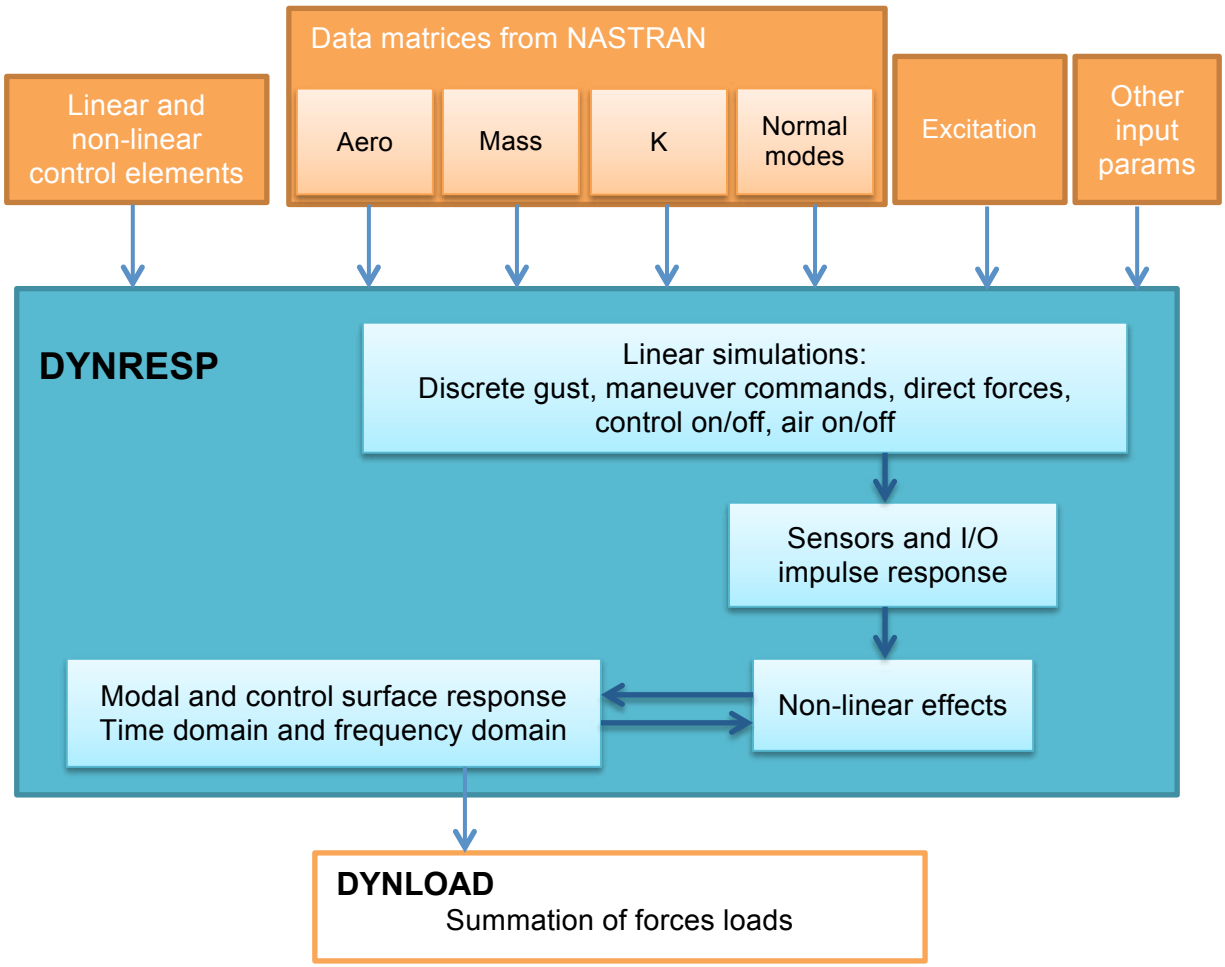

Figure 3.8 General flow chart of the DYNRESP solver

The resolution of the dynamic equations of motion consists of a mathematical model based on a set of low frequency natural modes of the structure that have the role of generalized coordinates. Then, unsteady aerodynamic matrices are combined with those modal properties in an aeroelastic model. Considering this, it is possible to express the aeroelastic equation of motion in the frequency domain where the modal displacements are the generalized coordinates. That equation is similar to the corresponding one for the case of a conventional gust excitation response, but now the vector of the velocity profile of a conventional gust is replaced by the velocity profile obtained in the previous computation using WESDE ($w_W(i\omega)$).

$$\left[-\omega^2\left[M_{hh}\right]+i\omega\left[B_{hh}\right]+\left[K_{hh}\right]+q\left[Q_{hh}(i\omega)\right]\right]\left\{\xi(i\omega)\right\}=-q\left[Q_{hj}(i\omega)\right]\frac{\left\{w_W(i\omega)\right\}}{V} \qquad [3.1]$$

The previous equation shows the dynamic equations of motion for the frequency domain expressed as function of the modal displacements. In the left-hand side are the matrix coefficients associated with the modal displacements $\{\xi(i\omega)\}$, such as the generalized mass $[M_{hh}]$, damping $[B_{hh}]$, stiffness $[K_{hh}]$ and aerodynamic influence coefficient $[Q_{hh}(i\omega)]$ matrices. The right-hand side shows the aerodynamic forces due to the velocity profile generated at the wake vortex expressed in the vector $\{w_W(i\omega)\}$.

This is a vector of separate signals obtained from the FFT (Fast Fourier Transform) of the normal velocity profile received from WESDE.

The DYNRESP tool solves the previous equations in the frequency domain in a very efficient way by means of FFT. The output obtained is the dynamic response in the time domain in modal coordinates. After that, the following step is to post-process, by means of the in-house software DYNLOAD, that modal response in the time-domain in order to obtain integrated loads in the whole aircraft or particular sections of it.

Another important characteristic of the DYNRESP solver is that admits flight control systems (FCS). Furthermore, one of the strengths of DYNRESP is the capability of solving non-linear problems, although it has not been used in the resolution of wake vortex encounter problem.

3.5. Post-process load output: DYNLOAD

After the computation of the modal response in the time domain, the last step consists of obtaining integrated loads for the whole aircraft or some specific areas in order to be able to compare those loads with the reference levels and assess the different cases where those levels are exceeded. With the aim of facilitate the load post process and evaluation, the Structural Dynamic and Aeroelasticity department has developed an in-house software that encompasses this step. The daily basis of the department involves the computation of several load cases and repetitive loops for the certification of the dynamic loads generated in all the possible defined scenarios, therefore, a tool such as DYNLOAD (Dynamic Loads Analysis) is very useful. This software is used in the department for the load computation of the different cases involving both flight and ground dynamic loads such as discrete gust, continuous turbulence, dynamic landing or taxi loads.

DYNLOAD takes as input the dynamic response of the aircraft in the time domain from different sources (DYNRESP or NASTRAN) and provides a various range of outputs:

1. Grids accelerations, velocities and/or displacements. It can provide position and movement characteristics of any grid point of the aircraft model. An output example of a grid point acceleration from DYNLOAD is shown in figure 3.9.

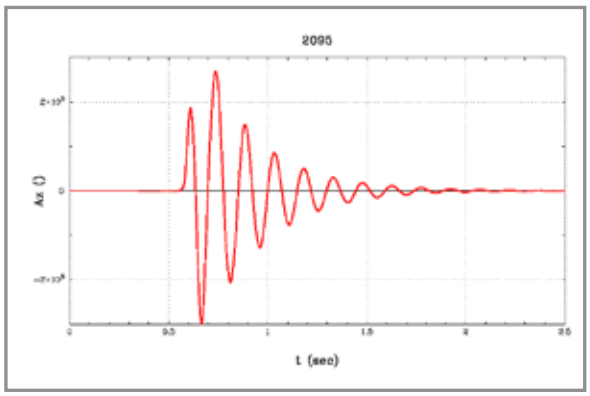

Figure 3.9 Example of a grip point acceleration output from DYNLOAD

2. Loads at monitoring stations. A monitoring station is defined as an area of interest and a reference system where the integrated loads for that area are obtained as can be seen in figure 3.10. Resulting loads (relative to some reference system) of the distributed forces and moments applied in a defined zone of the structure can be computed. Figure 3.11 shows a time-history of a monitoring station load component.

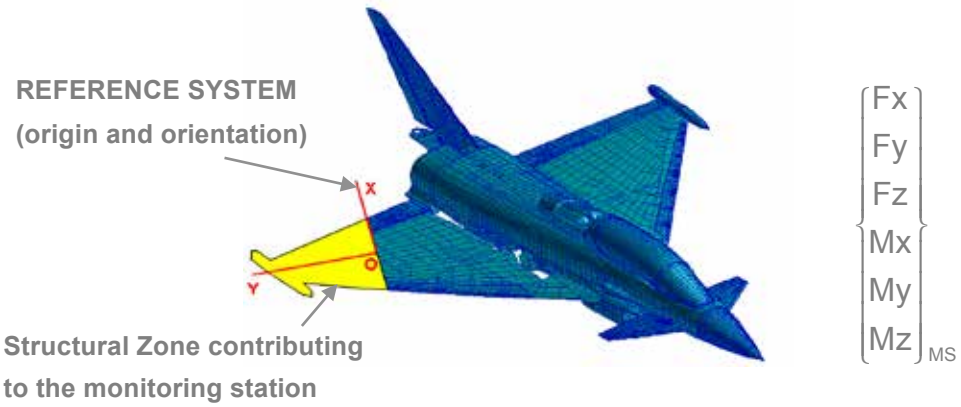

Figure 3.10 Example of a monitoring station definition

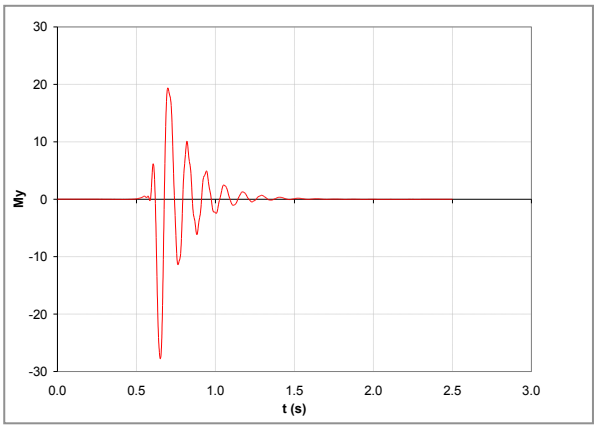

Figure 3.11 Time history example of a monitoring station load component

3. 2D Envelopes. With two time-histories of load components, it is possible to obtain the 2D envelope of both by combining the two in the same plot by eliminating the time, where each axis represents a load component. In this way, it is easier to understand where the relevant load values are. Figure 3.12 presents a scheme of how a 2D envelope is built.

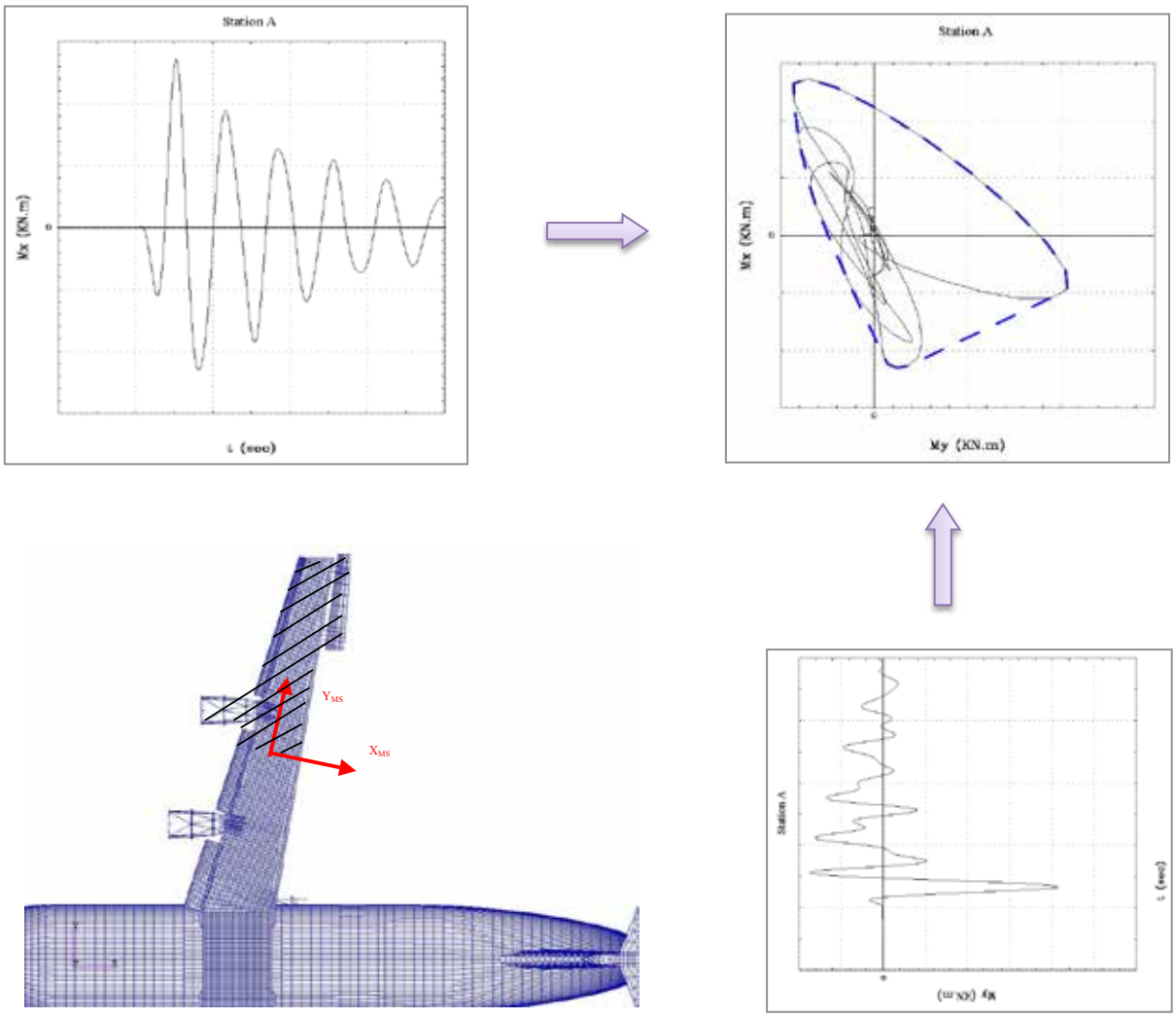

Figure 3.12 2D envelope example

Chapter 4

FLIGHT TEST RESULTS

4.1. Flight test results available

For the sake of a better understanding of the physical characteristics of the problem and to have real data for this type of scenario, the company set a series of flight tests where intentional wake vortex encounters were induced [17]. As said, these flight tests were carried out with the aim of refining the existing A400M wake vortex model and to complement the benchmark of the A400M wake vortex load analysis model.

Therefore, all the methodology and tools mentioned in the previous chapter have been validated with flight-test data. That fact allows to be able to use in this study excellent tools that represent very accurately the behavior of the aircraft and its response to a problem such as a wake vortex encounter.

4.2. Characteristics of the flight tests for wake encounters

The flight tests performed during June and August 2013 consisted of a wake generated by an A400M aircraft (MSN3 prototype) and another A400M (MSN1 prototype) crossing that wake at a certain separation distance and time after it. The leader aircraft is equipped with smoke generators located at the outer engines in order to facilitate the visualization of the wing tip vortices by the crossing aircraft. There was also a similar flight test campaign in the approximately same dates but it was performed by an Airbus A340 as the wake generator aircraft and an Airbus A400M crossing that wake. These were not the basis of the flight tests used in this study but they are referenced in further chapters and they were used to treat initial wake characteristics. Therefore, it is worth to mention them and to know that there were performed two flight test campaigns with different generator aircrafts.

The main characteristics of the leader aircraft for these flight test encounters is that is flying at a steady level of 1g (load factor of 1g) and at constant heading, speed and altitude in order to generate a very well formed and stable wake that can be identified and crossed by the follower aircraft. The crossing aircraft is also flying at a constant speed and with a certain heading angle with the wake trajectory established by the tests requirements. As the A400M aircraft presents a T-Tail configuration, there is a considerable distance between the reference wing surface and the reference horizontal tail plane (HTP) surface. For this reason, the excitation due to the wake vortex will not be comparable for both components when one of them is closer to the vortex core plane. In order to consider the two main encounter scenarios, two cases were set in the flight tests and they are summarized in figure 4.1. For the first type of encounters, the pilot intends to cross the vortex core center where the wings are close to the vortex plane including some deviation from the target (H=0m±4m, known

as ‘Nose impacts’). The second configuration is focused on crossing the wake vortex closer to the HTP reference surface. These last attempts were considered to maintain a path slightly below the vortex core center to position the tail zone through the wake vortex (H=8m±4m, named ‘Tail impacts’).

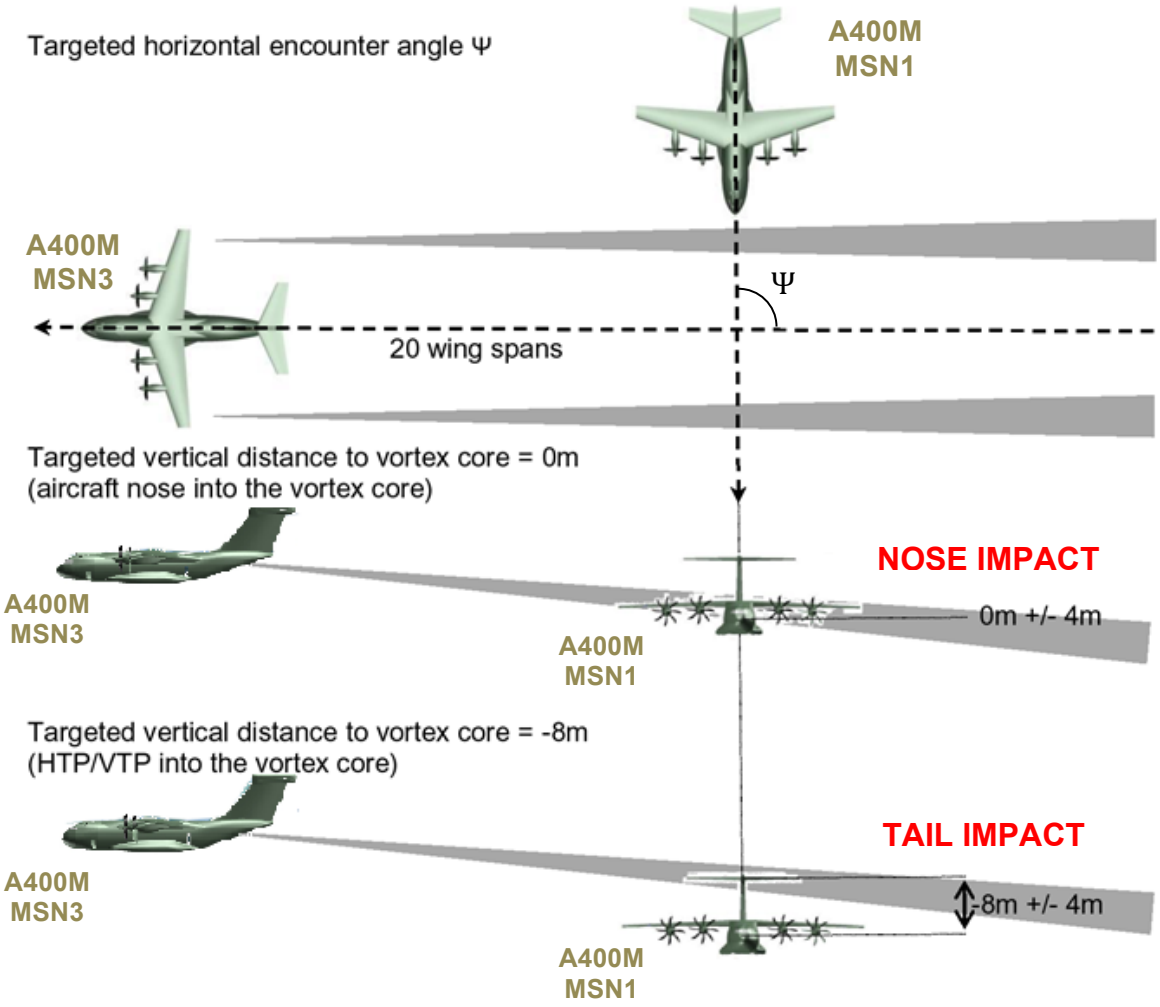

Figure 4.1 Flight test configurations

4.3. Methodology validation for the numerical simulations

Regarding the wake vortex encounters given in the flight tests, there is a parameter of the event that it is not known: the relative distance from the vortex core plane to the reference position of the aircraft. The crossing angle is very accurately defined due to the measuring precision of the heading of the aircraft but for the height variable, there is no possibility of knowing it exactly. The pilot tries to carry out nose or tail impacts, positioning the aircraft at a certain distance from the wake for each case but there is an uncertainty deviation from the desired impact height. For that reason, the validation methodology consists of an iterative process that adjusts the distances from the vortices until a satisfactory load match is achieved. This process

is shown in the Figure 4.2 and it starts with the consideration of a perfect vortex hit (H=0) to the corresponding reference point of the aircraft. Then the computation loop takes place and the obtained loads are compared to the flight test measurements. After the loads comparison, the distances to the vortices are changed consequently (H≠0). Another computation run is performed with that new configuration and the comparison is repeated. This process is performed until there is a good comparison between computed loads and flight test measurements and the vortices positions relative to the reference point of the aircraft are set.

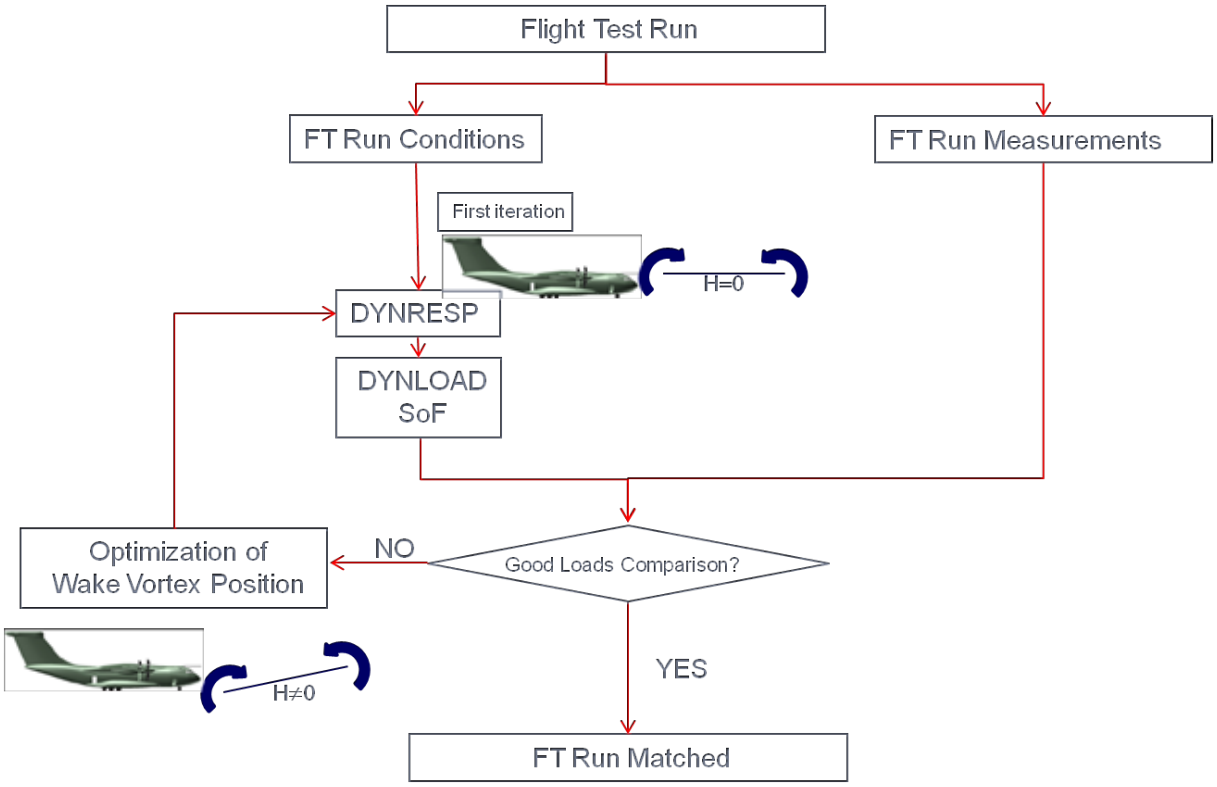

Figure 4.2 Iterative process followed to obtain vortices position with respect to the aircraft

Following that iterative process for the validation of the methodology presented before, the results obtained shows a great agreement with the flight test measurements. Therefore, it can be said that Airbus Defence and Space has satisfactorily validated all the tools used in this study and they can be used for further analysis that will be carried out in these pages. That good agreement can be seen in figure 4.3 for the case of bending moments for the wing root and the vertical accelerations of the wing tip, where the values have been normalized. Wing tip accelerations are shown in figure 4.4. Moreover, as the tail is the relevant part of the aircraft in this study, agreements for HTP and VTP loads and accelerations are presented in figures 4.5 and 4.6. It can be seen that for all the areas there is a satisfactory agreement between flight test measurements and numerical simulations.

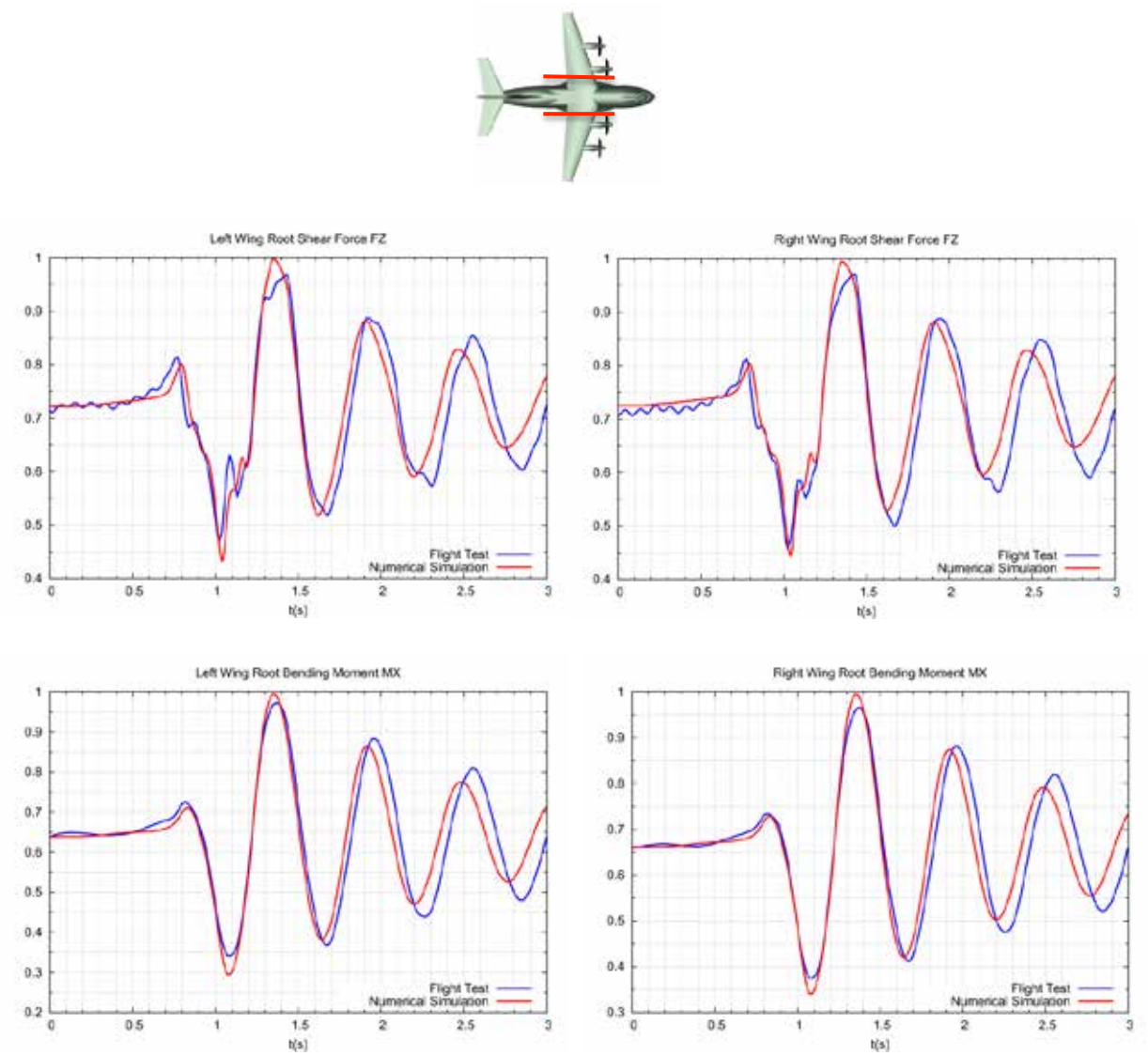

Figure 4.3 Adjustments of wing root bending moment to flight test results

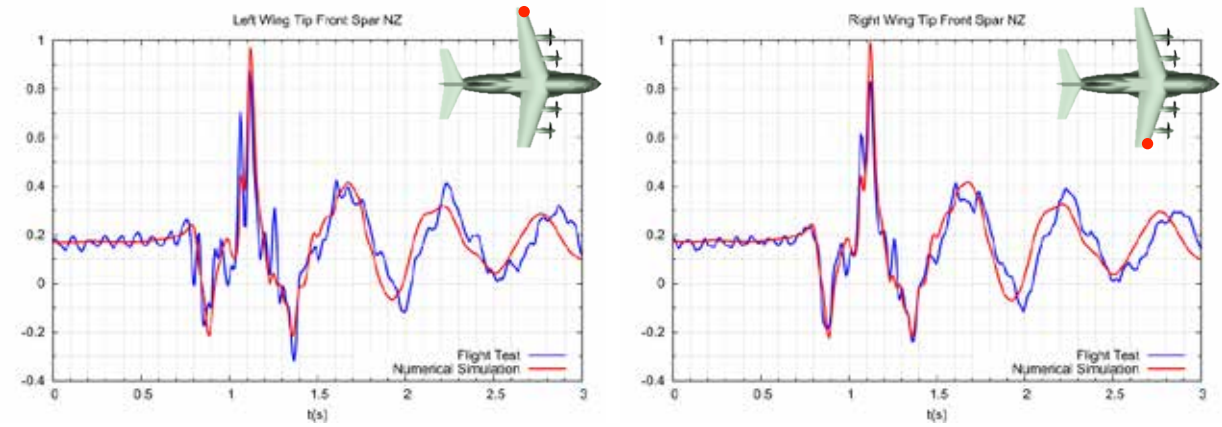

Figure 4.4 Numerical simulation results for wing tip accelerations versus flight tests

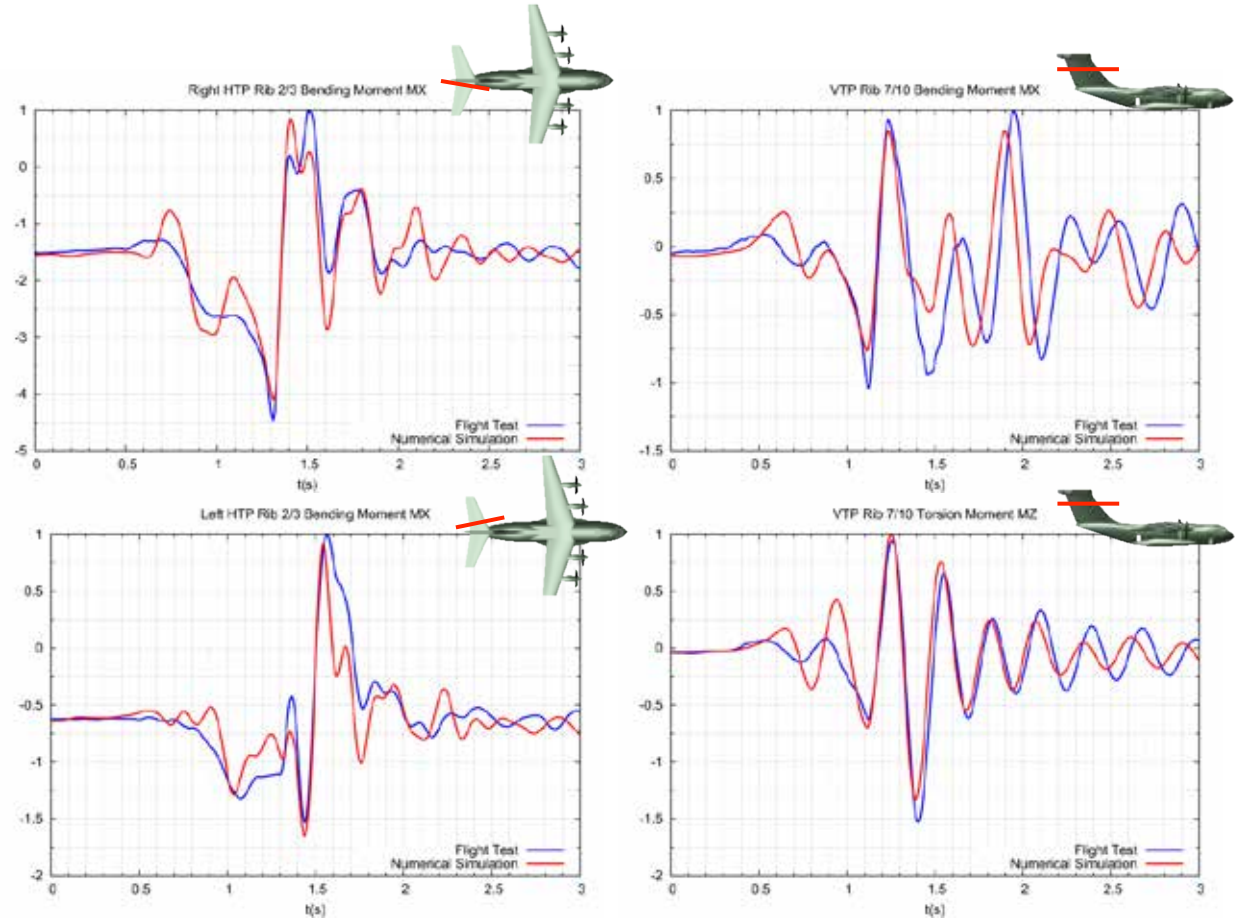

Figure 4.5 Agreements between flight test and simulations for HTP and VTP loads

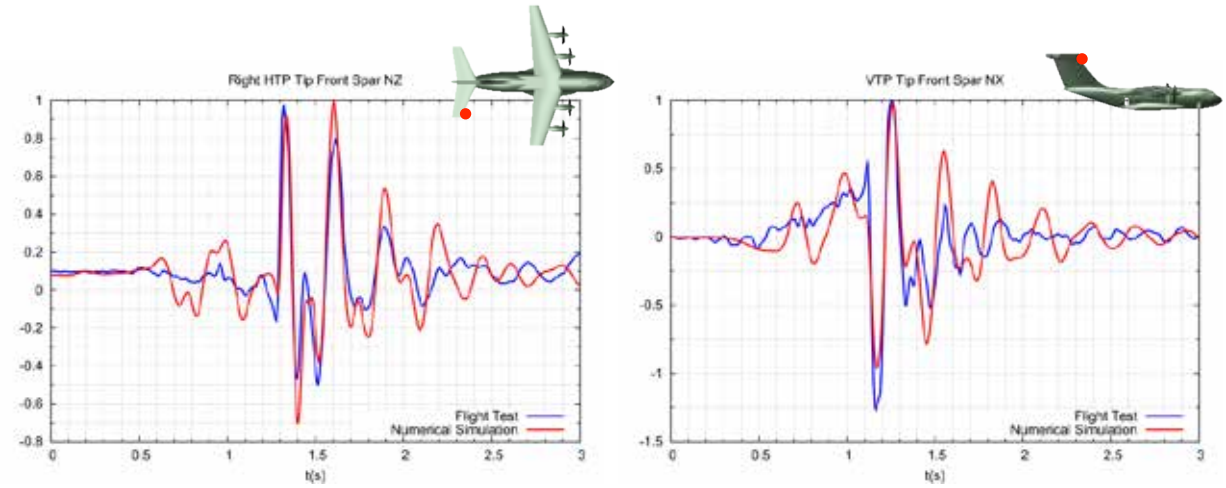

Figure 4.6 Agreements between flight tests and simulation for tail accelerations

Chapter 5

WAKE VORTEX MODELING

5.1. Wake Vortex model

In order to assess the response of the aircraft to an event such as a wake vortex encounter, it is necessary to establish a model of the physics involved in the wake generated which is the one that produces the excitation afterwards.

Going into detail of that model, the wake encountered by the crossing aircraft is assumed to be a far wake vortex sheet completely rolled-up. This vortex sheet is model by two horizontal straight parallel counter-rotating vortex tubes, where both lines of vortices do not necessarily be in the same horizontal plane. As far wake is assumed, the length of the vortex tubes is infinite compared to the characteristic length of the aircraft such as the wing span. The vortex tubes are separated a distance, b_0, that can be expressed as a fraction of the wingspan (s_0) of the leader aircraft, where $b_0 = s_0 \cdot b$, as it is shown in figure 5.1. This parameter of the wing span fraction will depend on the flaps configuration of the leader aircraft. As the vortices are assumed symmetrical and counter-rotating, the vortex circulation will be symmetrical. Thus, both vortices will have the same absolute value of circulation but opposite sign. The sign criterion is assumed to be positive for the vortex of the left wing of the leader aircraft and negative for the right wing vortex from the pilot perspective.

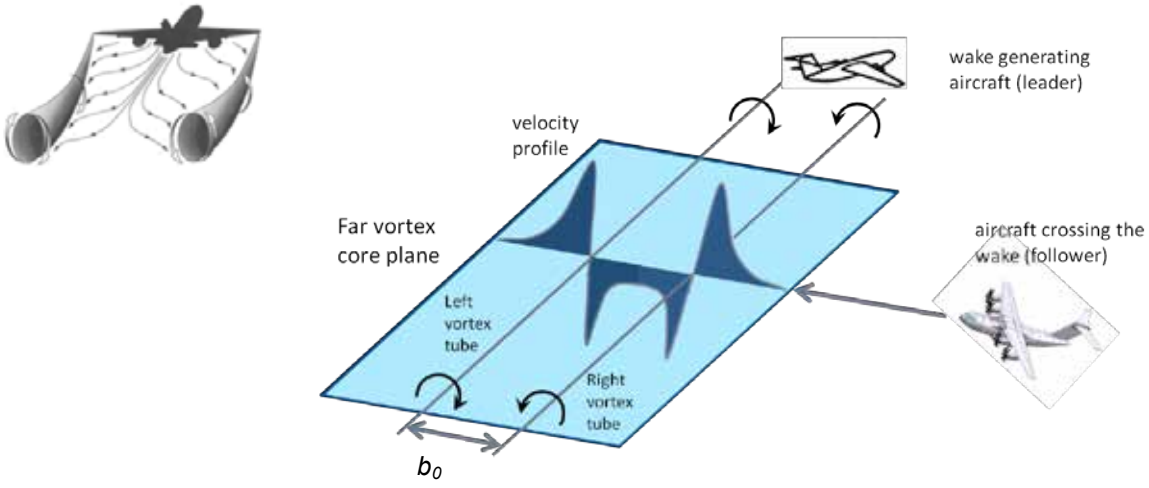

Figure 5.1 Far wake vortex model

5.1.1. Estimation of vortex circulation

In the wake model of two counter-rotating vortices assumed, a key parameter is the circulation assigned to those vortices. As it is the consequence of the flying path of the leader aircraft, the circulation of the vortices generated will depend mainly on parameters of that generator aircraft. Due to the consideration of far wake vortex, the wake is completely rolled-up and the circulation has to be in consequence with that assumption.

In order to find a relationship between the circulation of the vortices and other aerodynamic variables, the Betz assumption for the roll-up process was used [18]. The approach taken by Betz was to assume a final, axisymmetric form for the rolled-up vortices. Then, using conservation statements, he related the vortices circulation to the wing circulation and associated vortex sheet. A scheme of that is shown in figure 5.2. The initial assumptions of the process are that the circulation and the span-wise center of vorticity of each half of the wake are conserved during the rolled-up process. Then, Betz stated that the circulation of the final rolled-up vortex is equal to the integral of the distribution of circulation of the vortex sheet along the wingspan. That vortex circulation can also be expressed as the integral of its derivative along the radius as can be seen in equation 5.1. In the same way that differential trailing vortices that form the sheet are the result of circulation loss or gain along the wingspan, this distribution is equal to the derivative of the distribution of circulation of wing-bound vortices.

$$\Gamma_v(R) = \int_0^R \frac{d\Gamma_v}{dr}\,dr = \int_0^{\frac{b}{2}} -\frac{d\Gamma}{dy}\,dy \qquad [5.1]$$

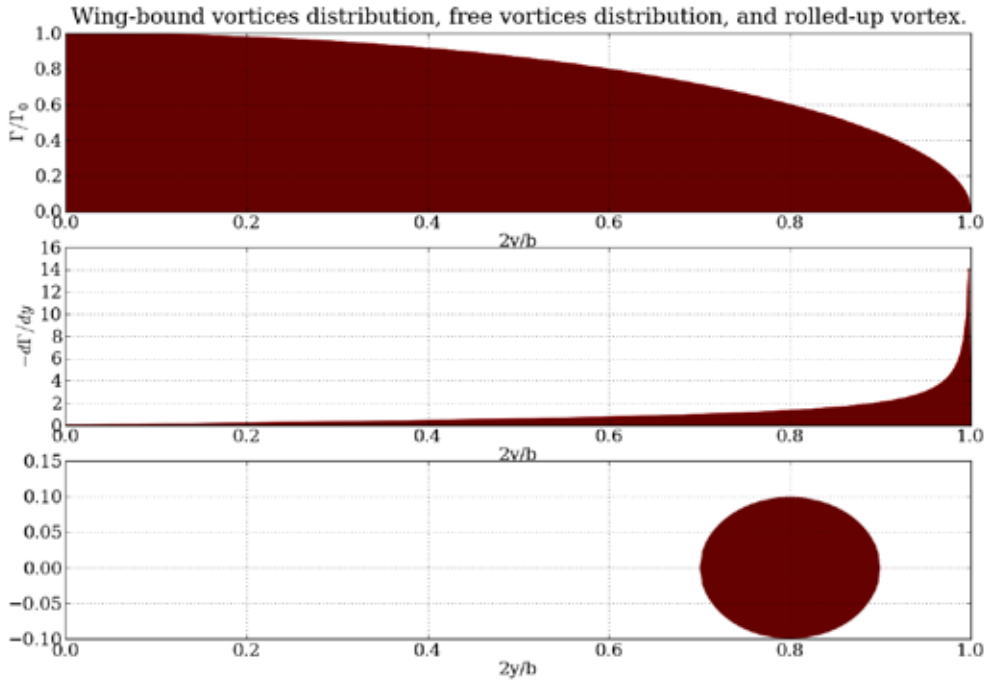

Figure 5.2 Vortices distribution scheme according to Betz assumptions

Applying Barrow's Law to the previous equation and considering zero circulation at the wing tip:

$$\Gamma_v(R) = \int_0^R \frac{d\Gamma_v}{dr} dr = \int_0^{b/2} -\frac{d\Gamma}{dy} dy = -\left[\Gamma\left(\frac{b}{2}\right) - \Gamma(y)\right] = \Gamma(y) \equiv \Gamma_0 \qquad [5.2]$$

Taking into account Betz's assumption of equal span-wise center of vorticity for both the rolled-up vortices and for the vortex sheet yields to the following equation where b_0 is the separation between the two rolled-up vortices.

$$\Gamma_0 \frac{b_0}{2} = \int_0^{b/2} -\frac{d\Gamma}{dy} y dy \qquad [5.3]$$

Now, integrating by parts the circulation from root to tip and considering zero circulation at wing tip gives:

$$\int_0^{\frac{b}{2}} \Gamma dy = \Gamma\left(\frac{b}{2}\right)\frac{b}{2} - \int_0^{\frac{b}{2}} y \frac{d\Gamma}{dy} dy = -\int_0^{\frac{b}{2}} y \frac{d\Gamma}{dy} dy \qquad [5.4]$$

The previous equation, 5.4, can be related with Betz's second assumption to obtain an expression between both the wing circulation and the rolled-up vortices' circulation:

$$\Gamma_0 \frac{b_0}{2} = \int_0^{\frac{b}{2}} \Gamma dy \qquad [5.5]$$

Now, the wing circulation can be obtained from the Kutta-Joukovsky formula:

$$L_w = \rho_\infty U_\infty \int_{-b/2}^{b/2} \Gamma dy = 2\rho_\infty U_\infty \int_0^{\frac{b}{2}} \Gamma dy \qquad [5.6]$$

Therefore, the circulation of the rolled-up vortices, as it is stated to be equal to the circulation at wing root, can be related to the aerodynamic variables as follows:

$$\Gamma_0 = \frac{L_w}{\rho_\infty U_\infty b_0} \cong \frac{nW}{\rho_\infty U_\infty b_0} \qquad [5.7]$$

As it was shown in the previous expression (equation 5.7), the vortex circulation for the wake model depends on several parameters of the leader aircraft and flight conditions. Those parameters are:

- Air density: ρ_∞
- Aircraft true velocity: U_∞
- Aircraft weight: W
- Load factor: n
- Distance between cores of vortex tubes: b_0

5.1.2. Velocity field induced by far vortex wake

The second aspect treated in the wake model is the velocity field induced by the rolled-up vortices and seen by the crossing aircraft. This velocity field is considered bi-dimensional, that means that it does not depend on the longitudinal position along the vortex tube direction and all the planes perpendicular to the vortex tubes have the same velocity field. The second assumption considers that the induced velocity is perpendicular to the vortices lines, so, there is no component parallel to the direction of the vortex tubes. After the previous assumptions are stated, the velocity induced by each of the infinite vortices tubes is given by the Biot-Savart law. Considering a generic point P of the velocity field, the velocity at that point contained in a plane perpendicular to the vortices tubes is bounded to the same plane and is the combination of the azimuthal velocities $v_{\theta 1}$ and $v_{\theta 2}$induced by each vortex tube as it is shown in the figure 5.3.

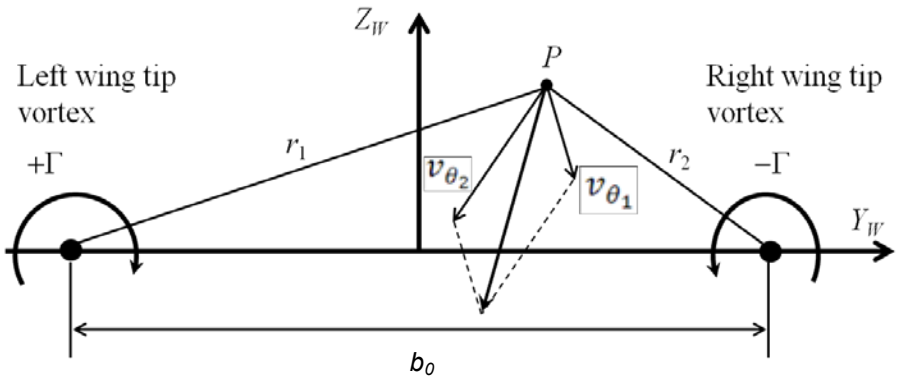

Figure 5.3 Velocity induced by the two vortex tubes

Regarding the azimuthal velocity induced by each vortex, there are several models derived by different authors that estimate that velocity. In this study, the model used was the one proposed by Hallock and Burnham [13]. This model is given by Airbus Military and is based in its previous expertise and experimental measurements. The Hallock-Burnham model defines the induced velocities as can be seen in equation 5.8, where r_1 and r_2 are the distances from each vortex core center to the point P and r_c is the vortex core radius.

$$v_{\theta 1} = \frac{\Gamma}{2\pi \cdot r_1} \frac{r_1^2}{r_1^2 + r_c^2} \qquad v_{\theta 2} = -\frac{\Gamma}{2\pi \cdot r_2} \frac{r_2^2}{r_2^2 + r_c^2} \qquad [5.8]$$

In this model the azimuthal velocity, v_θ, is zero at the vortex core center and increases with distance until it reaches its maximum value at a distance equal to the vortex core radius, r_c. Then, the induced velocity decreases towards zero as the distance increases.

5.2. Aging

The far wake vortex model presented before, considers a bi-dimensional velocity field where the induced velocity at each point depends only on the circulation of the rolled-up vortices and the vortex core radius. Those assumptions imply that the wake does not change as time goes by; it maintains the same circulation and vortex core radius no matter the time elapsed. This consideration does not represent accurately the physics of the problem because the wake characteristics will change as a function of the time passed since it was generated.

An actual wake experiments a degradation of its properties with time. This deterioration depends on several factors such as the initial intensity, the wake vortices sink rate, the atmospheric conditions and, of course, the time elapsed since its generation. Due to the complexity of the degradation of the wake, the effects have been reduced to two that apply to the main parameters of the vortices definition. The first is a decay factor in the circulation of the rolled-up vortices. This decay affects the wake intensity, diminishing it as the wake ages. The second factor considered in the wake aging is the diffusion effects summarized in the expansion of the vortices core radius as time goes by. The diffusion is the mechanism by which the vortices grow with time. Therefore, the wake model considered is going to include two parameters in order to catch the degradation or aging of the wake, which are circulation decay and vortex core radius diffusion. Before entering more in detail about both parameters, it is relevant to remark that the wake model is still bi-dimensional and does not change with time. Though the aging parameters are considered, they will produce and 'aged' velocity field, similar to the one presented before but now the induced velocity will depend on the aged characteristics of the wake. The velocity field will still be the same for all the points in the direction of the vortex tubes.

5.2.1. Circulation decay

Focusing on the first aging parameter, the decay of the circulation is a variable that influences all the velocity field of the wake vortex and thus the induced velocity. Remembering the expression of the induced velocity (equation 5.3), the vortex circulation is directly proportional to the induced velocity. Therefore, a reduction in the circulation by a certain factor will have the same consequences on the induced velocity. In this study and in the software used for computing wake vortex speed distributions (WESDE), the decay in the circulation will be introduced as a factor between 1.0 and 0.0 and it will multiply the nominal circulation of the rolled-up vortices in order to scale it consequently. As main points, the implications of the decay are:

- Intensity decay:

$$\Gamma_{aged} = \Gamma_{nominal} \cdot (\text{decay factor})$$

- Affects all the velocity field
- Attenuates the induced velocity proportionally to the decay factor

5.2.2. Vortex diffusion

The second aging parameter considered in the wake vortex model of this study is the vortex core radius diffusion. Once the wake vortex has been generated, this event will suffer an intensity reduction as time goes by, hence it will not maintain forever in time, and by the other hand, the vortex tubes expand in size due to energy diffusion mechanisms. This expansion of the vortex tubes is the one treated in the parameter of the vortex core radius diffusion. This is a more local effect and instead of the decay, does not affect the entire velocity field. Again, remembering the expression for the induced velocity, a change in the vortex radius will induce a variation on the resultant induced velocity but the total circulation will remain constant.

Therefore, the effects given by the application of a diffusion factor will be concentrated at the proximities of the vortex center where the parameter of the vortex core radius has more relevance. Modifying the radius of the vortices influences mainly the relative maximum values of the induced velocity. Thus, the peaks of the induced velocity decrease when a diffusion factor is applied due to the conservation of total circulation. The methodology to introduce the vortex diffusion in the simulations is a factor of the vortex core radius. This factor as the decay one, takes values from 1.0 to 0.0, but now it will divide the nominal vortex radius (note that 1.0 means no diffusion effects and 0.0 an 'infinite' vortex growth). The following scheme collects the mentioned implication of the vortex diffusion:

- Vortex core radius diffusion:

$$r_{c\ aged} = r_{c\ nominal} / (\text{diffusion factor})$$

- Local effects on the velocity field at the proximity of the wake vortex
- Redistributes the velocities, smoothing the peaks at the vortex core plane, but keeping the total circulation constant.

5.2.3. Comparison of aging effects

After the presentation of the two mechanisms considered for wake vortex aging, it is interesting to see the effect of each one in the excitation seen by the crossing aircraft. As it was said, the decay is a factor applied to all the circulation of the vortex tubes. Therefore, the effect is more global, producing a reduction of the excitation along the entire encounter. In the other hand, the diffusion mechanism is a more specific one and it only affects the dimension of the vortex radius. This is linked to the maximum value of the excitation, which now will be smaller, while the total circulation is maintained.

These effects on the induced velocity can be seen in figure 5.4 where both pure aging models are plotted along with the nominal case. The black curve is the nominal case where no aging is considered for the wake vortex. Then, two cases where the same factor of 0.7 is applied for the decay model first and diffusion pure model later. That means that the circulation is reduced by a factor of 0.7 for the decay model. In a similar way and following the model presented in section 5.2.2, the diffusion model increases the vortex radius by a factor of 1/0.7 (the factor less than one is dividing in order to produce a bigger radius).

As can be seen, the case where only decay is considered (red curve) gives a lower excitation for the entire spectrum of the wake vortex. A reduction of the vortex circulation implies a lower induced velocity. For the case of only diffusion aging model (blue curve), it is possible to appreciate that now only the peaks are lowered. The zones far enough from the vortices center maintain the same values of excitation as the nominal case (black curve). This makes sense considering that, in the diffusion aging model, only the vortex radius is modified. That has its relevance in the maximum value of induced velocity, which is obtained at the distance equivalent to the vortex radius.

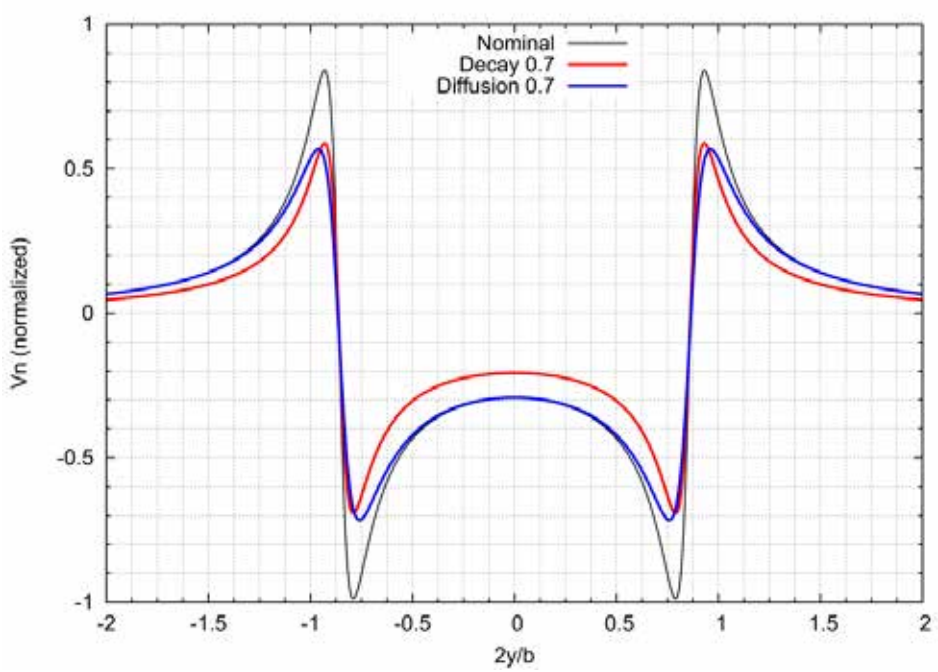

Figure 5.4 Comparison of aging effects on the normal velocity to the aerodynamic panels

Summarizing, the implications of the aging models considered in this study are the following:

- The decay of the vortex circulation produces a global reduction of the induced velocity.
- The diffusion model considers the growth of the vortex radius, affecting the values of maximum excitation and lowering the peaks of the induced velocity.

5.3. Decay and diffusion models

Once the aging models for the wake vortex are presented, they will be considered in more detail, explaining how the corresponding factors for each aging model are obtained. The decay model will be treated first, which is the most established inside Airbus Military for aging considerations of wake vortex. The diffusion model was not so studied and it will be treated in depth in the next chapter.

5.3.1. Decay model

The first of the aging models is the decay model that affects the circulation of the vortex tubes. Models for vortex decay are rather complex and depend, in first approximation, on:

- Circulation on wing
- Wake vortex sink rate
- Elapsed time since the generation of the wake (wake age)
- Atmospheric conditions:
    - Level of turbulence
    - Vertical temperature stratification
    - Vertical wind shear

Having this complex and very wide scope of parameters, some recommendations were presented by Airbus in terms of atmospheric conditions. Considering low winds and wind-shear, low temperature stratification and low to moderate ambient turbulence, the main mode of wake decay is through the combined effect of ambient turbulence and the natural long-wavelength instability of the wake, called Crow instability [26]. This mechanism of decay is the one assumed in this study.

Besides the consideration of the decay mechanism, the decay model to be followed is the Sarpkaya model [27]. A worst-case scenario is assumed by defining low atmospheric turbulence and low temperature stratification. Then, the Sarpkaya model interpolates a dimensionless atmospheric turbulence (ε^*, equation 5.9) to a dimensionless critical time $\left(Tc^*\right)$.

$$\varepsilon^* = \frac{2\pi\sqrt[3]{\varepsilon \cdot b_0^4}}{\Gamma_v} \qquad [5.9]$$

After that, the D2P model developed by DLR [28] is the one chosen to obtain the decay factor of the aging model. The procedure consists of defining a dimensionless time, $\widetilde{T}$, from the wake age using a characteristic time, T_0, where Δt is the time elapsed until the wake encounter takes place or the wake age. That time could be derived from a coordinated turn maneuver where the aircraft crosses its own wake or an estimated time when it crosses the wake generated by another aircraft.

$$T_0 = \frac{2\pi \cdot b_0^2}{\Gamma_v} \qquad \widetilde{T} = \frac{\Delta t}{T_0} \qquad [5.10]$$

The last step of the model compares the dimensionless time with the critical one obtained from the Sarpkaya model and assigns the corresponding values of the decay factor. This goes in hand with the behavior of the circulation decay of the vortex, where there is an initial slow decay followed by a rapid reduction of circulation. The change between the two modes is the meaning behind this model of decay for vortex circulation. Figure 5.5 shows an example of decay factor (Γ/Γ_0) versus the time elapsed since wake generation (wake age) for particular conditions of aircraft and flight parameters. There, it can be seen the behavior mentioned before, with two differentiated slopes.

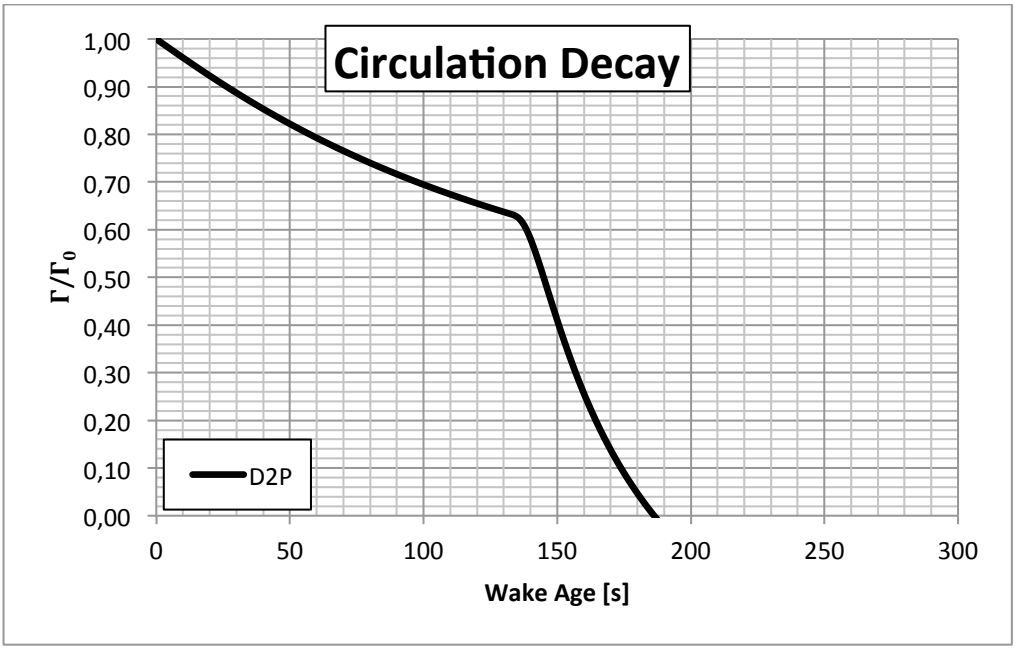

Figure 5.5 Example of decay factor model

5.3.2. Diffusion model

The wake vortex diffusion model is the second of the models treated in this study for considering wake aging. It will be revisited more in deep in the next chapter, where it will be used for fitting flight test results with an aging model of pure diffusion. The basic model used for wake vortex diffusion is the one presented by Winckelmans et al [22]. In this model they developed an analytical expression for vortex core growth as it shows equation 5.11.

$$\frac{dr_c}{dx} = \frac{2\upsilon\lambda}{Ur_c}\left(1+\frac{\mu_t}{\mu}\right) \Rightarrow r_c^2 = r_{c0}^2 + 4\lambda\upsilon\left(1+\frac{\mu_t}{\mu}\right)\Delta t \qquad [5.11]$$

Where r_{c0} is the nominal vortex core radius, υ is the kinematic viscosity, Δt is the vortex age and λ is called the entrophy constant, which for the Hallock-Burnham model is equal to $\lambda = 0.6667$.

For practical Reynolds numbers, the laminar model predicted a very low vortex core growth. Therefore, turbulent wakes should essentially be considered. Capart & Winckelmans [29] showed that the wake development in a low turbulence environment such as the one considered in this study, can be predicted by using an effective viscosity concept, as the effective viscosity turbulence model from Owen [30].

Hence:

$$\frac{\mu_t}{\mu} = \frac{1}{\beta}\sqrt{\frac{C_L}{2ARb_0}}\sqrt{\frac{Ub}{\upsilon}} \qquad [5.12]$$

Where β is a constant whose value is 8, C_L is the lift coefficient, AR is aspect ratio, b is the wing span, U is the aircraft velocity, b_0 is the distance between vortices expressed as a fraction of the wing span and υ is again the kinematic viscosity.

This vortex diffusion model presented in equation 5.11 is the one that will be treated in the next chapter for further considerations. It will be analyzed along with the decay model to study the combined effects of both models. After that, apply the corresponding modifications to the model in order to fit flight test results considering numerical simulations with only vortex diffusion as aging mechanism.

Chapter 6

WAKE VORTEX DIFFUSION MODEL

6.1. Objective of the analysis

This chapter is oriented to the understanding and improvement of the vortex diffusion model developed by Winckelmans et al [22]. In one hand, the decay model for the vortex circulation it is where Airbus Military has taken steps forward and they have an acceptable model to implement that aging mechanism in the wake vortex encounter simulations. However, the vortex diffusion is another aspect of the wake aging that seems feasible to happen from the physics point of view and it should be worth studying and extend the knowledge about this model.

For these reasons, the idea of following the procedure of fitting flight results considering different aging models and then, compare the results, was presented. Remembering the aspects of the wake vortex encounter, the main parameter in the loop of fitting flight results with numerical simulations was the distance at which the reference surface of the aircraft crosses the vortex tubes line. These distances are the ones that are iterated until a good match with load results is achieved because the exact value is not known.

Therefore, the main goal of the revisiting of the diffusion aging model is the consideration of a modified model of the proposed by Winckelmans that provides satisfactory adjustments with flight results when only the diffusion mechanism is considered as aging factor.

6.2. Methodology

The strategy followed in this analysis consists of setting three cases of wake vortex aging and then adjust the flight test results of several different runs with those three aging models. Hence, the distances to the vortices lines are modified for each case and they can be different. The three aging models considered can be classified as follows and are shown in table 6.1.

- **Nominal case**: Conditions used in previous loop calculations, carried out by Airbus Military. These are: circulation decay factor of 0.8 and a diffusion factor of 1.00. The heights with respect the vortex core are already set for them too.
- **Decay and diffusion model**: Here, both decay and diffusion are considered as aging factors. A combination of both factors at around 0.8 is chosen. Distances from vortices are iterated to obtain the best adjustment possible.
- **New adjustment considering only diffusion**: Circulation decay factor set to 1.00 and the diffusion factor is introduced in the numerical computations to obtain the best possible adjustments. Here the diffusion factor will be less than

0.8. Then, the distances are adjusted to obtain the best fit with flight test results.

Table 6.1 Decay and diffusion factors for the three aging models

	Nominal case	***Decay + Diffusion***	***Pure Diffusion***
Decay factor	0.80	0.80	1.00
Diffusion factor	1.00	0.80	> 0.80

6.3. Simulations results and model modifications

The three aging models presented before were considered for different flight test conditions. Then, the computation procedure explained in chapter 3 is repeated for each one, iterating the values of the distances to the vortices until a satisfactory match is reached.

6.3.1. Adjustment results

As a first output, several figures showing the adjustment between flight test results and the numerical simulations considering the different aging models are presented. This is the main step in order to obtain equivalent models of the wake that can be analyzed afterwards.

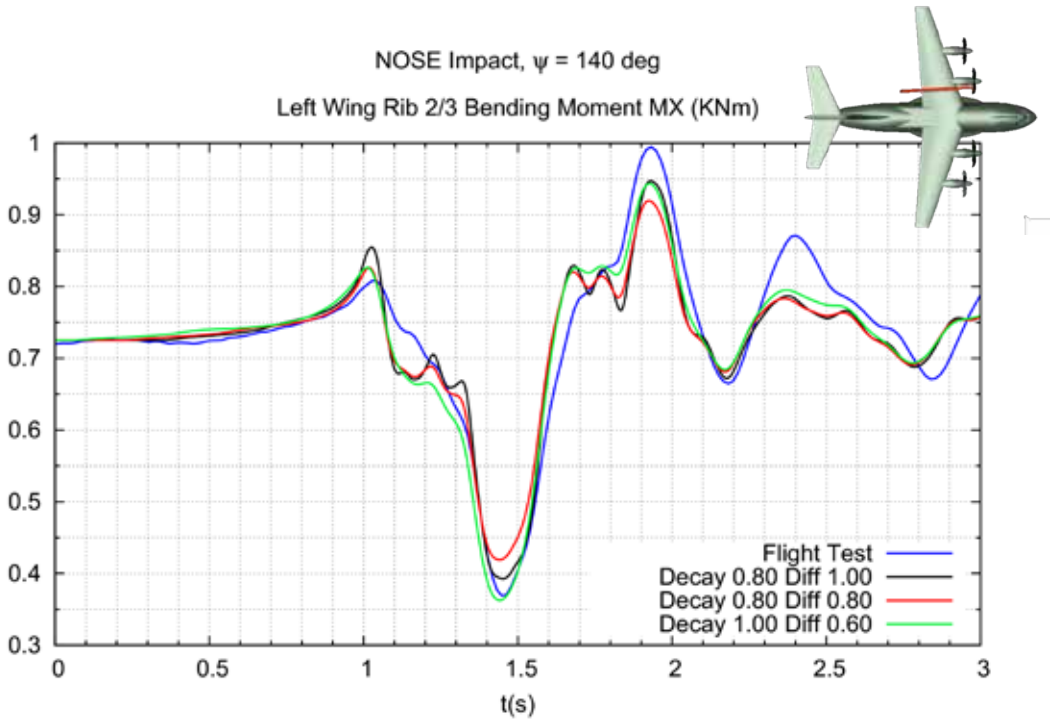

Figure 6.1 Comparison between aging models, wing loads

Focusing on the three main areas of the aircraft, three figures with load adjustments for representative monitoring stations of each one of them are presented. All three are from different flight tests in order to increase the verification of the adjustments. Figure 6.1 shows the results of the bending moment (MX) at the left wing root. The next one, figure 6.2, presents the bending moment at the HTP root while figure 6.3 gathers the torsion moment (MZ) at the VTP.

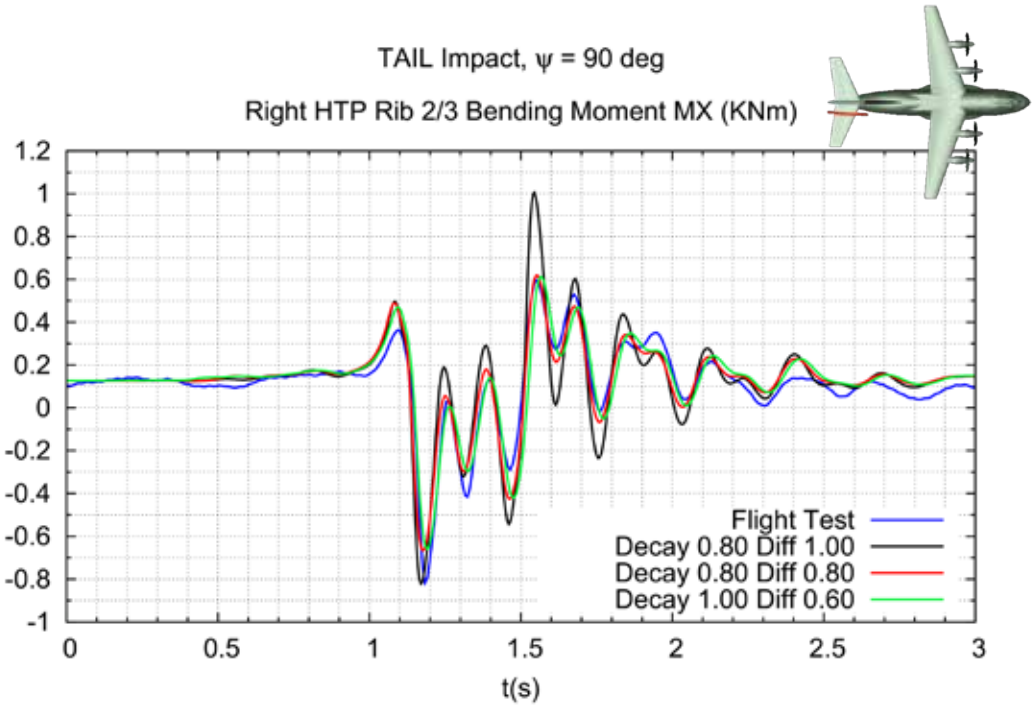

Figure 6.2 Comparison between aging models, HTP loads

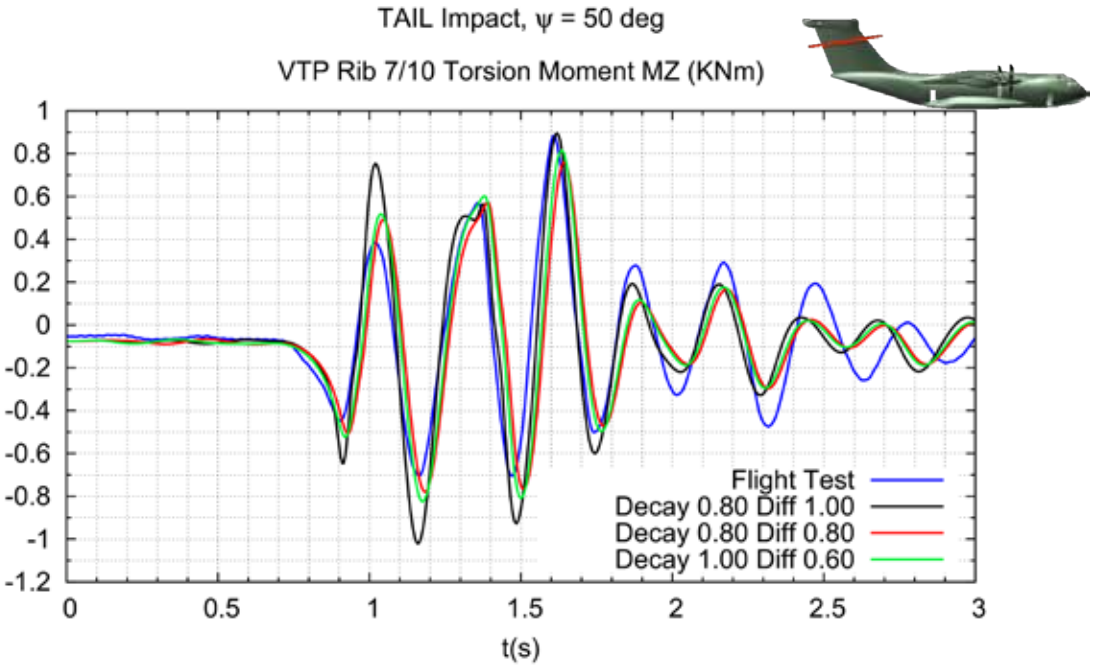

Figure 6.3 Comparison between aging models, VTP loads

The previous results showed a satisfactory adjustment between flight test results and numerical simulations for the two additional aging models considered: the one combining decay and diffusion and the corresponding with only vortex diffusion applied. It is also remarkable, the improvement that produces both models against the previous simulation performed in the department considering only decay as aging factor. It can be appreciated that several peaks are lowered when diffusion is included in the aging model, as it is seen in figure 6.3. Once these results are analyzed, more relevant information can be obtained considering the distances to the vortices for each aging model. In other words, how the vortices have moved from the nominal position when other aging factors are taken into account. Concentrating on a single flight test, table 6.2 shows the values of decay and diffusion factors as well as the distances to the vortices for each type of aging model.

Table 6.2 Parameters for each aging model of a particular flight test adjustment

	Decay factor	Diffusion factor	H_1	H_2
Nominal case	0.8	1.00	+1.90	+1.90
Decay + Diff	0.8	0.80	+3.00	+3.00
Only Diff	1.0	0.60	+4.20	+4.20

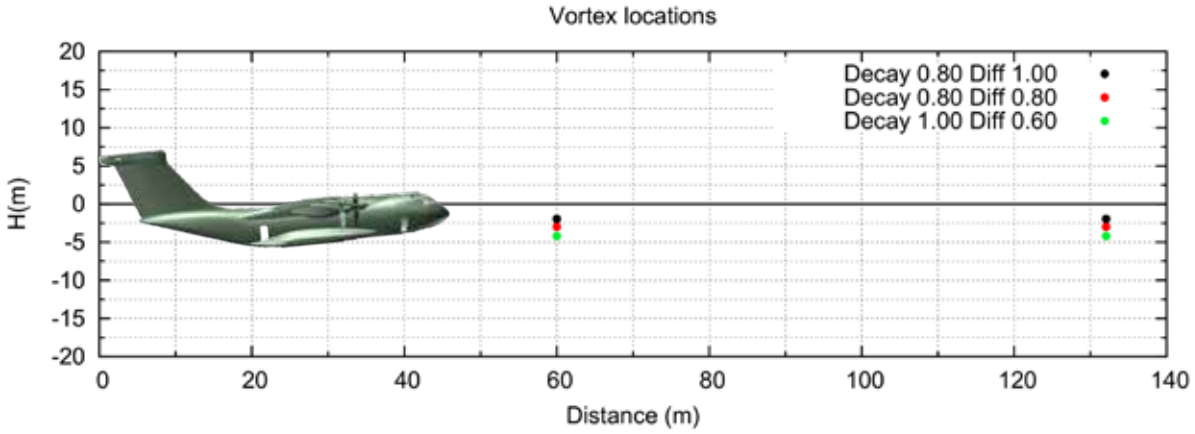

Figure 6.4 Vortex locations for different aging models

Table 6.2 shows that for aging models that include decay and diffusion or only diffusion, the distances to the vortex line increase and they are even more than the double of the value for the nominal case when only diffusion was considered. This difference in the vortex distance is presented in a more graphic view in figure 6.4. There, it can be seen that as the vortices grow (lower diffusion factor means larger core radius), the distance to a better fit also increases. This makes sense with the idea that the larger the vortex core radius, the further should be the excitation located to obtain the same values of flight test adjustments.

Nevertheless, the relevant parameter here is the value of the diffusion factor. This factor has been defined between 0.0 and 1.0 and is the one by which the initial core radius is divided in order to obtain a larger and aged vortex radius. In the model with only vortex diffusion, the vortex core radius has been set manually to a value that provides accurate adjustments between flight test and numerical simulations. This tuning has been performed without considering the model of vortex diffusion with the aim of finding a modification of that model that provides better results. In the middle between the nominal case and the pure diffusion model, it has been considered a combined model with decay and diffusion. In this case, the model developed by Winckelmans was followed to establish the corresponding diffusion factor applying the suitable elapsed time. In that way, it is possible to compare between the original Winckelmans model and the new proposed factor and try to make the adequate modifications.

The value of the diffusion factor obtained for the different flight test runs is similar and approximate to 0.6. Remembering the definition of the diffusion factor, that means the relation between the initial and the aged vortex core radius is equal to 0.6, as it is shown in equation 6.1.

$$diff \equiv \frac{r_{c0}}{r_c} = 0.6 \qquad [6.1]$$

6.3.2. Aging model and modifications

The vortex diffusion model proposed by Winckelmans et al [22] and presented in section 5.3.2 relates the growth of the vortex core radius with several parameters of the generator aircraft and atmospheric conditions. The analytical expression is written again in equation 6.2.

$$r_c^2 = r_{c0}^2 + 4\lambda\upsilon\left(1 + \frac{\mu_t}{\mu}\right)\Delta t \qquad [6.2]$$

Dividing by the initial vortex core radius, a dimensionless relation for the vortex growth is obtained, which is the inverse value of the diffusion factor.

$$\frac{1}{diff} \equiv \frac{r_c}{r_{c0}} = \sqrt{1 + \frac{4\lambda\upsilon}{r_{c0}^2}\left(1 + \frac{\mu_t}{\mu}\right)\Delta t} \qquad [6.3]$$

Where it is relevant to remember that:

$$\frac{\mu_t}{\mu} = \frac{1}{\beta}\sqrt{\frac{C_L}{2ARb_0}}\sqrt{\frac{Ub}{\upsilon}} \qquad [6.4]$$

If this model is applied for a specific aircraft and flight conditions, it is possible to represent the evolution of the diffusion factor (the relation of vortex core radius growth) with time. Relevant data as the initial vortex core radius is given by the

Aerodynamics department of Airbus Military, who also has worked in the wake vortex problem and in the model of the wake generation. Figure 6.5 shows the evolution of the diffusion factor for a generic case when the A400M is the leader aircraft flying at 10000 feet altitude and 200 KCAS speed.

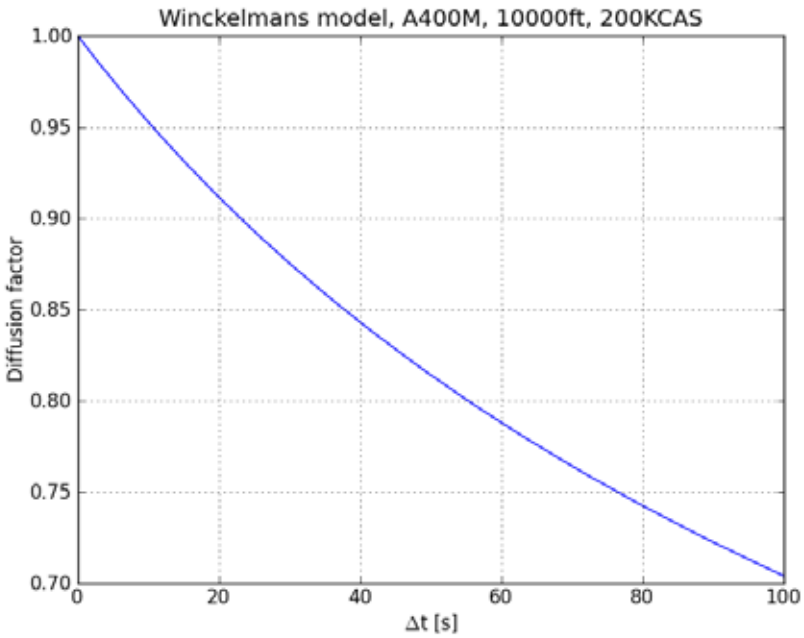

Figure 6.5 Evolution of the diffusion factor for the Winckelmans model

Regarding the previous plot, entering with the corresponding time gives the value of the diffusion factor to be applied in those conditions. In the flight test campaign, the characteristic time for the encounters was considered at around 45 seconds after the wake was generated. Therefore, this will be set as the elapsed time for the aging models presented in this section.

Now, considering the three aging cases mentioned in the previous chapter, there was the case of pure diffusion that gave lower values for the diffusion factor. These lower values induce a larger vortex radius growth that tries to compensate the combined effect when decay is also considered, as it was the second aging case where decay and diffusion are both applied. Starting from the original vortex diffusion model developed by Winckelmans, it was not possible to achieve such diffusion factors at the characteristic aging time of 45 seconds. Therefore, a modification of the Winckelmans model is proposed for the case when only vortex diffusion is considered as aging factor.

The value of the diffusion factor for the last aging case was 0.6. That means that the analytical expression of the model should give that factor for 45 seconds of aging time. This is shown in equation 6.5.

$$\frac{1}{diff} \equiv \frac{r_c}{r_{c0}} = \sqrt{1 + \frac{4\lambda\nu}{r_{c0}^2}\left(1 + \frac{\mu_t}{\mu}\right)\Delta t} = \frac{1}{0.6} \qquad \Delta t = 45s \qquad [6.5]$$

The model proposed by Winckelmans takes into account several parameters of the aircraft and atmospheric conditions as well as turbulent viscosity. As it was the same aircraft flying at the same conditions, those parameters were considered to remain constant. It was in the definition of the viscosity turbulence model where the modifications were made. Remembering that expression, it involved a β constant, whose value was 8. This constant is the one that is modified to achieve the new value of the diffusion factor as it can be seen in equation 6.6.

$$\frac{r_c}{r_{c0}} = \sqrt{1 + \frac{4\lambda\upsilon}{r_{c0}^2}\left(1 + \frac{\mu_t}{\mu}\right)\Delta t} = \frac{1}{0.6} \quad \rightarrow \quad \frac{\mu_t}{\mu} = \frac{1}{\beta^*}\sqrt{\frac{C_L}{2ARb_0}}\sqrt{\frac{Ub}{\upsilon}} \quad \rightarrow \quad \beta^* \approx 2.7 \qquad [6.6]$$

Hence, the new value of the β constant is 2.7. Representing now both models, original and modified Winckelmans for the same flight and aircraft conditions, it can be seen that for the second one, the diffusion factor obtained is around 0.6 for the aging time of 45 seconds. Both representations are shown in figure 6.6, where the models are plotted for the same case as the one considered in the table 6.2 and figure 6.4.

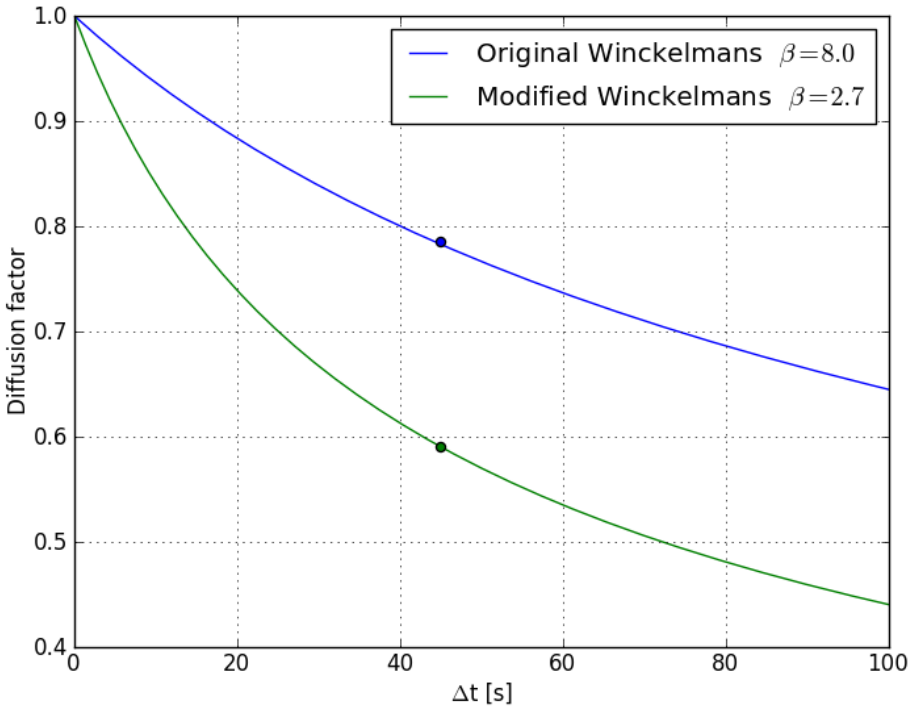

Figure 6.6 Comparison between vortex diffusion models

6.4. Application of modified diffusion model

Once the vortex diffusion model is modified to adapt the new diffusion factors, the next step consists of applying that modified model to numerical simulations and compare it with flight test results. In other words, the proposed modification of the diffusion model should be validated with flight test in order to assess its validity.

The procedure in this section is similar to the previous one where the three aging cases were adjusted and compared among them. The difference is that now instead of setting the diffusion factor manually, it is determined by the modified diffusion model applied to the corresponding flight parameters.

First, the results for the modified diffusion model only compared with flight test results are presented. It is important to note that the simulations for the modified diffusion model have been performed with different flight tests than the ones presented before, in order to assess the reliability of the proposed model. Figure 6.7 shows load results in sections of the aircraft tail (HTP and VTP).

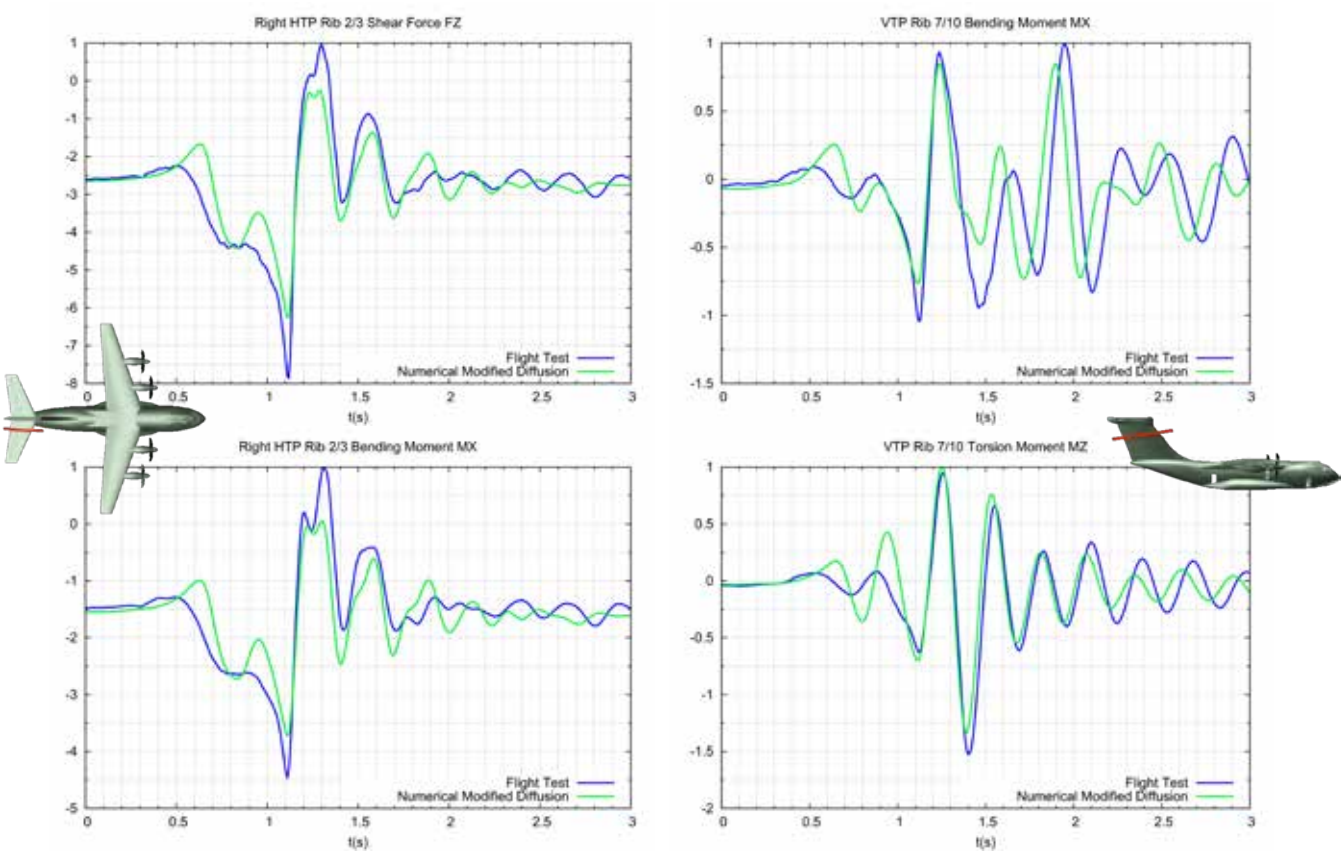

Figure 6.7 Numerical results for the modified diffusion model at HTP and VTP

In the same way, accelerations in those sections of the aircraft are also obtained for simulations where only vortex diffusion is considered as aging factor. They are presented in figure 6.8.

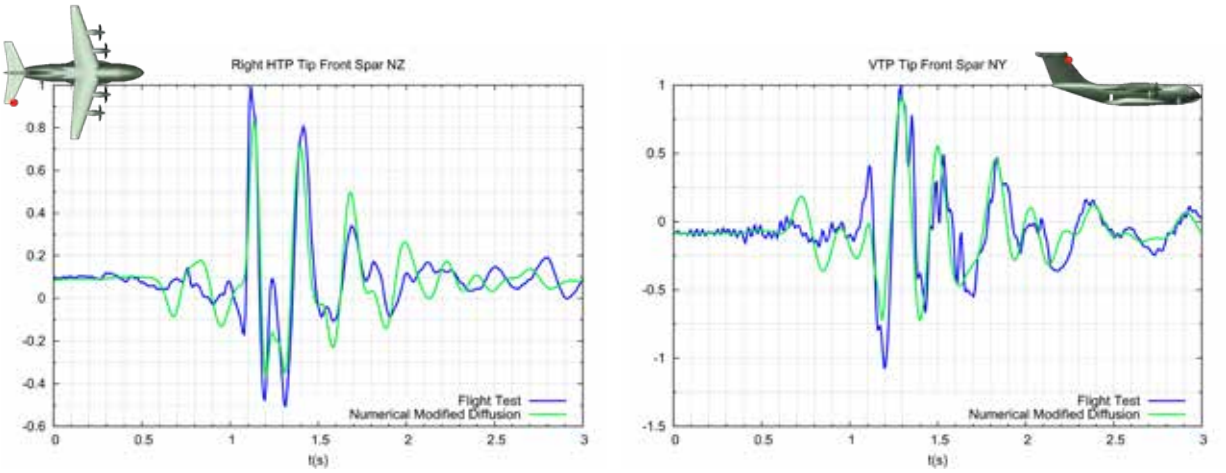

Figure 6.8 Numerical accelerations obtained using the modified diffusion model

The previous results showed a satisfactory agreement between numerical simulations and flight test results both in loads and accelerations. Therefore, the modified diffusion model could be reliable when applying only vortex diffusion to the wake model. However, it is important to compare that model with the other aging cases presented before in order to determine its complete response and behavior to the problem resolution. In that way, three aging cases as before are considered in the comparison with the modified diffusion. As before, the first is the nominal case considered by the department of Structural Dynamics in which only a decay factor of 0.8 is applied and no diffusion factor is involved. The second is a combined one that has a 0.8 decay factor but also includes a diffusion factor given by the original Winckelmans model. The last aging case is the proposed one in this study where no decay factor is applied and the modified diffusion model gives the value of the diffusion factor.

Focusing only in load results in the horizontal and vertical tail plane of the aircraft, the three aging models mentioned in the previous lines are executed for the same flight test case as the one in figures 6.7 and 6.8. The following figures 6.9 and 6.10 show an example of the loads obtained from the simulations with the different aging models. In them, it is possible to notice that both aging cases where diffusion is considered produce an improvement for the adjustment with the maximum peaks. The nominal case provided by the department is a conservative approach that overestimates the maximum load values in order to provide a safer design. Between the combined model with decay and diffusion and the proposed one with only diffusion, there are no relevant differences and both models are able to reproduce the same response. This is a consequence of the other important parameter of the analysis that should be taken into account, which are the distances at which the reference surface of the aircraft crosses the vortex line. These distance parameters seem to play an important role in the response to the event and they will be discussed in the next section.

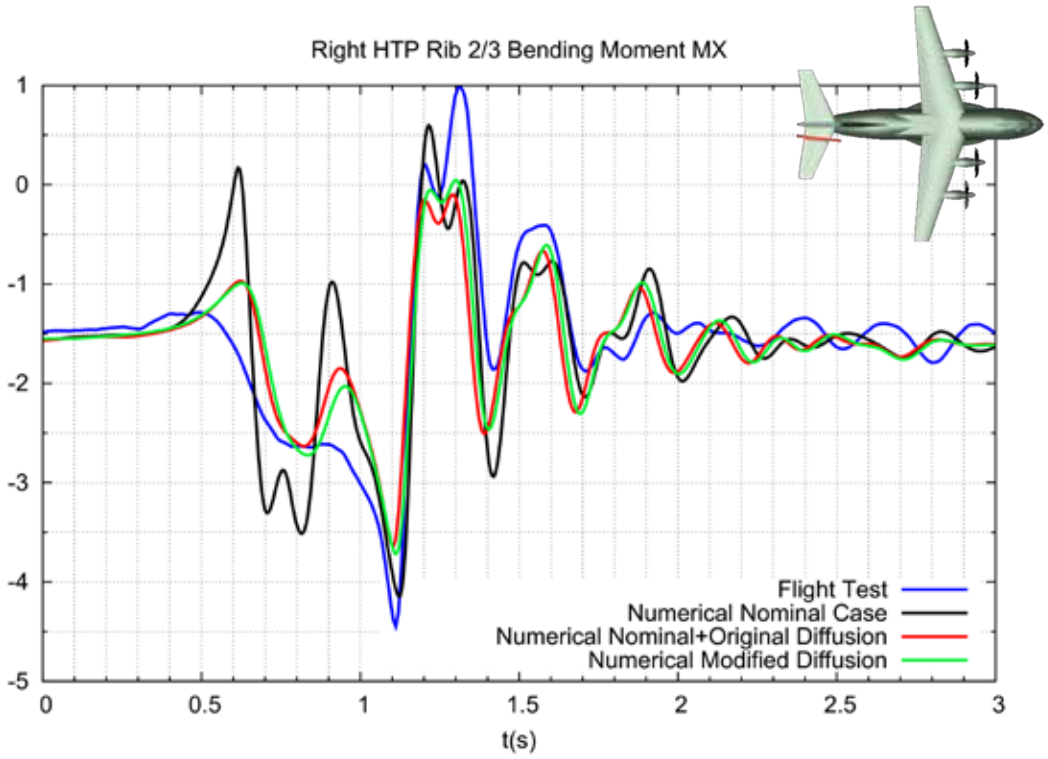

Figure 6.9 Comparison of HTP bending moment for different wake aging models

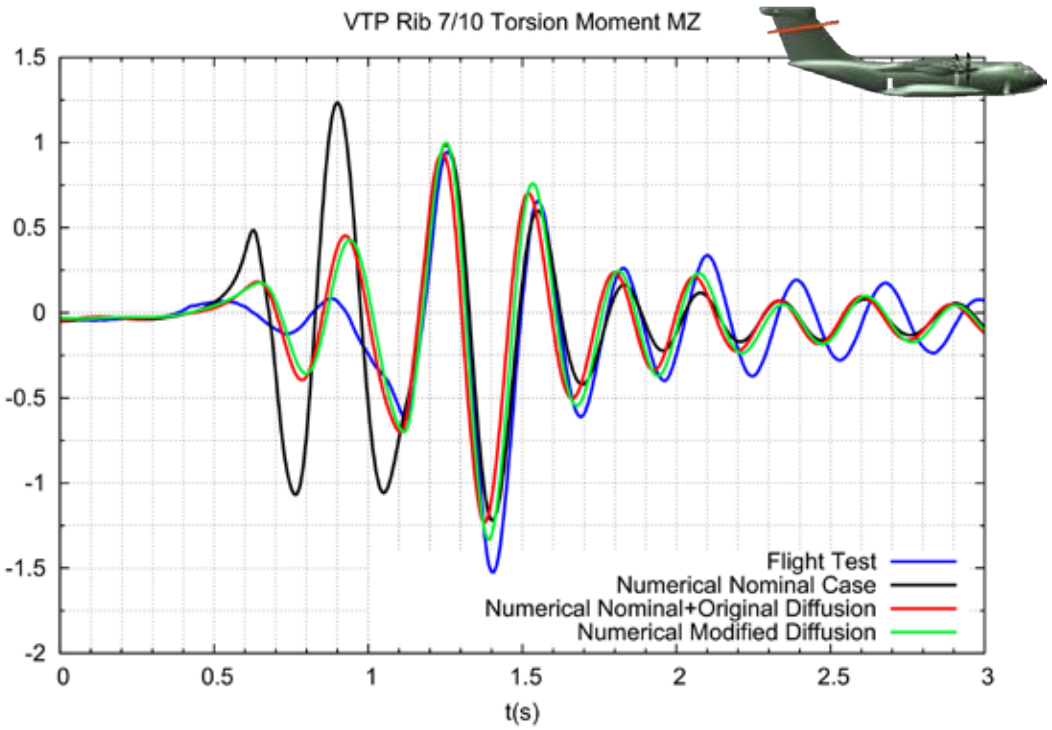

Figure 6.10 Comparison of VTP torsion moment for different wake aging models

6.5. Results discussion

In the previous figures, time histories for characteristic loads of the HTP and VTP obtained in the numerical simulations applying different wake aging models have been presented. All of them show acceptable behavior in the adjustment of the response to the wake encounter. Nevertheless, there is another unknown parameter of the event that should be also compared and understood. For that reason, it is presented a table and a figure similar to table 6.2 and figure 6.4 where the distances to the vortices, H1 and H2, are compared for the three aging models. Table 6.3 presents the numerical values while figure 6.11 shows a realistic visualization.

Table 6.3 Values for aging factors and distances to vortices

	Decay factor	***Diffusion factor***	H_1	H_2
Nominal case	0.80	1.0	+0.50	+0.50
Nominal + Original Diffusion	0.80	0.80	-4.00	+0.30
Modified Diffusion	1.00	0.60	-5.00	+0.50

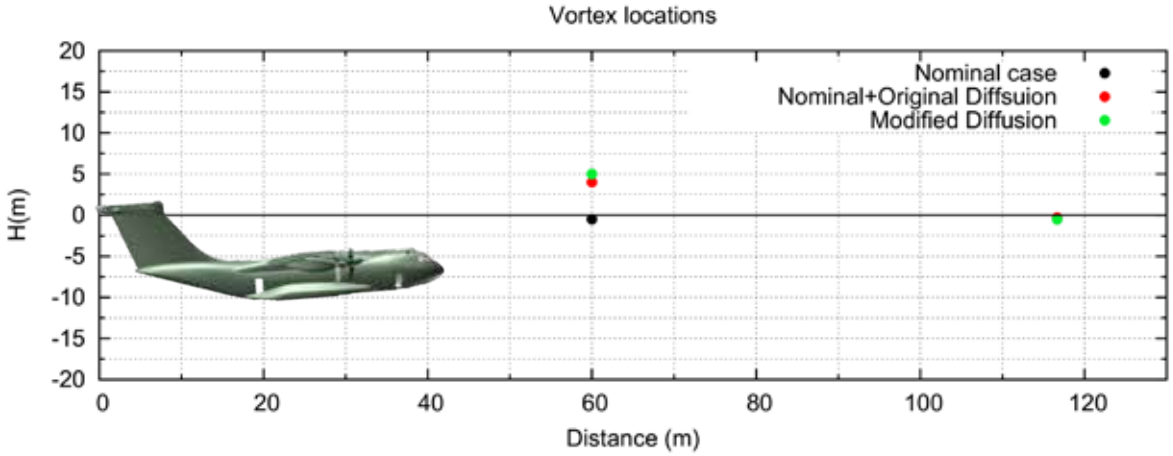

Figure 6.11 Vortex locations for different wake aging models

The previous values show the variation in the parameter of the distances to the vortices. The nominal case of wake aging used by Airbus Military considers a critical distance in order to be conservative with the load results. When other aging models are considered, the distances to the vortex changes considerably. With respect to the distance to the first vortex, the variation is larger than a factor of 5 times the nominal value. With these relevant differences, it is clear that a parameter such this, whose exact value is not known, has a key importance in the problem resolution.

Therefore, the analysis of the wake aging models has provided a few ideas about the wake model and its aging factors. First and most important is that the problem of the

wake aging is extremely complex and depends on several parameters difficult to determine as the atmospheric turbulence. Second, it is fair to think that there are two main mechanisms of wake degradation: the circulation decay and the vortex diffusion. These two mechanisms produce different effects on the induced velocity and the consequent excitation seen by the crossing aircraft. Both effects can be complementary and used for finer adjustments of maximum loads and peak responses.

Nevertheless, for a general adjustment between flight test results and numerical simulations, the most important parameter can be the distance from the vortex core center to the reference surface of the crossing aircraft. Since the exact value of that distance is not known for each encounter, this parameter should be iterated with good criterion to obtain a satisfactory adjustment. For the case when another wake model is applied, this distance is still unknown and could be modified adequately to achieve the same or, sometimes, better adjustments. Furthermore, the sensitivity of the response to the variation of the distance to vortices is much bigger than the one for the wake aging model. A small change in those distances produces an important variation in the output of the problem and modifies the load results significantly.

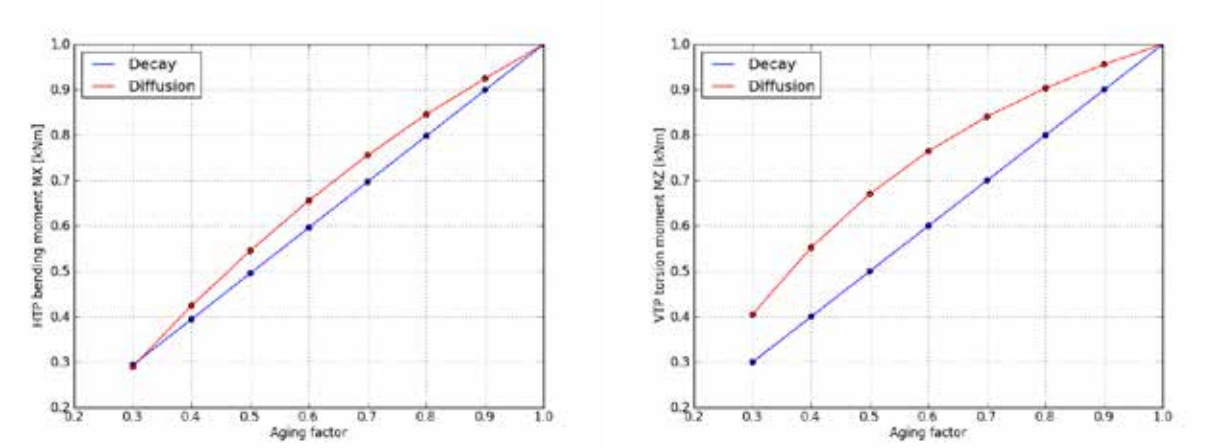

Figure 6.12 Sensitivity of load results in HTP and VTP to aging factors

As it is shown in figure 6.12, the effect of the decay factor is linear with the load results. Since it is a factor that multiplies the nominal circulation of the vortices, it affects the induced velocity in the same way. Hence, the excitation is proportionally reduced and the loads obtained follow that trend. The diffusion factor was based on a quadratic expression for the vortex radius growth. Therefore, the effect on the response is also quadratic. In figure 6.13, the sensitivity of the load results in the same areas of the aircraft to the distance to the first vortex, H1, is presented. It is relevant to remember that this parameter is the distance from the vortex center line to the reference surface of the aircraft. It can be appreciated that the behavior is now more severe, and that changes of small scale (~1-2m) produce significant variation in the loads generated in the aircraft. These scales are easily exceeded because the dimensions of the aircraft and the geometry of the encounter are much larger.

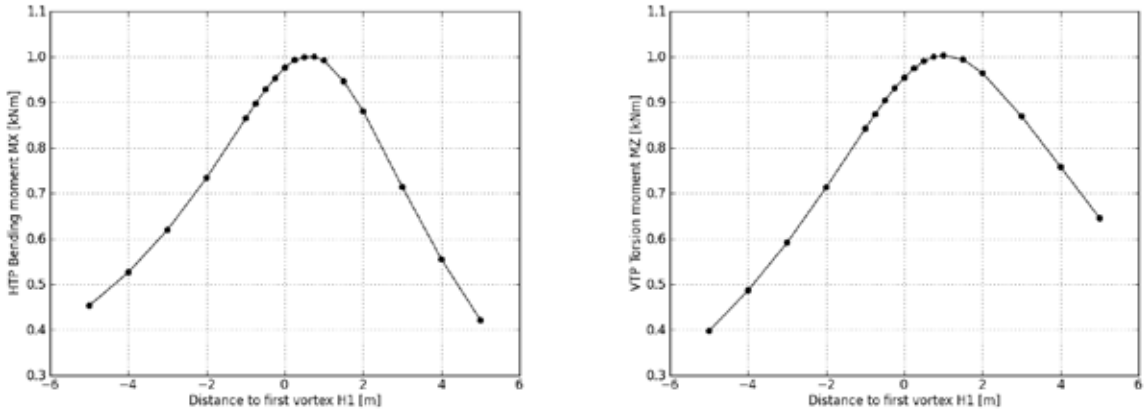

Figure 6.13 HTP and VTP loads sensitivity to crossing distance to first vortex

In conclusion, the wake aging models are necessary in the resolution of the wake vortex encounter problem since it is realistic to consider the wake degraded due to the time elapsed since its generation. However, there are also important variables that are relevant in the characterization of the encounter and they need further study.

Chapter 7

STOCHASTIC ANALYSIS OF WVE

7.1. Analysis objective

In the previous chapters some relevant aspects of the problem were presented, such as the methodology used in the numerical simulations, the validation with flight results and the models used both for the aircraft and the excitation. However, the loads induced in the aircraft structure by an event such as a wake vortex encounter are the valuable information in later studies or analysis. As it was mentioned in the first pages, a wake vortex encounter is an event that is not regulated by any Aviation Authority. Therefore, there is not any requirement or recommendation about this type of problem. In other scenarios such as discrete gusts, there is a clear specification about what conditions the aircraft structure must pass in order to get the approval. That is not the case about wake vortex encounter, so it is very difficult to derive a scenario for safety events.

Considering the previous reasons and the fact about the complexity of the problem definition, the solution proposed was to perform a stochastic analysis of this kind of event. A stochastic analysis consists of scattering the input parameters a high number of times and then collecting the output results. In that way, it is possible to obtain the characteristic behavior of the problem. The higher the number of analysis, the more accurate will be the obtained response of the problem.

In this case, the problem was very suitable to perform a stochastic analysis. There are several input parameters that define the problem and they are not precisely known. Computing many simulations of the problem where those parameters vary following a certain distribution, it is possible to obtain load results that have certain relevance in terms of probability. Therefore, the objective of the stochastic analysis is to obtain load results for a very wide range of the input parameters. In that way, the nonexistence of regulation is mitigated by an exhaustive number of simulations that cover all the possible events and are performed with software that has been satisfactorily validated.

7.2. Methodology

7.2.1. Generic procedure and tools

As in any other stochastic analysis, the procedure to follow starts defining the parameters that influence the analysis. Then, trying to determine how they behave, how are their values distributed within an expected range. Once the relevant parameters of the problem are defined, random shots of their values are performed

and all the computation loop of the problem is completed. Repeating that process as many times as possible produces useful levels of loads that can be analyzed for the characterization of the problem.

During the process of the stochastic analysis, a tool to help in the implementation of the problem was used. This tool is a software program called ST-ORM developed by CASA División Espacio. ST-ORM is an advanced Meta Computing tool programmed for performing stochastic analysis of generic physical problems. This tool helps to select a set of variables, which are known to scatter within a certain range of tolerance. Then, for each variable, pick 'randomly' a value from that range. After that, replace the value of each variable with the random one and execute the analysis. Finally, it extracts and stores the value of the response parameters of the system. These steps are repeated until significant statistics of the output parameters are obtained. This procedure of the tool was adapted to the problem of the wake vortex encounter and is presented in figure 7.1.

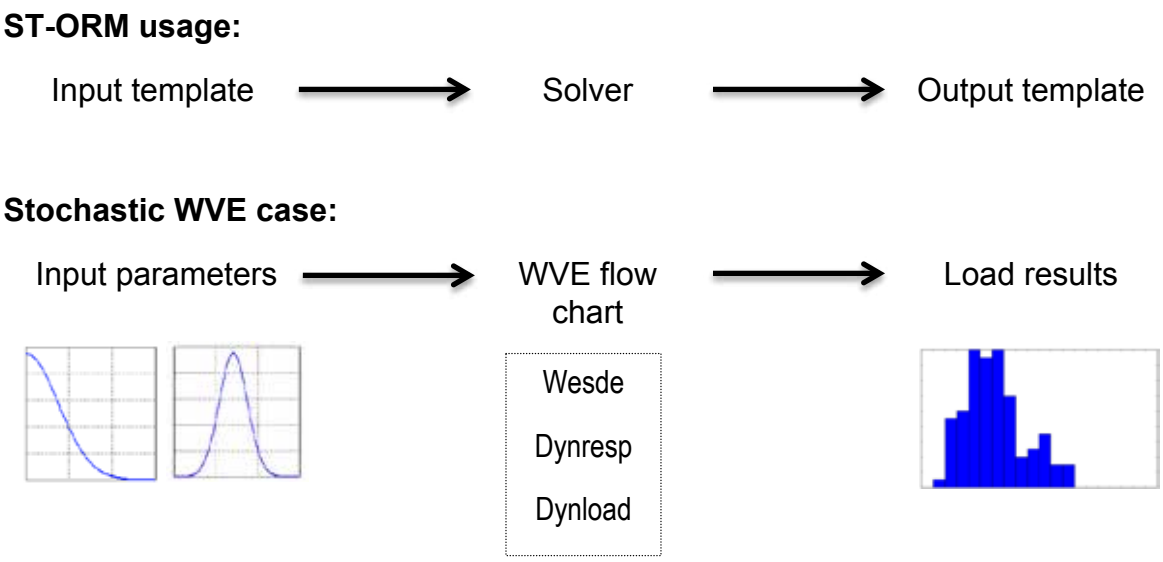

Figure 7.1 Procedure for the stochastic analysis

Having in mind that procedure, the main work is focused on determining the input parameters and their distributions. That is, how the 'random' values are going to be picked for each analysis. Understanding the probability distributions of those parameters is essential to implement a realistic problem in which the values of the inputs are the same as they may occur in a real event. Therefore, it was necessary to study again the variables of the problem and within what range they may vary.

After that, the core of the analysis is to execute the computation loop of the wake vortex problem in order to evaluate the problem with the values of the inputs assigned for each particular execution. This consisted mainly of programming the necessary instructions that the execution of all the software should follow each time. Essentially, the task was to put in contact the existent tools of the wake vortex encounter with the stochastic software ST-ORM that is the one in charge to assign the inputs. Once the execution of each stochastic shot is finished, the outputs

obtained are aircraft loads in the desired areas in order to evaluate the response of the aircraft to the excitation.

7.2.2. WVE problem application

In the process of application the wake vortex encounter problem to the stochastic analysis, it was necessary to define the event scenario that will be computed in each execution. For that reason, among the several possibilities of a wake encounter, particular ones that are considered significant for the problem were selected.

The first aspect to consider in the scenario definition is the aircraft and the maneuver that produces the encounter. In this study the aircraft was already presented and is the Airbus A400M. Regarding the type of encounter, it was considered to be an A400M crossing its own wake, in despite of other possibilities such as crossing other aircraft wakes. This implies that some of the parameters of the problem will be the same for both the leader and the crossing aircraft because they are the same.

Thus, there is an A400M crossing its own wake due to a turn maneuver. The next step is to select between the two types of encounters that could be defined. Remembering previous chapters, there were two definitions of crosses. When the reference surface of the aircraft is the wing root, that is the point where the distances to the vortices are referenced and it is called a ‘nose impact’. The other possibility is to take as reference the root of the horizontal tail plane. Then, that is the point considered to be the one to which the distances to the wake are measured. These are called ‘tail impacts’ and are the ones considered in this stochastic analysis. Since the aircraft tail was the area where more interesting loads are obtained, that was chosen to be the area of study. Therefore, the corresponding parameters of the distance to the vortex center will be referenced to the HTP surface of the aircraft.

The next points in the scenario definition are the parameters of the wake generation and encounter. Due the type of maneuver that is assumed, the leader aircraft is considered to have a certain load factor in order to represent the turn maneuver. That load factor will have influence in the nominal circulation of the vortex tubes of the wake model. Also, the load factor of the leader aircraft determines the orientation or bank angle of the turn maneuver. This orientation is related to the position of the vortices in the space. It is not the same if the wake is generated horizontally where both vortices are in the same horizontal position or if the wake is generated with a significant bank angle where each vortex will be at different heights. Then, the follower aircraft will enters the wake at a certain yaw angle, Ψ, and at 0º roll angle. The later is assumed for simplicity of the load calculations and further sensitivity studies will demonstrate that the crossing roll angle can be assumed to be null and then apply a correction probability factor. Finally, the wake model considered in this stochastic analysis is the same as the one considered by the Structural Dynamics department in previous computations. This wake model only considers circulation decay as aging mechanism and no diffusion effects. Therefore, each execution performed in this analysis will have its corresponding decay factor obtained from the model presented in section 5.3.1. This model considered the elapsed time since the wake generation that, for this case, will be the turning time of the maneuver and also

takes into account all the involved parameters such as the aircraft and flight conditions, load factor and atmospheric turbulence.

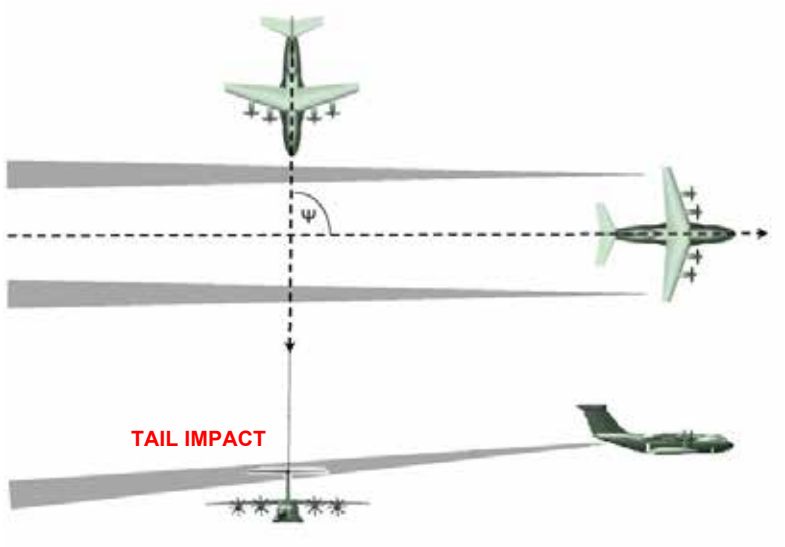

Figure 7.2 Scheme of the scenario for the stochastic analysis

Figure 7.2 shows the conditions of the tail impacts considered in the stochastic analysis. Summarizing all the mentioned before, the main characteristics of the considered scenario are:

- A400M aircraft crossing its own wake.
- Encounter takes place at the HTP/VTP reference distance (Tail impact).
- Leader aircraft: corresponding maneuvering load factor (vortices are generated at consequent heights)
- Follower aircraft: crossing wake vortex at horizontal position (0º roll)
- Wake model: only decay factor. No diffusion.

7.3. Input parameters

When the scenario for the analysis is defined, is is possible to go further in the stochastic analysis definition. Note that the first aspect to consider was to determine the inputs parameters of the problem. Those parameters are the relevant variables that define the problem and will be scattered within a range in order to serve as inputs.

Due to the conditions assumed for the analysis, where the aircraft crosses its own wake, there will be some parameters that are shared by both leader and follower aircrafts. Then there will be some inputs for the aircraft that generates the wake and other ones that are for the crossing aircraft alone. These variables will be deeper explained one at a time in the next sections. Now, as an introduction, table 7.1 summarizes the inputs parameters considered for performing the stochastic analysis. The general conditions of the flight and aircraft characteristics are the same for both aircraft because it is the same one crossing its own wake. Therefore, it is acceptable

to assume that both are flying at the same height and at the same speed. Also, aircraft parameters such as aircraft mass and flaps configurations are assumed to be the same for both of them. Regarding the leader aircraft, it is the one that generates the wake and starts the turning maneuver. Therefore, one of the input parameters considered for it is the load factor that is related to the bank angle and the turning maneuver and also defines the vertical distance between the two vortex tubes. This relation is treated deeply in section 7.3.2. There is also an input variable that determines the bank orientation. That is, at which side is the leader aircraft banked to perform the turn. The last input parameters are related to the crossing of the wake and, thus, the follower aircraft. First there is the vertical distance at which the first vortex is crossed. As tail impacts are considered, this distance will be measured from the center of the first vortex to the root of the horizontal tail plane (HTP). The other input parameter of the crossing configuration is the yaw angle. That is the angle relative to the course of the leader aircraft at which the follower enters the wake. These are the main input variables considered for the stochastic analysis of the wake vortex encounter. They are summarized in table 7.1 and will be treated more in deep in the following sections.

Table 7.1 Input parameters of the stochastic analysis

Both Aircrafts	• **Aircraft and flight point parameters**: Altitude, A/C speed, A/C mass, flaps configuration, etc. Obtained from *A400M fatigue missions*.
Generating A/C	• **NZ**: Load factor of the leader aircraft. This determines the position of the second vortex H2. • **Bank orientation**: Parameter set to define the orientation of the maneuver. It only has two options, right wing down and right wing up.
Crossing A/C	• **H1**: Distance in meters from the first vortex encountered to the checkpoint (HTP Root, tail impacts). • **Yaw angle**: crossing angle at which the following aircraft enters the wake. Ψ<90° means left wing first while Ψ>90º means right wing first.

7.3.1. Aircraft parameters and flight conditions

The first input parameters presented are the aircraft configuration and the flight conditions of the event. This will determine the characteristics of the flight, which are shared for both, leader and follower aircraft, due to the aspects of the encounter. Essentially, these variables consist of the aircraft characteristics in terms of mass state and flaps configuration and also the parameters defining the flight point, which are altitude and speed.

There were two possible approaches in the determination of the aircraft and flight variables. The first one was to choose a reduced number of mass configurations and flight points that are characteristic of the Airbus A400M life and perform the analysis with those values. The other approach was more ambitious. It involved the consideration of the entire fatigue life of the aircraft and it was the one chosen for the definition of the aircraft configuration and flight conditions parameters. The fatigue mission definition is a document provided by Airbus Military that gathers the characteristic life of the A400M. It defines the mission profiles the aircraft is more likely to perform, specifying how many flight cycles are of each mission type. Then every mission profile is exhaustively defined in each one of their flight stages from takeoff to landing. With the fatigue missions, the entire estimation of the aircraft configurations and flight conditions is covered for its whole service life. This gives a good approximation of what are the most likely flight points that the aircraft will be flying and what mass states are the most common for the A400M. For all these reasons, this was the chosen approach. Because it was not limited to a reduced number of aircraft weights, altitudes and speeds, and instead, the entire range of those variables is included as input parameters for the stochastic analysis.

The first aspect of the fatigue missions of the A400M is the definition of the different mission types. In this case, four mission profiles are defined that correspond to two logistic missions, one long and other short, which are mainly a flight between two points, a tactical mission for military operations, and a training mission for pilot preparation and practice. Each one of the four profiles has defined a mission duration time and a number of cycles, which is the number of times that the aircraft perform that mission. Multiplying the duration of each mission type by the number of cycles, the total number of hours that the aircraft spend in that mission profile is obtained. Then comparing that number to the total number of hours of the aircraft life, it is possible to produce a histogram of probability of each mission type. This can be seen in figure 7.3 where the number of hours of each mission type for 1000 flight hours is represented.

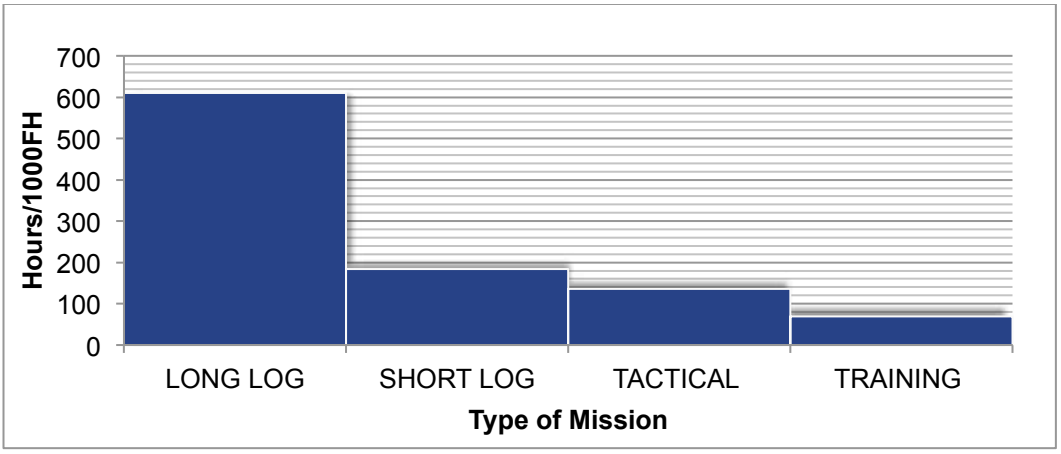

Figure 7.3 Number of flight hours for each mission profile

As expected, the most probable types are the logistic ones due to their long duration. This means that, considering the entire life of the aircraft, most of the time, it will be performing a logistic mission. In order to introduce this variable into the analysis, it

was necessary to adapt these values to the specific problem of the wake vortex encounter. The logistic missions are the most probable in the operation life of the aircraft. However, since the scenario considered is a crossing with its own wake, it is not realistic to have a higher number of analyses executed for the logistics missions. In other words, it is more likely to have a wake vortex encounter in a tactical or in a training mission where the mission profile has more variability. In a logistic mission where the aircraft takes-off, climbs, flights a long cruise stage and finally lands, it is more difficult to have a turn that produces a wake self encounter. For that reason, it is proposed a correction factor that is applied to the mission types in order to provide a larger weight to the tactical and training missions, where the event studied is more likely to occur. Table 7.2 shows the factor applied to each type of mission; it establishes a factor of 1 for the long logistic missions, where it is very improbable to have an event. Then the short logistic flights are multiplied by 2, the tactical missions by a factor of 4 and the training ones by a factor of 8. In this way, the original distribution of hours for each mission type is weighted for consequent factors that give more importance to the missions that are more likely to induce a wake encounter.

Table 7.2 Weighting factor applied to mission types

Mission profile	WVE weight factor
Long Logistic	1
Short Logistic	2
Tactical	4
Training	8

After the application of the WVE weighting factor to the mission types, the distribution of the mission profiles is more uniform because the less frequent missions (tactical and training) are the ones with higher factors for wake encounter likeliness. The procedure for applying that factor consists of multiplying the number of hours for each mission profile for the corresponding weighting value. Following that, the resulting distribution for the four different mission types is presented in figure 7.4.

Figure 7.4 Distribution of mission profiles after wake encounter weighting factor

In that figure, the weighted values for the mission profiles distribution are showed. Then, the probability distribution that best fits that values and which is the one introduced in the tool ST-ORM is presented. This probability distribution is the one used by the tool when picking the values for each execution. Finally, in grey color, the values obtained after the assignation of values made by ST-ORM as an example of 1000 random shots are shown. It can be observed that the assignation assembles satisfactorily to the considered values for the mission profiles. Therefore, the first input variable for the stochastic analysis will be the type of mission in which the aircraft is flying. That variable has been approximated using real data of the missions of the aircraft and it has been validated to present the same distribution after the assignation made in the stochastic tool.

After the determination of the previous variable of mission type, the next input variable will be the flight stage of that mission profile in which the aircraft is flying. That flight stage will determine the aircraft weight and mass state, the flaps configuration and the flight conditions such as altitude and velocity. The specific profile of each mission type is defined in the fatigue missions' document of the aircraft and the particular values of the flight stages are omitted in this document due to confidentially issues. Essentially, the mission profiles are defined from takeoff to landing thorough several flight stages. As an example for a logistic mission, the takeoff and climb stages are defined in a number of segments in which the aircraft takes off and then gains speed and altitude. Once the cruise conditions are reached, the cruise segment is defined with the corresponding altitude and speeds. Finally, the descent approach and landing phases of the mission are defined in a similar way. This procedure is repeated for the four mission profiles and a symbolic example is shown in table 7.3.

Table 7.3 Example of a symbolic mission profile definition

	MASS (kg)	**Flaps**	**Z (ft)**	**KCAS**	**M**	**ρ**	**Time (min)**
TAKE-OFF	mass1	20º	H1	V1	M1	ρ1	T1
	mass1	20º	H2	V2	M2	ρ2	T2
CLIMB	mass2	0º	H3	V3	M3	ρ3	T3
	mass3	0º	H4	V4	M4	ρ4	T4
CRUISE	mass3	0º	H5	V5	M5	ρ5	T5
DESCENT	mass4	0º	H6	V6	M6	ρ6	T6
	mass4	0º	H7	V7	M7	ρ7	T7
APPROACH & LANDING	mass4	40º	H8	V8	M8	ρ8	T8
	mass5	40º	H9	V9	M9	ρ9	T9
	mass5	40º	H10	V10	M10	ρ10	10

As can be seen in the example of table 7.3 the mission profiles have several flight stages and within them, different segments that determine the aircraft configuration and flight conditions are defined. The proposed idea to use these definitions was to create another input variable that is the flight segment. This will determine the desired parameters of the aircraft and the flight. Therefore, this variable will be 'randomly' picked among its possible range depending on the time spend in each one of them, in a similar way carried out for the mission type variable. For instance, if a particular mission profile has 20 flight segments, the corresponding stochastic variable will take values between 1 and 20 and the probability of each one will be determined by the duration of each segment over the total time of the mission.

After that, the task consists of determining the histogram of segment times for each mission profile. Then, adjust a probability distribution so that the stochastic tool ST-ORM can pick the values of the segment variables accordingly to the real values. The first histograms of the flight segments showed that the cruise segments of the mission were considerably longer in duration than the other ones. Hence, it was particularly difficult to fit a predefined probability distribution such as a Gaussian distribution as it is shown in figure 7.5.

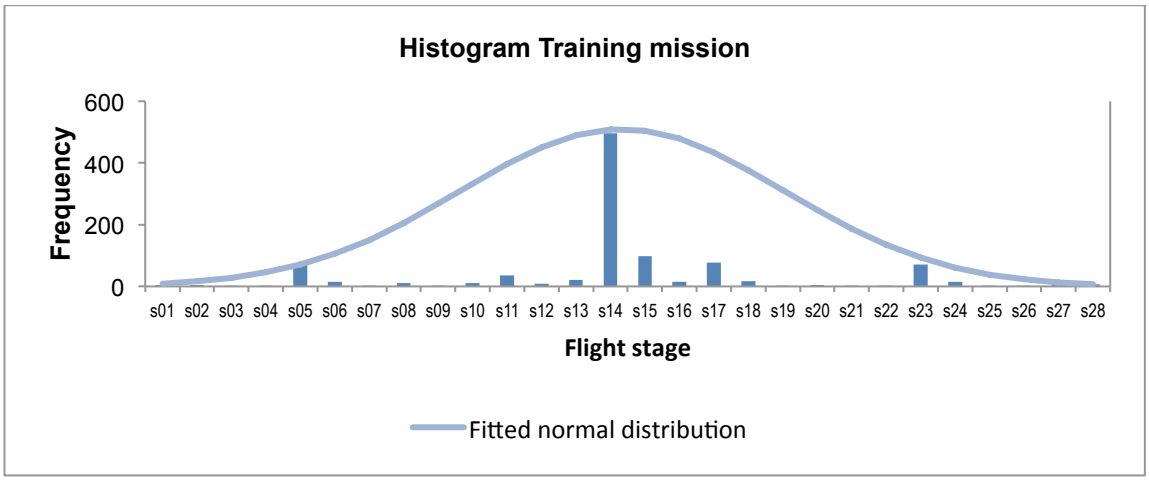

Figure 7.5 Example of flight segment distribution for a training mission

Considering the previous figure, it is clear that the distribution obtained is far from a Gaussian one and the cruise stage is more frequent in time that the other ones due to its long duration. After seeing that, the proposed solution was to eliminate the cruise segment of the mission profiles to have a neater histogram for the flight segments. This was assumed because it was very unlikely to have a wake vortex self encounter in a cruise segment. The suppression of the cruise segment involves the posterior treatment in the probability factors. Since the cruise segments of the four mission profiles last more than the 50% ($0.5=5\cdot10^{-1}$) of the total time, a factor of 10^{-1} was proposed for later application to the results probability.

Thus, the procedure involved the elimination of the cruise segments from the total number of segments and then sorting the rest of the flight stages in order to obtain the closer to a normal distribution. When the cruise segment is removed the rest of the stages have similar durations. Therefore, instead of having them in order from first to the last, the idea is to have a variable from 1 to 25 for example but each value

corresponds to different flight stages. That is to say, that the value 1 of the stochastic variable corresponds to the segment 6 of the real mission profile. In that way, the histograms obtained for the flight stages without the cruise segment can be adjusted by a Gaussian distribution that will determine the value for that variable assigned by ST-ORM in each execution.

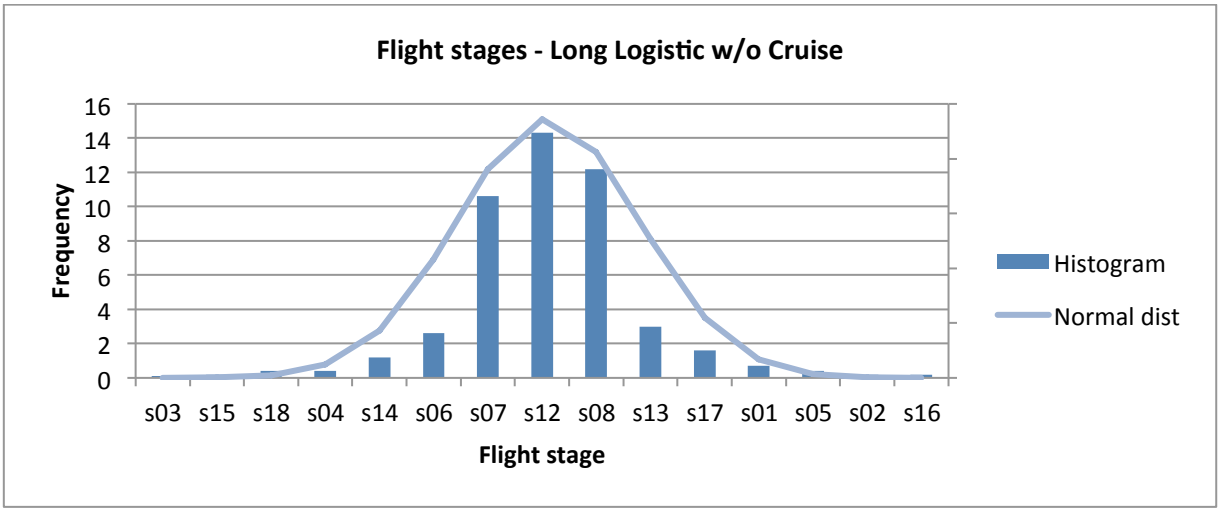

Figure 7.6 Histogram LL

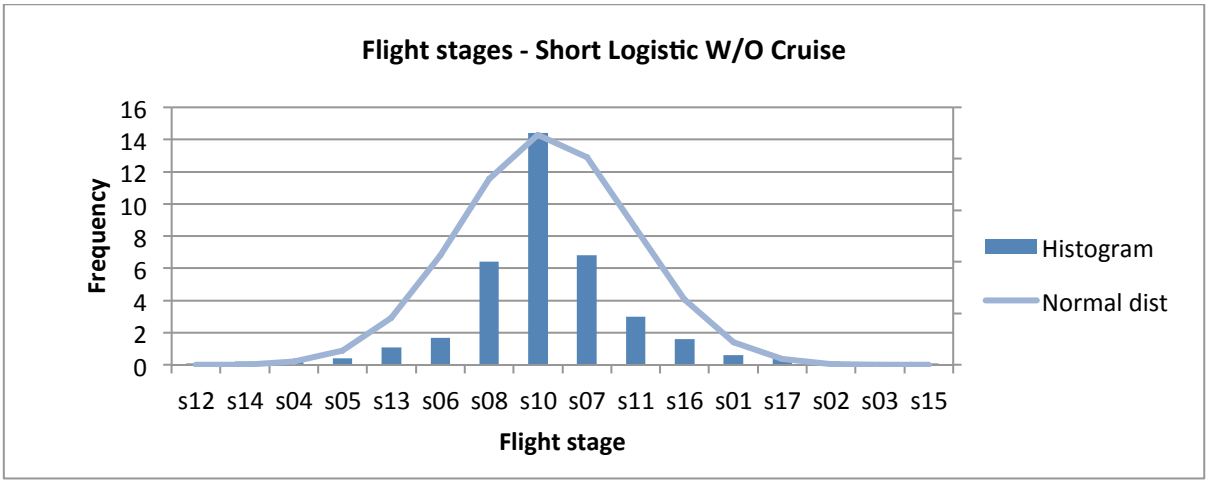

Figure 7.7 Histogram SL

Figures 7.6 to 7.9 show the histograms for the flight stages of each one of the mission profiles with their corresponding normal distributions adjusted with that data. It can be observed that now the adjustment is more representative and do not present the incoherencies of the previous one with the cruise segment. With that, the next input parameter of the stochastic analysis will be the flight segment at which both aircrafts are flying. This variable will follow its corresponding distribution depending on the type of mission assigned by the previous variable for each execution. Table 7.4 shows the ranges of the flight segment variables and the parameters of the normal distributions fitted for each mission profile.

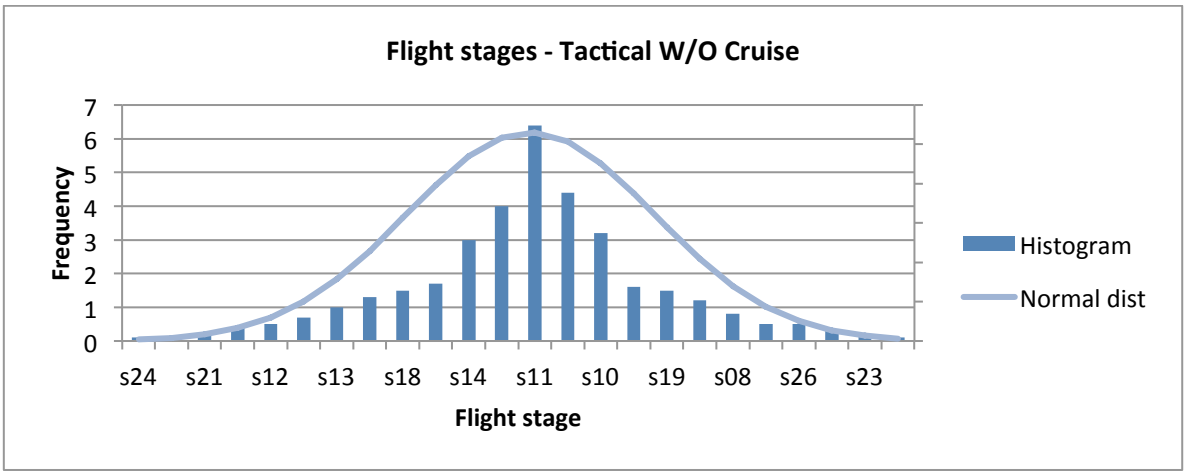

Figure 7.8 Histogram TC

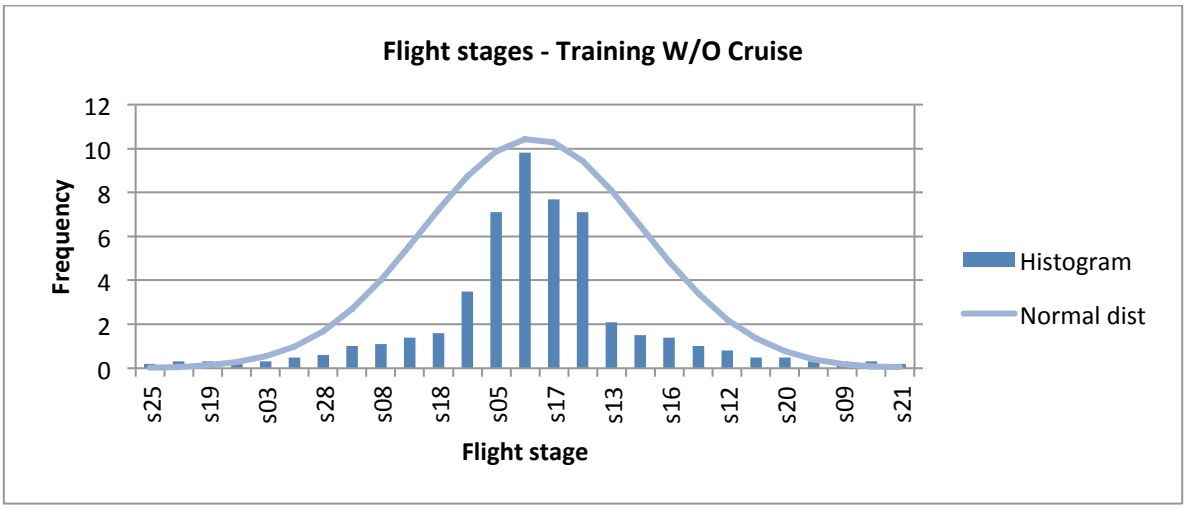

Figure 7.9 Histogram TR

Table 7.4 Summary of the flight segment variables and their probability distributions

	Range values	Mean value μ	Standard deviation σ
Long Logistic	[1 – 15]	8.1	1.7
Short Logistic	[1 – 16]	8.2	1.8
Tactical	[1 – 24]	12.9	3.7
Training	[1 – 27]	14.3	3.8

After all the explained in this section, the first input parameters of the stochastic analysis have been defined. They are two variables, one for the mission type and the other for the flight stage. When these two variables are selected within its range following the corresponding probability distribution, the aircraft configuration in terms of weights and flaps and the flight conditions, altitude and speed, are completely determined. These are the characteristics shared by both aircraft, leader and

follower, in the wake encounter due to the assumptions made for this stochastic analysis.

7.3.2. Load factor nz

The next type of input parameters of the analysis is the leader aircraft depending variables. After the determination of the flight conditions and aircraft parameters that both aircraft share, the leader aircraft defines the following input variables and they influence the wake generation.

The first variable to consider is the load factor of the leader aircraft. Remembering basic knowledge of flight mechanics the load factor is the relation between lift and weight of the aircraft. Therefore, it is related to the bank angle of the coordinated turn maneuver. A coordinated turn is a maneuver where the aircraft perform a turn at a constant inclination (bank angle, ϕ) and at a constant speed. Performing basic operations, it is showed that the load factor is related to the bank angle with the following expression:

$$nz = \frac{1}{\cos\phi} \qquad [7.1]$$

Considering the current scenario for this analysis, the load factor of the leader aircraft will determine the turning maneuver to be performed. The inclination of the maneuver determines the position at which the wake vortices are generated as can be seen in figure 7.10. Starting from that inclination, it is possible to obtain the vertical distance between the two vortices using basic geometry. Then, knowing the crossing vertical distance to the first vortex, the second one is also known. Another aspect influenced by the load factor is the vortex circulation. Remembering the expression of the circulation, the load factor was directly proportional. Thus, the higher the load factor (greater bank angle), the higher the circulation of the vortex tubes of the wake.

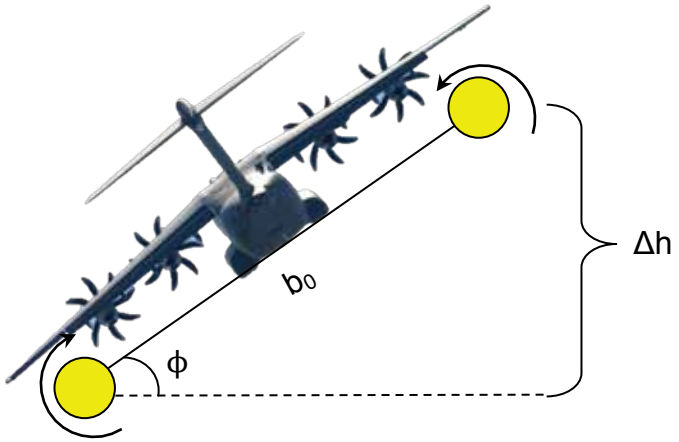

Figure 7.10 Vortices position due to the turning maneuver

In order to determine the distribution of the load factor variable, the documentation of the fatigue life of the Airbus A400M was used. In that, there is provided data of load factor occurrences for each of the four mission profiles of the aircraft. Essentially, there is an experimental expression that gives the total occurrences for different types of maneuvers. Applying them, histograms for load factor occurrences for the four mission types are obtained. All the values vary within the admissible range of load factors, which starts at 1.0 (horizontal) to the maximum load factor that is 2.5 for the logistic and training missions and 3.0 for the tactical ones.

The procedure to include that variable in the analysis is similar as the previous ones. The histograms are adjusted with defined probability distributions in order to give them to the stochastic tool ST-ORM. Figure 7.11 shows the data of load factor occurrences for a particular mission profile. As can be seen, the behavior of the distribution is linear in a logarithmic scale. Therefore, representing the data in a linear scale, the distribution that can be fitted to the obtained values is an exponential distribution as in figure 7.12.

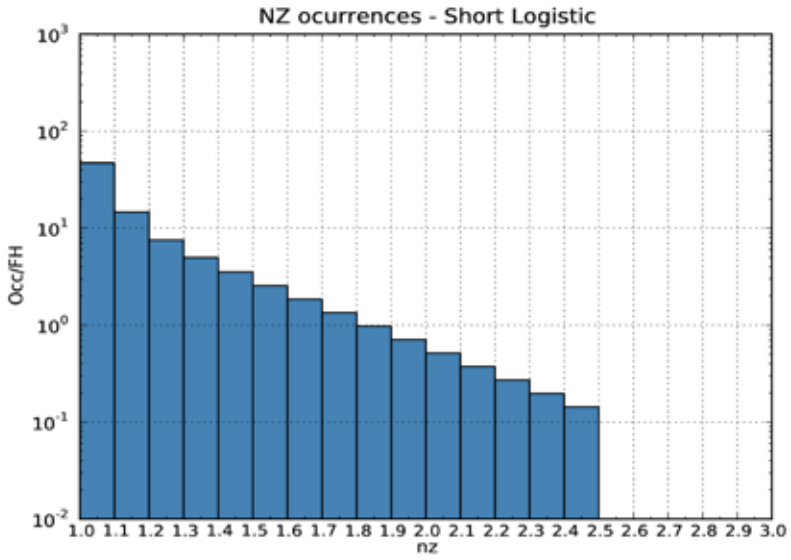

Figure 7.11 Load factor occurrences for short logistic missions

This procedure of adjustment is repeated for the four types of mission profiles. These are the next input parameters that the stochastic tool will assign at each execution. Therefore, after the determination of the first input variables, the next one to be considered in the analysis is the load factor of the leader aircraft. This load factor follows an exponential distribution for the four mission types where the higher values are much less probable to occur. Thus, the assignation of the value for the load factor by the stochastic tool will depend on the mission profile and the corresponding exponential distribution of each one.

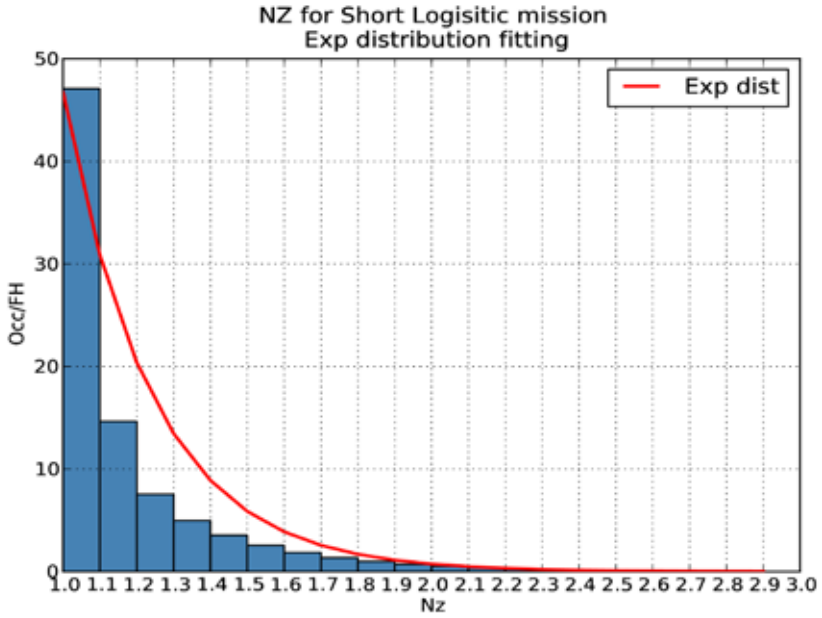

Figure 7.12 Example of exponential distribution adjusted to values of load factor

Finally, as a summary, the following table collects the admissible ranges of the load factor for each mission profile and the main parameter of the fitted exponential distribution. Equation 7.2 shows the expressions of the probability density function and variance of an exponential distribution.

Table 7.5 Relevant values for load factor distributions

	Load factor range	**λ parameter**
Long Logistic	[1.0 – 2.5]	4.64
Short Logisitc	[1.0 – 2.5]	4.15
Tactical	[1.0 – 3.0]	4.24
Training	[1.0 – 2.5]	3.63

$$f_X(x) = \lambda e^{-\lambda x} \qquad Var(X) = 1/\lambda^2 \qquad [7.2]$$

7.3.3. Bank orientation

Another important variable to consider in the definition of input parameters is the orientation of the maneuver. There are two possibilities for the turning maneuver; turn to the right or to the left. The previous two will produce a different configuration of the aircraft. Using the sign convention of flight mechanics, a turn to the right of the course is produced by the right wing from the pilot perspective going down and the left wing going up. The opposite configuration, right wing up and left wing down, gives the opposite maneuver.

This fact is important to be considered in the analysis due to the vortices position. As said before, the turning maneuver will give the vertical position of the vortex tubes in the space. Considering the reference distance to the first vortex, each configuration will produce different vertical distances for the second vortex. Depending on the orientation of the maneuver, the second vortex is placed below or above the first one. A scheme of both orientations is showed in figure 7.13.

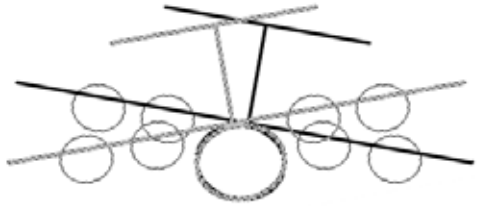

Figure 7.13 Scheme of turning maneuver orientation

This parameter is included in the analysis as a simple variable with only two possible values 1 and 2. Each value corresponds to each one of the possible turning orientations. Since there is no real data for this parameter, the probability assigned to each value is a uniform distribution where all the values have the same probability of occurrence, in this case, 50%.

7.3.4. Distance to first vortex H1

Regarding the follower aircraft, there are some geometrical parameters of its flight that define the wake encounter. The first of those parameters is the vertical distance from the first vortex center to the reference surface of the aircraft that in this case is the horizontal tail plane root. A scheme of the geometry assumed for the analysis can be seen in figure 7.14.

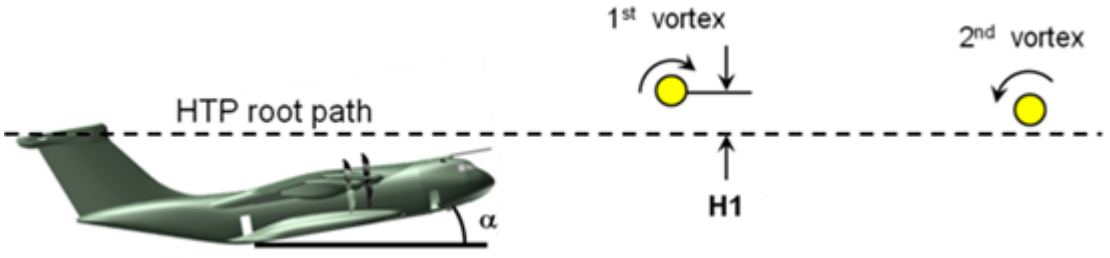

Figure 7.14 Outline of the encounter vertical geometry

Considering that scenario, the parameter that will be varied in the stochastic analysis is the distance H1. Once that variable is fixed, the other H2 is also known using the load factor and maneuver characteristics as it is explained in the previous section. The main decision was to establish a feasible range for the H1 in order to represent

possible wake encounters. The first attempt was to set a small range close to the vortex center in order to capture only the relevant shots where significant loads were obtained. However using this approach, there were some cases that were not considered. Such cases that, given the vortex position due to bank angle configuration, the follower aircraft crosses far from the first vortex but closer to the second one. This effect is showed in figure 7.15 where are plotted the H1 versus the distance to the second vortex, H2. It can be seen that for lager values of H1, there are some shots that are very close to the center of the second vortex.

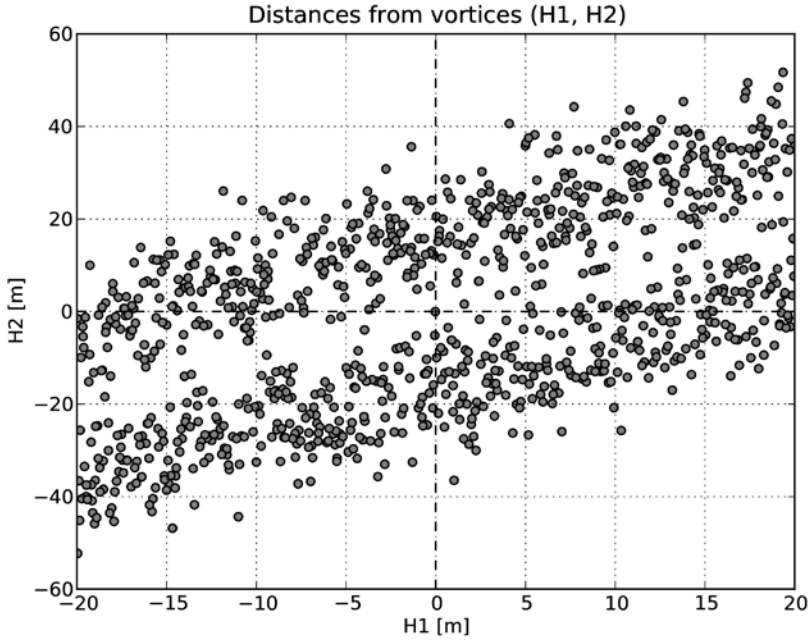

Figure 7.15 Distance to the second vortex H2 as a function of H1

Taking into account the previous fact, the range of the values for H1 was extended to ±20 m. In this way, the possibilities that the aircraft crosses far from the first vortex but relatively close to the second one were also included in the stochastic analysis. The behavior of this variable is assumed to be constant. Therefore, a uniform distribution is assumed for the H1 variable where all the possible values have the same probability of occurrence. Figure 7.16 shows a representation of the probability distribution for H1.

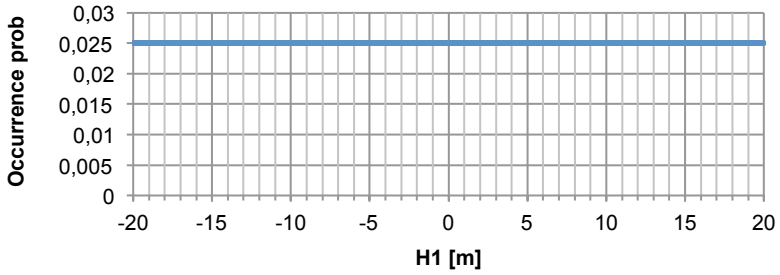

Figure 7.16 H1 probability distribution

7.3.5. Yaw angle Ψ

The last of the parameters of the follower aircraft and also of the input variables is the yaw angle at which the aircraft crosses the wake. This variable completes the definition of the geometry of the wake encounter as it was presented in section 3.3 where it was treated the geometry definition of the event. This yaw angle have influence in the excitation seen by the aircraft as flying through the wake and, hence, in the load response itself.

In order to consider the majority of the possibilities this parameter is assumed to be arbitrary. Therefore, its distribution is also uniform where all the possible values have the same probability of occurrence, as it was the case for H1. The only remaining aspect was to determine the range of admissible values for the yaw angle. Instead of sweeping the 180º of possible crossing angles, some limits were imposed to ensure a non-parallel crossing that could induce numerical problems in its resolution. For these reason, it was set the range between 15º and 165º for the yaw angle. It is important to remember that values below 90º means that the left wing of the follower aircraft enters the wake in first place while angles greater than that, gives an encounter where the right wing enters first. This makes sense with the definition of the crossing angle made in the software for computing the excitation (WESDE). Summarizing, the yaw angle will vary between 15º and 165º where all the values have the same probability of occurrence. This means a uniform distribution similar to the case of the first distance, H1. Figure 7.17 shows the outline of the variation for the yaw angle parameter considered in this stochastic analysis.

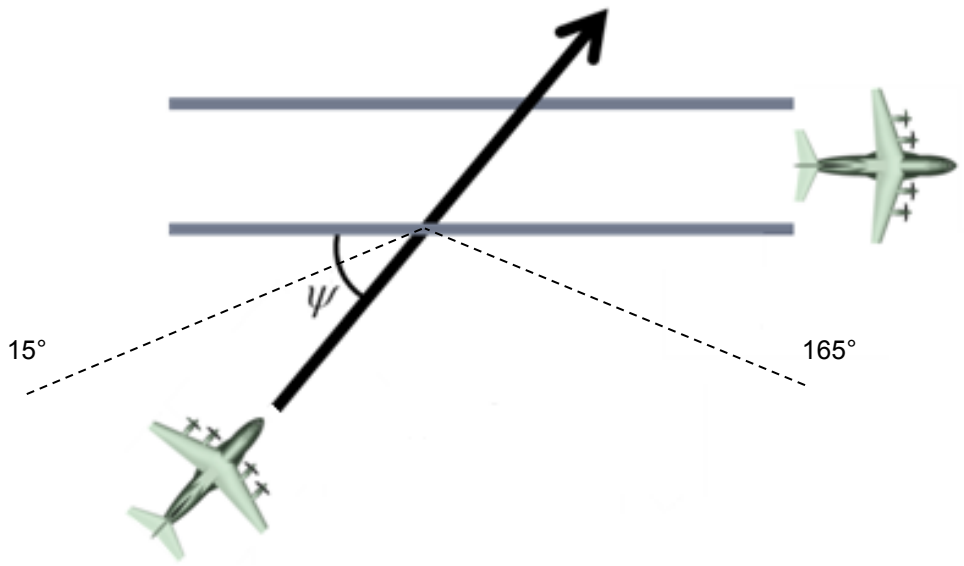

Figure 7.17 Outline of yaw angle variation

7.4. Output results

Once the main characteristics of the analysis have been defined in the input parameters definition, the following consideration are focused on explaining and analyzing the output results obtained from that analysis. Since it is a stochastic analysis where several executions of the same problem have been computed, the type of outputs will be in the sense of gathering the statistical behavior of the results. For that reason, three main types of outputs can be obtained and they will be treated separately in the following sections.

It is important to remark the characteristic areas of the aircraft where the load outputs are going to be computed. As presented in the scenario configuration, the types of encounters treated in the analysis are tail impacts where the reference surface of the plane is the horizontal tail plane. Therefore, the monitoring stations considered for computing integrated loads will be focused only in the rear part of the aircraft. Those monitoring stations are located in the vertical tail plane and in the horizontal tail plane. Considering that, the results presented in the stochastic analysis are all about HTP and VTP integrated loads and moments.

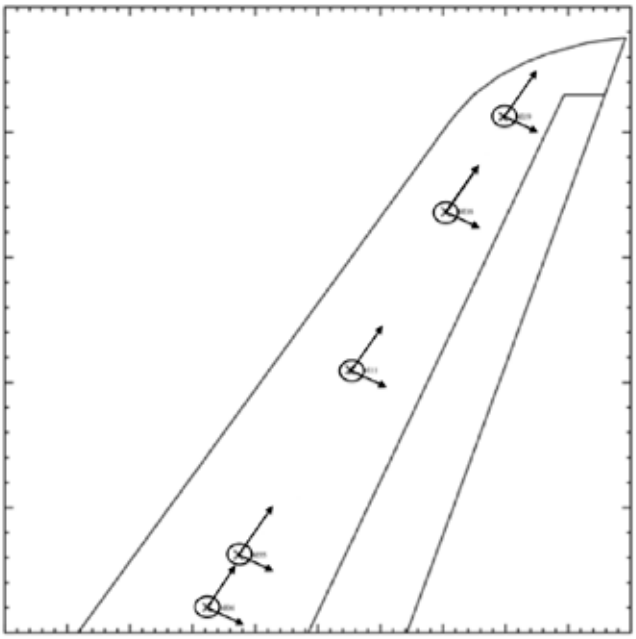

Figure 7.18 HTP monitoring stations for load computations

Figures 7.18 and 7.19 show the location of the monitoring stations considered in the analysis where the six components of loads (forces and moments) will be integrated and computed in each execution. It can be seen that there are 5 monitoring stations in the horizontal tail plane distributed from root to tip and for the surfaces of both sides. For the VTP is considered a similar arrangement, having 4 monitoring stations capturing the loads at those four sections of the surface. They are located also distributed from root to tip of the VTP.

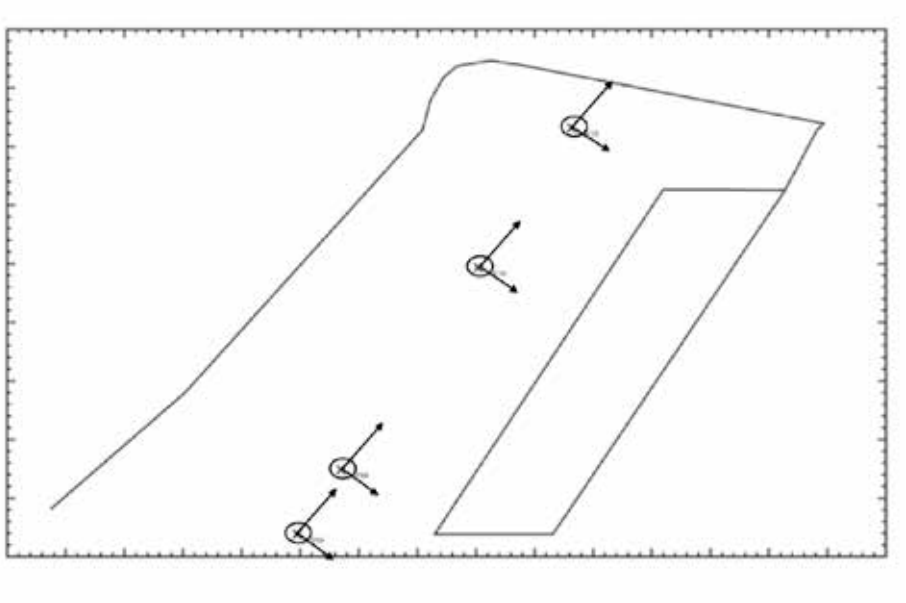

Figure 7.19 VTP monitoring stations for load calculations

Therefore, the six load components (3 forces and 3 moments) at each one of these sections of the HTP and VTP will be the outputs of this stochastic analysis. With those outputs, different kinds of post-processing tools can be obtained and they are treated in the following sections. Essentially, they can be classified in three categories: histograms of the load results, stochastic envelopes where the individual 2D envelopes are combined in a major one considering all the number of shots, and ant-hill plot where any load component is plotted against an input variable to represent its dependency.

7.4.1. Histograms

The first type of statistical output of the stochastic analysis is the histogram. This is a representation of the frequency of occurrence of a variable within its assumable range. Between the maximum and minimum values of a variable, a certain number of bins are considered and each bin represents the number of occurrences of that variable for the range of the particular bin. Histograms are a very used tool in statistical and population representations.

The idea is to represent all the results of a certain force or moment of a monitoring station in order to see its behavior and the most probable values of the results. Along with the histogram, it is possible to add the values of the maximum assumable loads in order to have an idea of the number of analysis that exceeds the maximum value. An example of histogram is shown in figure 7.20 where it can be seen the bins for the corresponding range normalized to the admissible values of maximum loads.

The information obtained from these outputs is mainly to verify that the results are coherent with the expected values and there is not any peculiarity or non-sense. It is difficult to relate the hazardous analysis with the maximum reference value for that

variable. Often, it is more suitable to use the 2D envelopes were two magnitude are plotted one against the other. These gives more information because it is possible to have a combination of two components that produces exceed levels that is not seen in a plain histogram of 1 variable. For that reason, those last are the outputs that will be used in the majority of the analysis of the results.

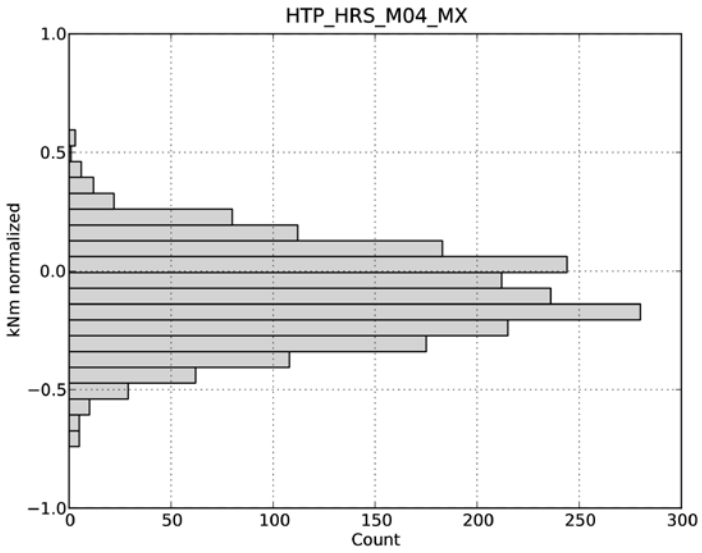

Figure 7.20 Example of histogram for the bending moment MX at HTP root

7.4.2. Stochastic envelopes

The next type of output obtained in the stochastic analysis is the total envelope of all the particular 2D envelopes obtained in each execution. In this study, this total envelope is called stochastic envelope because it represents the combination of all the singular 2D envelopes and provides information of the total number of shots of the analysis. This type of representation was explained in section 3.5 and is one of the possibilities that allows DYNLOAD in the computation and post-processing of integrated loads. Essentially is the combination of two time-histories of different load components where the time has been eliminated between the two and one magnitude is plotted against the other.

The software DYNLOAD also allows the possibility of obtaining such stochastic envelopes. In one of its modules, it has the option of computation the total 2D envelope of several 2D envelopes. Therefore, the procedure is to select all the 2D envelopes obtained for each run of a particular number of executions to combine all of them in a single total envelope. Figure 7.21 presents an example of this kind of envelope where there are different 2D envelopes of different executions plotted and the total envelope is plotted in red. This total envelope gathers all the maximums of its participants. The same procedure is repeated for a higher number of shots performed in the stochastic analysis.

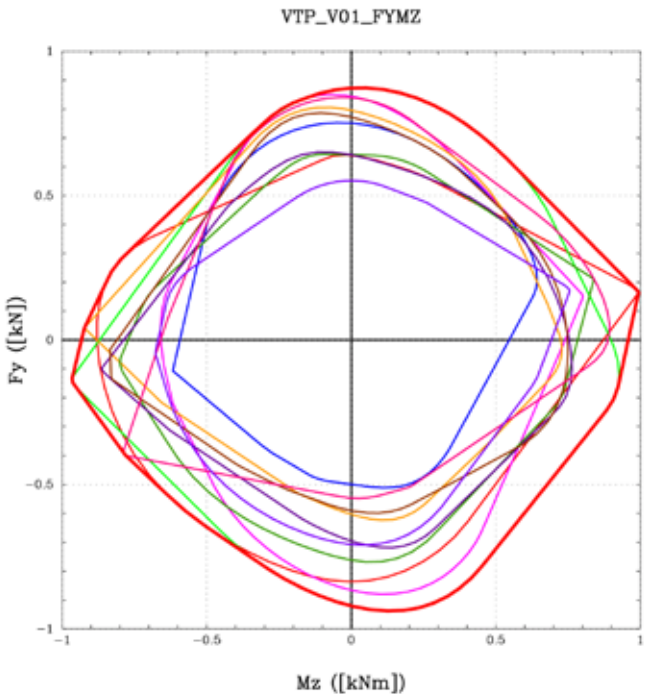

Figure 7.21 Example of enveloping particular 2D envelopes

This type of output provides the most complete information about the load results because they are comparing two magnitudes. Thus, each combination of loads is compared to the same point of the reference loads and gives more detail of what is happening that a unique magnitude. For these reasons, the stochastic envelopes will be the bases of the outputs analysis. The loads obtained will be compared to the reference loads and represented with the correct criterion to analyze possible exceeds and hazardous results.

7.4.3. Ant-hill plots

The third kind of output that can be obtained from the stochastic analysis is an ant-hill plot relating two variables of the analysis. These plots represent the values of one variable against the values of the other for all the executions of the analysis. The result is a significant point cloud where each point represents a shot of the stochastic analysis and the coordinated axes are two variables of that analysis.

Ant-hill plots can be useful to clarify the dependency of outputs or in this case load results to different input variables. Hence, these plots will be used in the determination of critical values of input parameters for certain load components from aircraft sections of interest. Figure 7.22 shows an example of an ant-hill plot. In that case, an output load is represented versus an input parameter, H1.

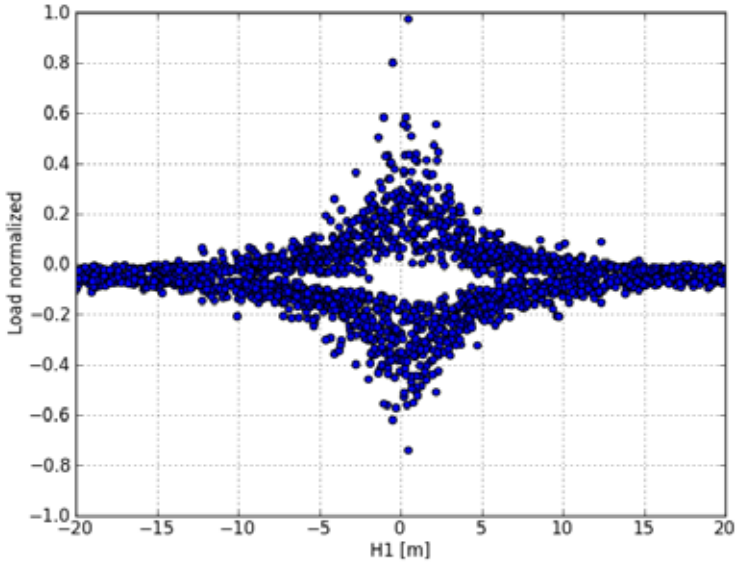

Figure 7.22 Example of ant-hill plot

7.5. Computation loop

Once all the input parameters and output results have been defined, the procedure of the analysis consists of establishing a computation loop. That loop is repeated each execution until the total number of shots desired for the stochastic analysis is reached.

In this case, the center of the analysis is the software flow chart for the wake encounter presented in chapter 3. This comprises the solver part of the stochastic analysis, were the computations are performed. Ahead of that central part, there is the stochastic tool ST-ORM that assigns the values of the input variables for each execution. Then these values are passed to the computation loop were the wake vortex encounter is executed completely with that parameters. It starts obtaining the excitation of the wake in WESDE, then the dynamic equations of motion are solved for that excitation using DYNRESP, finally, integrated loads are obtained in different parts of the aircraft using DYNLOAD. Once that loop is completed, the last module of the stochastic analysis is the post-processing of the results obtained. This last part involves the representation of the load responses in different forms such as histograms, stochastic 2D envelopes and ant-hill plots. The procedure for the stochastic analysis is outlined in figure 7.23.

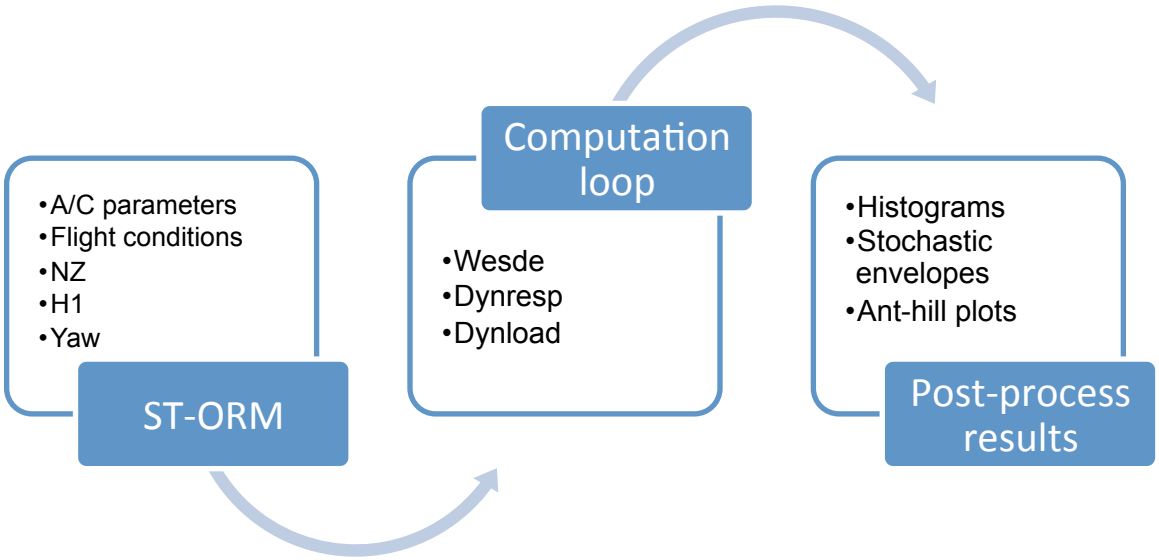

Figure 7.23 Outline of the methodology for the stochastic analysis

The methodology to follow is to implement the computation loop of the wake vortex encounter inside the stochastic tool ST-ORM. That way, the stochastic analysis can be started and the input parameters are varied as designated by their distributions and the load results obtained are an acceptable statistical measurement of the response to that kind of event.

Therefore, once all the implementation has been thoroughly verified and works correctly, it is possible to start a discrete number of runs of a controlled number of executions each. Choosing a coherent number of shots gives the possibility of having a suitable probability scale for the output results. Applying that in an example, if executions of 1000 cases are performed, the results obtained will have a probability of occurrence of 10^{-3}. Then, these probability factors can be related to the reference loads and derive a probability level of occurrence for the response to wake vortex encounter.

Chapter 8

STOCHASTIC RESULTS

8.1. Analysis procedure

Once the stochastic analysis is presented and all the parameters involved are defined, the efforts are focused on the implementation of the corresponding tools for the analysis and start to perform the computations. As said in the previous chapter, the stochastic analysis is based in the execution of a controlled and significant number of shots of the entire computation loop for the wake vortex encounter. This means that the stochastic tool ST-ORM assigns random values for the input variables following certain probability distributions. Then, with the corresponding values of the inputs, the numerical simulation of the wake vortex encounter is executed and the output results for integrated loads are obtained. Repeating that procedure the corresponding number of times, a statistical behavior for the loads generated in the event considered can be obtained.

Entering in the number of shots for the executions, the stochastic analysis started with low numbers of 300 and 500 shots per execution. These were the initial analysis, were all the parameters were being checked in order to assure that they behave in the desired way. Those initial executions also allowed analyzing the coherence of the outputs results and starting to obtain the first plots after the corresponding post process. Therefore, the first runs of the stochastic analysis was focused on starting all the modules, check the correct distributions of the input variables, and assure that the computation loop is executed correctly until the load results are obtained.

The final runs of the stochastic analysis started after the initial assuring executions. These final runs form the base of the stochastic analysis and their outputs are the ones that establish the probability levels for the dynamics loads in terms of forces and moments for the select sections of the aircraft. The strategy consisted of defining a number of executions that could be representative for the occurrence of a wake vortex encounter.

Usually, in structure design, the reference loads that should resist the structure in its service life are assumed to have a probability of occurrence of 10^{-5}. In other words, there is a probability of 1 over 100.000 that the design loads occur in the normal operation of the aircraft. This is the standard reference used in structural design when determining the dynamic loads generated in all the regulated scenarios provided in the regulations and certifications. Since there is no regulation about wake vortex encounters, the ideal scenario would to simulate 10^5 events. In that way, the loads obtained would be comparable to the reference ones and the probabilities of occurrence will be all covered.

However, due to limitations in the computations time and other probability factors involved in the problem, the stochastic analysis consisted of performing 10 runs of 1000 shots each one. In that way, the total number of simulations of wake vortex encounters will be 10.000 and the probability event will be 10^{-4} as can be seen in table 8.1. This is a significant number of simulations and thanks to the probability factors applied afterwards, it could be increased and be compared to the reference loads. As the input variables of the flight conditions are based on fatigue missions and these are based on flight hours of the missions, the probabilities presented in the stochastic analysis are all per flight hour. Therefore, when the reference loads are said to have a probability of 10^{-5}, these are 1 per 100000 flight hours of the aircraft and similar for the probabilities of the stochastic simulations.

Table 8.1 Simulations of the stochastic analysis

Number of runs	Shots per run	Total simulations	Event probability
10	1000	10000	10^{-4}

8.2. Probabilities study

As said in the previous section, there are some probability factors to be applied to the event probability of 10^{-4} describe before. These factors take into account the variability of some parameters that is not included in the probability distributions of the inputs. After applying those factors, the probabilities for the stochastic results will decrease and will become more remote than the ones for the reference loads. The probability factors applied are explained in this section and they will be treated separately, considering the influence of each one. Essentially, there are three uncertainty factors involved in the stochastic analysis:

- Roll angle.
- Cruise time.
- Other uncertainties, altitude, time.

These three parameters are the roll angle of the follower aircraft, the cruise time of the mission that is not considered and other uncertainties related to the altitude and time of the crossing. All these factors are explained in the following sections and they will be applied to the event probability of the total number of stochastic analysis.

8.2.1. Roll angle

The first variable that could introduce a probability factor to the output results is the roll angle at which the crossing aircraft enters the wake. It was said in the presentation of the scenario for the stochastic analysis (chapter 7) that the follower aircraft is assumed to enter the wake at 1g horizontal flight, that is 0º roll angle. This was fixed to that value for relevancy of the load responses. The case that induces

greater loads is the one where the aircraft enters the wake horizontally and the entire surface of the horizontal tail plane impacts the vortex tubes. The cases where the crossing aircraft enters with a particular roll angle or inclination will produce lower responses since not all the surface is excited by the wake. Due to the maneuver definition for the encounters, it is possible that the aircraft enters with a relative roll angle. For that reason, it is necessary to find the probability factor to apply to the load results in order to consider also the cases with nonzero roll angle.

In order to assess the dependency of the load results and the roll angle of the crossing angle, a sensitivity study was developed. In that, the rest of the variables were maintained fixed and only the roll angle of the follower aircraft was varied. Figures 8.2 and 8.3 show the results of the sensitivity study for the torsion moment at the VTP root and tip.

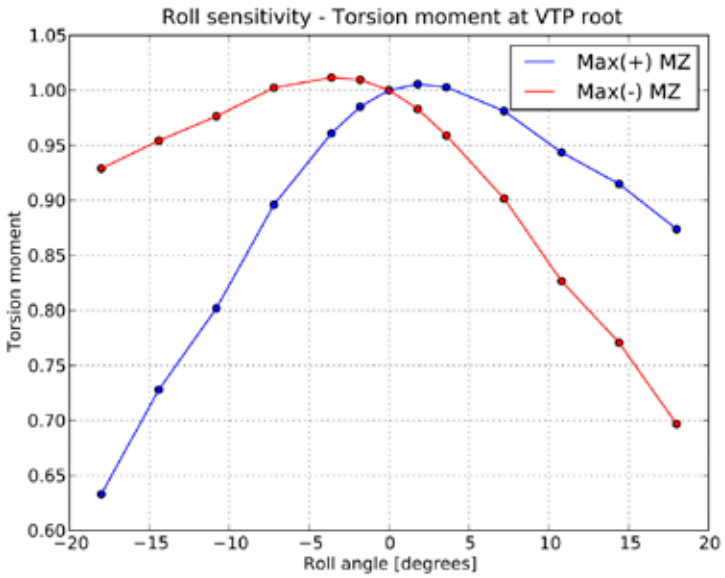

Figure 8.1 VTP torsion moment against roll angle of crossing angle

As can be seen in those figures (8.2 and 8.3) the load response is reduced considerably for small variations of the roll angle. If the range of that variable is assumed to be around 160º (from -80º to 80º for structural limitations) a variation of about 20º gives reductions in the maximum values of the VTP torsion moment of around 30%. For that reason, the approach was to set the roll angle of the crossing angle at 0º for the simulations and afterwards apply the corresponding probability factor to consider all the range values that are also possible but do not produce relevant load results. Based on the sensitivity study, this probability factor can be set to 0.125 (20º/160º). Therefore, the first parameter treated in the probability study, introduces a factor of approximately 10^{-1} in the final probability occurrence.

- Probability factor due to roll angle = 20º/160º = 0.125 = **$1.25 \cdot 10^{-1}$**

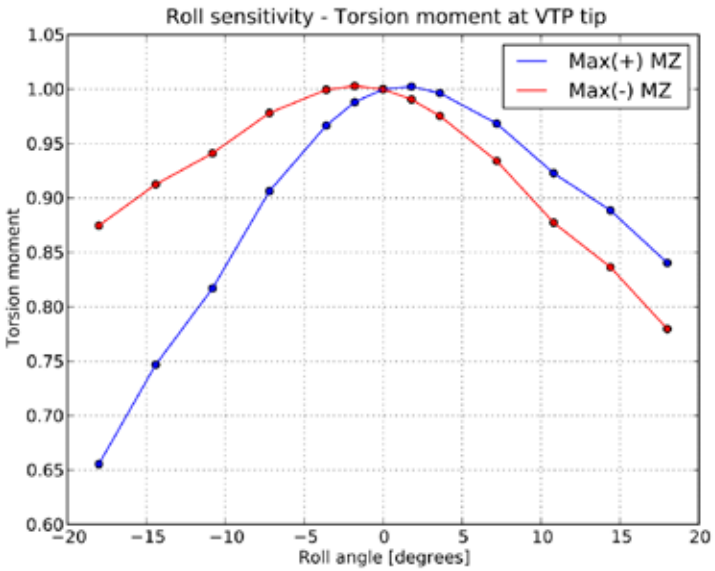

Figure 8.2 VTP torsion moment against roll angle of crossing aircraft

8.2.2. Cruise segment time

The second aspect in this probability study is to analyze the probability factor to be applied for considering the flight time of the cruise segments that are not included in the stochastic definition. To do so, the strategy consists of determining the time of the cruise time for all the mission profiles and then compare that time to the total one. With that, it is obtained the fraction of time that the stochastic analysis included in the definition of the flight stages variable.

Table 8.2 Cruise time for each mission profile

Mission profile	Cruise time (%)
Long Logistic	89,8%
Short Logistic	50,1%
Tactical	71,2%
Training	49,0%

Table 8.2 shows the cruise time in percentage for each mission profile. With those values, it is possible to obtain the total cruise time for all the operational life of the aircraft given by the fatigue missions. Considering the number of cycle of each mission profile, the duration of each one and the percentage of cruise time, the total time that the aircraft spend in that flight stage is around 77%. That means that the stochastic analysis is only considering the 23% remaining of the operational lifetime. Remember that the cruise stages were eliminated in the flight segments definition

because it was considered that the kind of event studied in the analysis was not likely to occur in those stages. Therefore, a factor of 0.23 should be applied to the output results in order to consider the entire operational life of the aircraft as it is showed in table 8.3.

Table 8.3 Probability factor applied for not considering cruise stages

Total cruise time (%)	Remaining time considered	Probability factor to be applied
77%	23%	0.23 = $\boldsymbol{2.3 \cdot 10^{-1}}$

8.2.3. Other uncertainties

The last uncertainties involved in the stochastic analysis are the ones related to the characteristics of the crossing. In this problem, there are defined a crossing altitude from the center of the first vortex tube through the variable H1 and an elapsed time depending on the turn maneuver. However, these two variables can vary in a wider range than the ones considered. First, the crossing altitude H1 was assigned to a uniform distribution between the values of -20m and +20m, where all the range values have the same probability of occurrence. Given the characteristics of the variable H1, the stochastic tool performs a sweep of 40 m for the crossing altitude of the wake vortex encounter. Although, this crossing altitude can take other values that are not considered in the variable range because they are too far from the vortex center and they do not induce significant load responses. Due to the maneuver defined for the wake encounters of this problem, it is possible that the aircraft vary its altitude or lose it in the completion of the turn. Based on the performance of the aircraft, the total range of altitudes for the wake encounters can vary in wider range of about 100 meters as can be seen in figure 8.1. This means that the stochastic input variable is only considering 40% of the total crossing distances of the encounters (40 meters of the variable definition over the total 100 meters). This wider range was not considered in the definition of the input variable for computation savings. For wake encounter at such far distances, the excitation is very low and the response is much lower than the cases considered. Therefore, those values can be not included in the analysis knowing that they do not produce representative results for the stochastic analysis.

Another uncertainty is the turning time of the maneuver that defines the characteristic time for the wake aging model. This time was derived from basic flight mechanics of a coordinated turn with constant velocity and constant load factor. Though, the maneuver could be not so constant and one of those variables can have slight variations along the complete turn. As a consequence, the turning time can experiment also slight variations from the theoretical value of the coordinated turn. This uncertainty should be included in the post treatment of the outputs probabilities. Hence, the combination of the time and altitude variation will determine the probability factor to apply in the last consideration of this probability study.

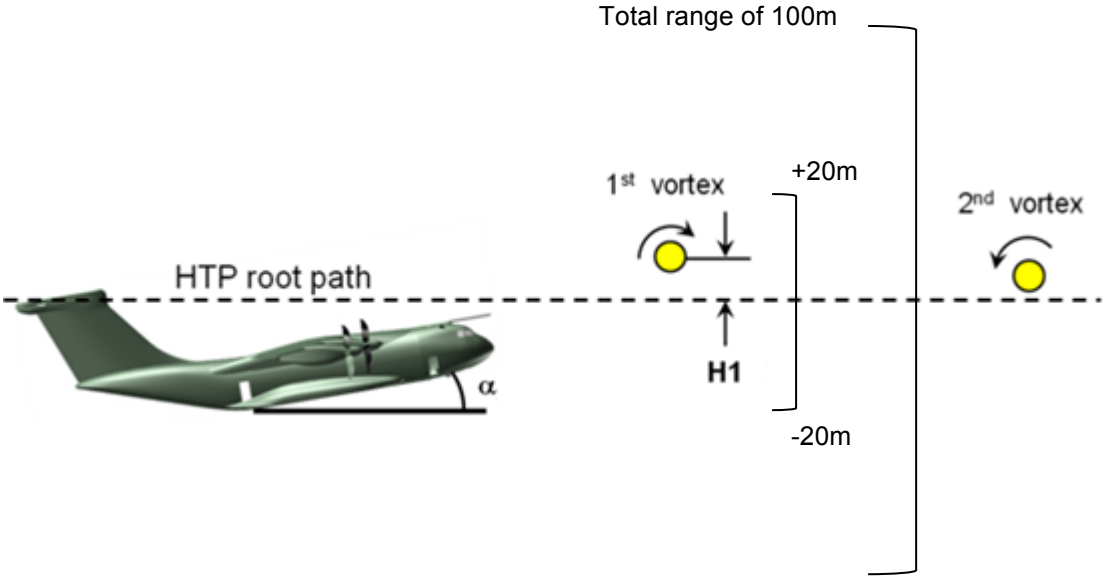

Figure 8.3 Crossing altitude due to maneuverability and aircraft performance

If the two uncertainties are considered, the probability factor of 0.4 from the crossing altitude should be reduced by the maneuver time factor. Including both parameters in a global probability factor, the $4 \cdot 10^{-1}$ factor value from the crossing altitude can be reduced to a global factor of $1 \cdot 10^{-1}$. This was established for being conservative in the analysis. It was considered that 10^{-1} was a suitable probability factor to include all the uncertainties related to the maneuverability and performance of the aircraft.

- Probability factor due to aircraft maneuverability and performance = **$1 \cdot 10^{-1}$**

8.2.4. Final probability

After the analysis of the probability factors to be applied to the output results due to the stochastic considerations, the event probability of 10^{-4} reduces to about 10^{-7}. The methodology presented was to perform 10.000 wake vortex encounter simulations, thus the event probability for that results is of 10^{-4}. These values should be multiplied by the three probability factors presented before in order to have a complete occurrence probability per flight hour of the output results. In table 8.4 are presented all the values and the corresponding final value for the probability of the load results obtained in this analysis.

Table 8.4 Final probability for the stochastic analysis

Event probability	10^{-4}
Roll angle	$1.25 \cdot 10^{-1}$
Cruise stages	$2.3 \cdot 10^{-1}$
Maneuverability	$1 \cdot 10^{-1}$
Final probability	**$2.875 \cdot 10^{-7}$**

Therefore, the total probability of the results of the stochastic analysis will be around 10^{-7}. That means that the load results obtained will be referenced to a probability factor of occurrence of 10^{-7} per flight hour.

8.3. Stochastic results

Once the stochastic probabilities have been determined with all their considerations, the results obtained will be presented. It will start with the 2D envelopes for the 10 runs of 1000 shots each in order to visualize the results and ensure that they are comparable. The presentation of results is based on 2D envelopes because is the fastest way to determine the behavior of the loads with respect to the reference design loads of the aircraft. This kind of output provides more information than simple maximum and minimum values for the forces and moments. As 2D envelopes combined two time-histories of respective magnitudes, the resultant provides information about all the combination of possible pair values for the two magnitudes considered. For these reasons, these envelopes are the most used in the determination of dynamic loads obtained for different events in the Structural Dynamics department and are the base of the outputs of this stochastic analysis of wake vortex encounters. From now on, the envelope plotted in black line represents the reference loads envelope. The other kinds of outputs are more related to particular magnitudes, their distribution in histograms and relation to other input variables. The later will be used in the specific study of particular forces or moments.

As said before, the first output obtained were the 2D envelopes of the 10 runs of 1000 shots each one. The following figures show the results for the different sections considered in the area of interest, the aircraft tail. For that, there are plots for sections in the horizontal tail plane root, the vertical tail plane at root and tip and the junction between HTP and VTP.

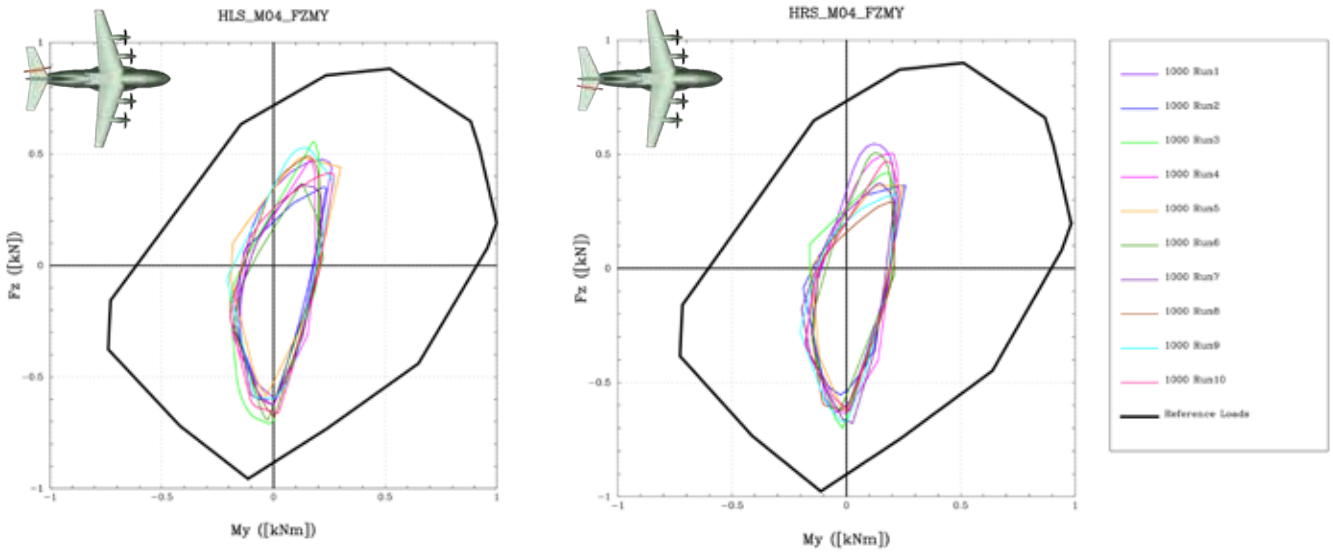

Figure 8.4 Envelope for shear force (FZ) and torsion moment (MY) for both sides of HTP

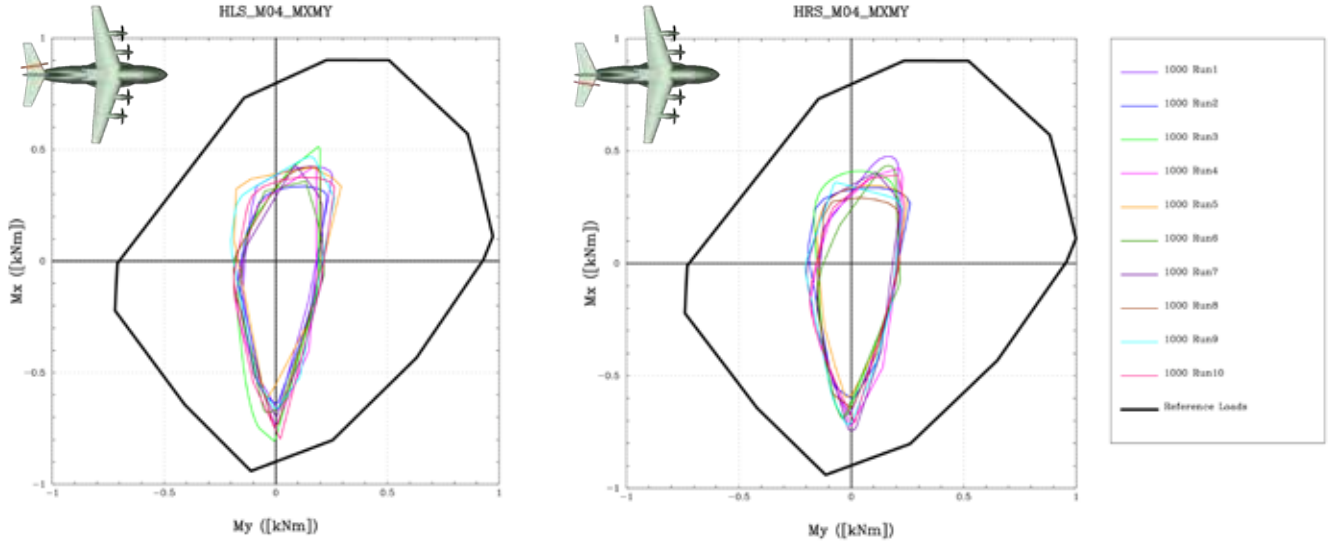

Figure 8.5 Envelope for bending moment (MX) and torsion moment (MY) for both sides of HTP root

Figures 8.4 and 8.5 show the 2D envelopes obtained for the section of the horizontal tail plane root. The first figure represents the combinations of shear force and torsion moment, while the second shows the bending and torsion moment. These envelopes are obtained for both, left and right sides of the HTP and in there, the stochastic envelopes of the 10 runs of 1000 shots each along with the reference loads plotted in thicker black lines are represented. It can be seen that the 10 runs are comparable among them and are all inside the reference with a significant margin. Going a step further, it is possible to obtain the total envelope of the ten particular runs but they are all very similar and the total envelope will maintain its location safely inside the reference loads envelope. These means that the HTP is not a critical area in the wake vortex encounter events and the loads induced in that area do not pose a compromise for the structure of the aircraft.

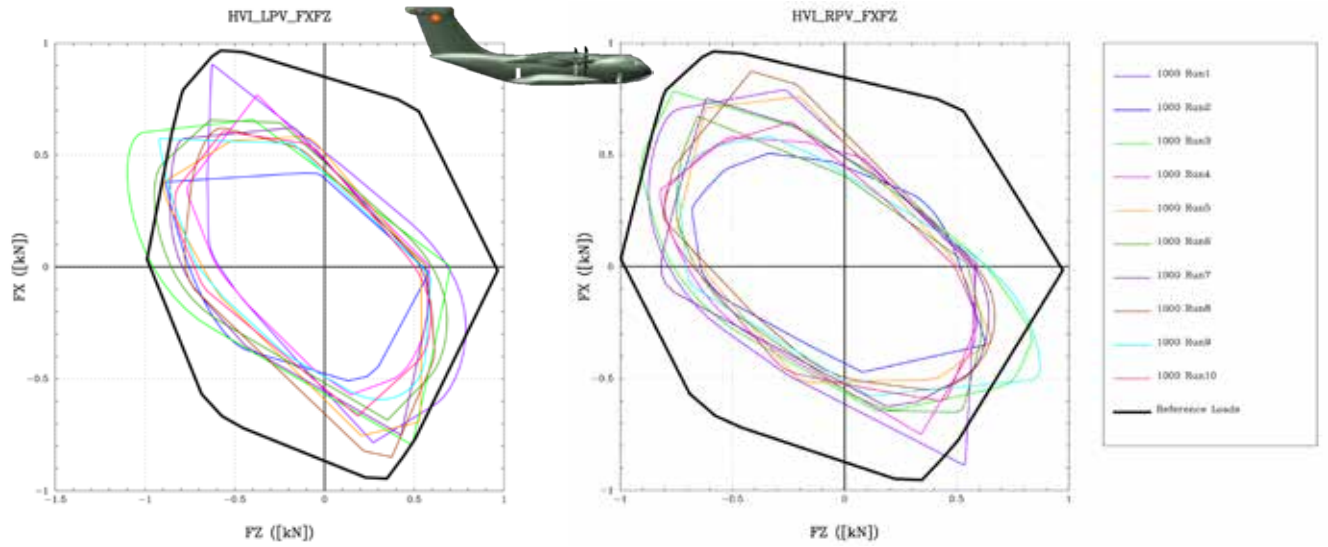

Figure 8.6 Envelopes for the axial (FX) and shear (FZ) force at the junction HTP-VTP

Focusing on another area of the aircraft, figure 8.6 shows the results of axial and vertical forces for the junction between the HTP and the VTP. This is a particular point of the structure and the results obtained are specific forces and not integrated loads as was the case for other sections. Analyzing this point is interesting because it gives the idea between what happens between the two surfaces and whether there are significant forces in that area. The results show that there are several runs that produce exceeds compared to the reference loads. This is the first sign that possible high loads can be induced in the structure, as it will be shown in the results for the vertical tail plane (VTP) sections.

Figure 8.7 presents the results for the 2D envelopes of the ten runs of 1000 shots each for the section of the vertical tail plane root. This is the lower part of the VTP, closer to the tail fuselage. The load components analyzed are five, two forces FY and FZ and the three moments MX, MY and MZ. Being now a vertical surface, FY is equal to the shear force while FZ is the axial force for the VTP. Regarding moments, MX is the bending moment, MY is the in-plane moment and MZ is the torsion moment. It can be seen that all the runs are comparable again but there are greater variations compared to the HTP results. Now, there are some runs that have given higher values for certain magnitudes, especially for the torsion moment, MZ. Essentially, for this lower section of the VTP, the results are acceptable for all the load components and only the torsion moment is the one that presents higher variations having some runs that are close to the reference loads.

The last section analyzed in the output results is the VTP tip. This is a higher section, closer to the HTP and the junction between both. For this section, the load components are the same as for the previous one, considering two forces and the three moments. Figure 8.8 shows the combinations of envelopes for the load components of this section. It can be appreciated the trend pointed out previously, the runs are comparable among them with significant variations in certain magnitudes. Again, the component that presents highest variations is the torsion moment, MZ. The rest of the components are inside the envelopes of the reference loads. The ones involving the torsion moment shows slight exceeds for certain runs. This means that there have been particular shots of those runs in which the numerical simulations have given higher load responses than the ones of the reference envelope. That is a potential issue for the aircraft structure and it should be treated further. Since the first results show that the only load component that produce exceeds levels is the torsion moment at the VTP tip section, the following analysis will be focused on that particular magnitude and section, not showing again all the load components for the other aircraft sections.

Therefore, the next step is focused on understanding the relationship of the VTP torsion moment with the input variables in order to assess the values that produce high responses in wake vortex encounters.

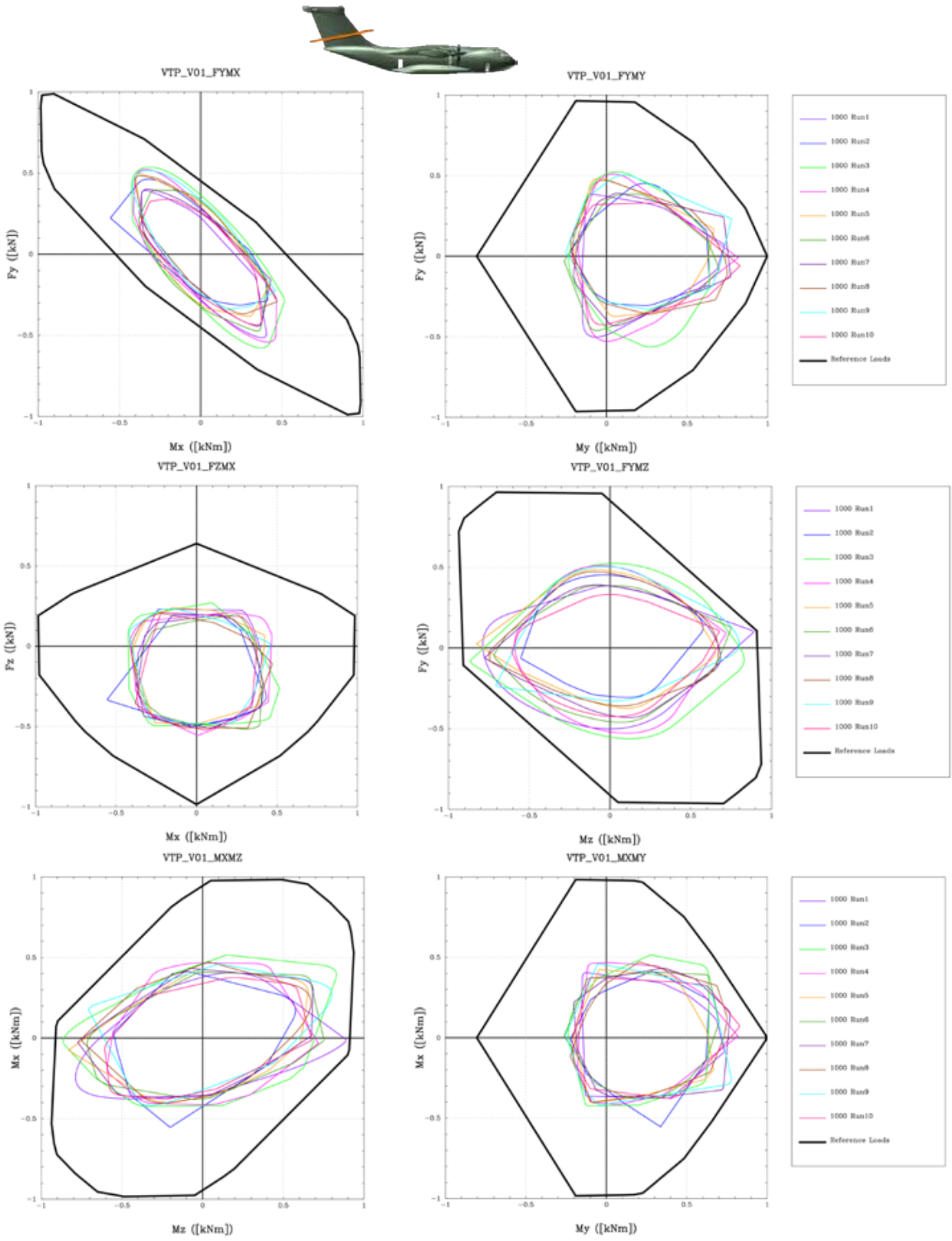

Figure 8.7 Ten runs envelopes for VTP root section

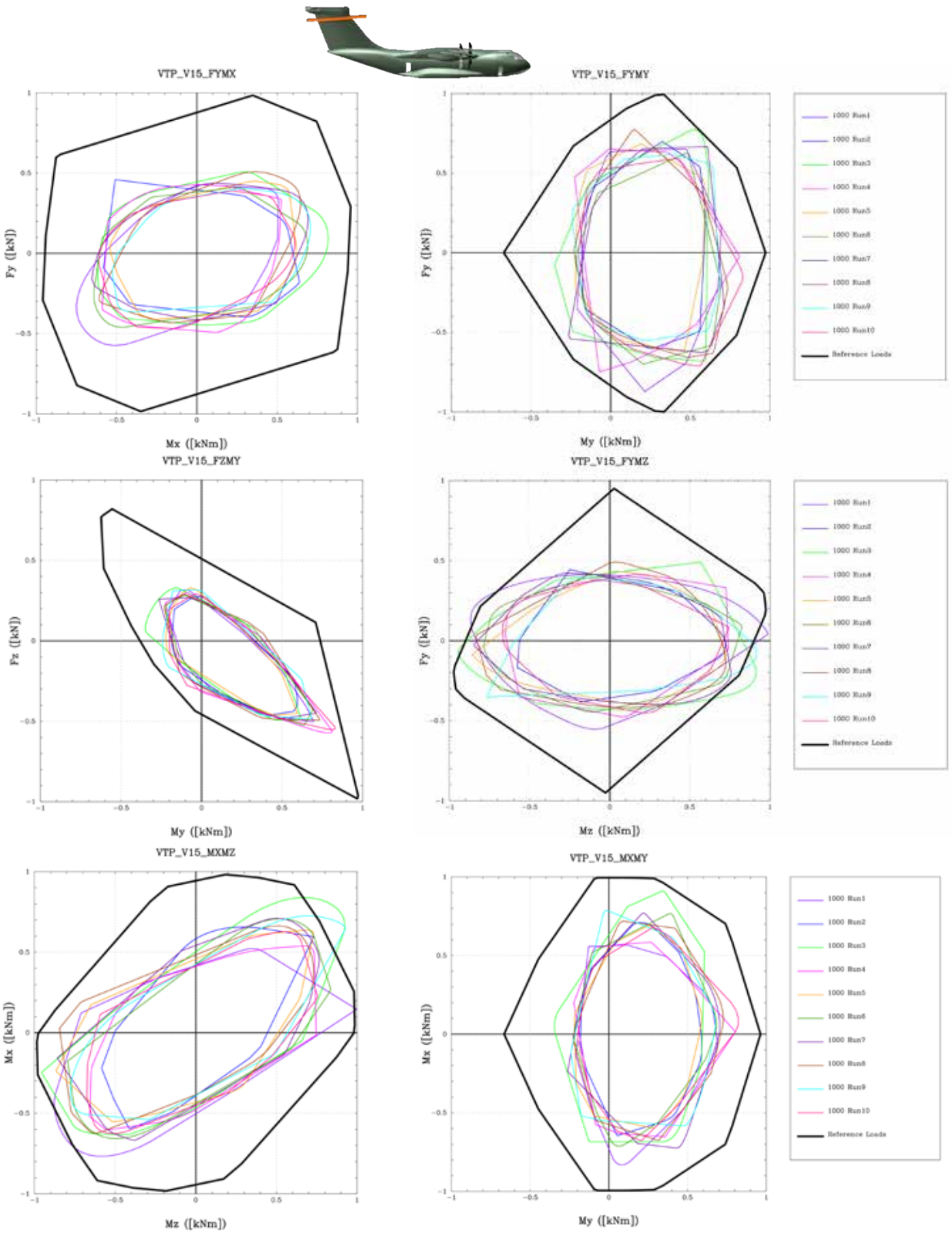

Figure 8.8 Ten runs envelopes for VTP tip section

8.4. Histograms and Ant-hill plots

As explained in the previous section, the magnitude of interest of the analysis is the torsion moment at the vertical tail plane (VTP). In order to go on a more specific detail, there are two post-process tools that will be used. First, the histogram of the values of that load component will give information about its behavior and will allot to identify possible odd results. The second tool is the ant-hill plot. This kind of plot represents two variables of the analysis against each other and shows the position with respect them of all the shots performed.

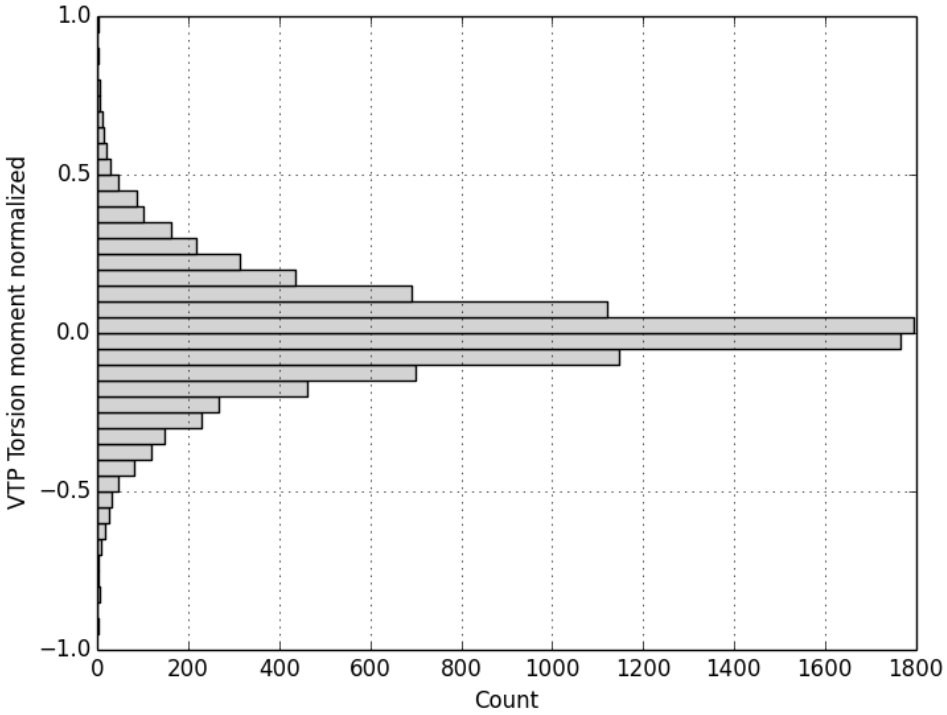

Figure 8.9 Histogram for the torsion moment maximum values at VTP tip section

Starting with the histogram, figure 8.9 shows it for the case of the torsion moment (MZ) maximum values at the VTP tip section. This gives an idea of the behavior of that magnitude. As it can be seen the distribution follows the trend expected with a higher number of shots giving low load responses. While fewer shots produce the high values of torsion moment. This indicates that the stochastic analysis does not have any odd behavior in its results and the high responses are due to certain combination of parameters that are expected to be of a very low probability.

Once it has been checked that the response is correct, it should be analyzed the relationship between the magnitude of interest, VTP torsion moment, with respect to the input variable that are scattered in the stochastic analysis. To do so, the best plotting resource is the ant-hill or scatter plot. Regarding this plot, the results presented will be focused on the VTP torsion moment to compare it with different input variables. The inputs considered are the ones that follow continuous distributions:

- Minimum distance to any vortex, min(H1,H2).
- Yaw angle, Ψ .
- Load factor, nz.

The other inputs are more discretized as they are based on the establishment of flight stages for the aircraft missions. Therefore, focusing on those three variables, it will be easier to understand the dependency of the VTP torsion moment response for wake vortex encounters.

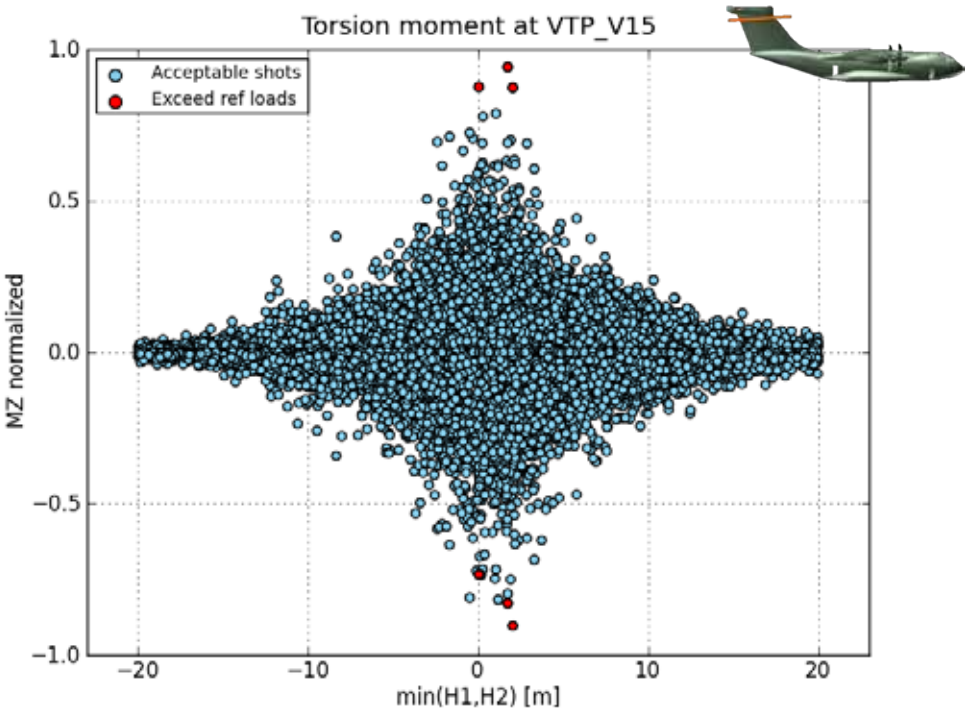

Figure 8.10 VTP torsion moment against the minimum distance to vortex center

As can be seen in figure 8.10 the relation of the response with the distance to one vortex of the wake is consequent with the definition of excitation of the wake model. The higher values of the torsion moment are close to the distance values nearer to zero. That means, the closer to the vortex center, the higher is the response in terms of VTP torsion moment seen by the aircraft. The maximum is slightly moved to the right positive axis of distances due to the angle of attack of the aircraft. As it is flying with a small angle of attack the reference surface (HTP) is not horizontal. Therefore, this surface sees a higher excitation if it passes at a certain distance, this way all the vortex tube impact to the reference surface. Thus, distances closer to 1.0 meter from the vortex center gives the highest load values.

The next figure (8.11) represents the ant-hill for the same magnitude as before (VTP torsion moment) but now comparing it with the yaw angle of the crossing event. In there, it can be seen that the torsion moment increases as the crossing turns less perpendicular. For encounters at 90º, the excitation is symmetric and there is not torsion moment at the VTP. As the angle of entrance increases, the excitation becomes non-symmetric and that generates high torsion moments in the VTP. The

trend seems to be increasingly for the torsion moment with respect to the yaw angle. The higher values of the response are obtained for relatively high values of the yaw angle at around 40º or 150º, depending which wing crosses the wake at first place.

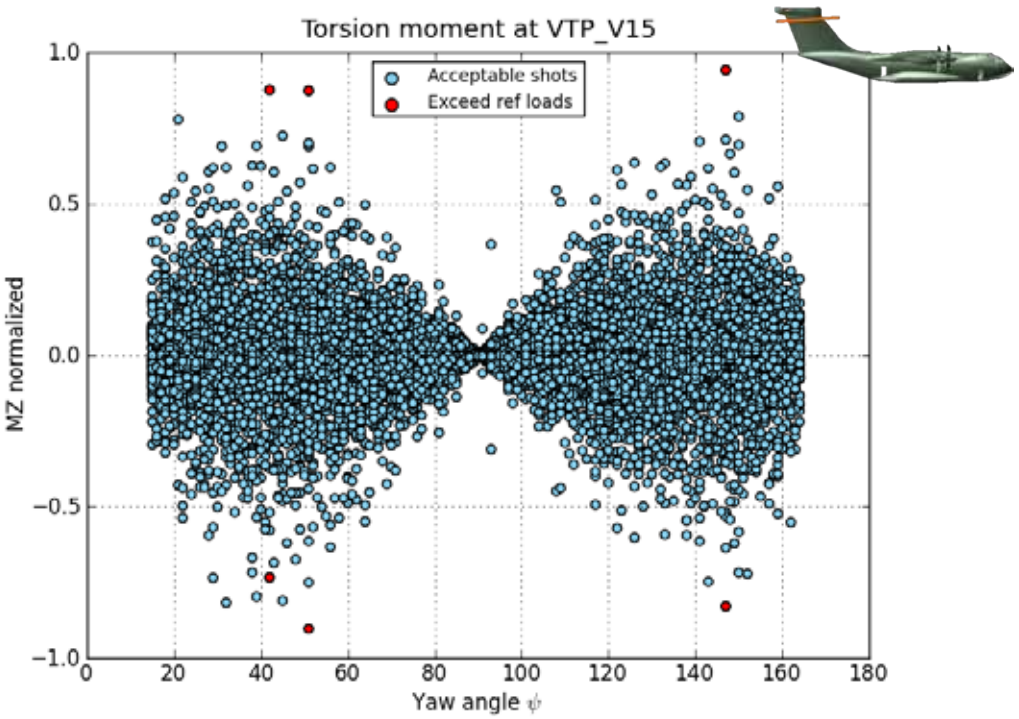

Figure 8.11 VTP torsion moment against the yaw crossing angle

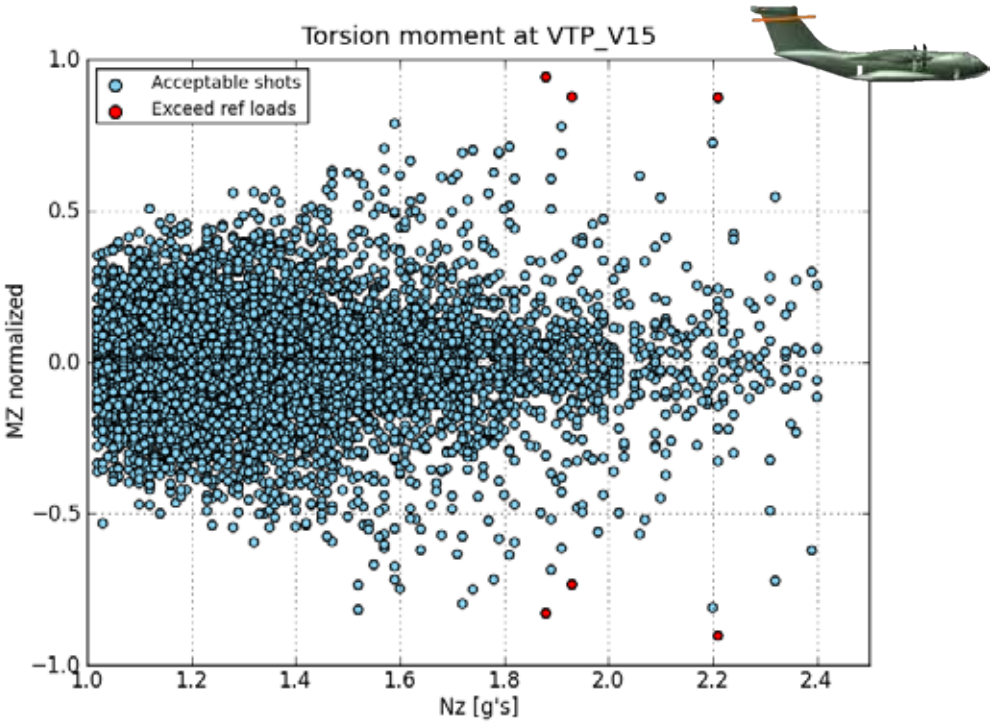

Figure 8.12 VTP torsion moment against leading aircraft load factor

The last of the ant-hill plots (figure 8.12) shows the relation of the VTP torsion moment with the load factor of the leader aircraft when it started the turn maneuver. It is relevant to remember that the load factor has influence in the nominal circulation of the vortex tubes, being directly proportional. Therefore, the higher the load factor, the higher the vortex circulation and the excitation induced by it. Hence, as the plot shows, the highest values of the response are obtained for higher values of the load factor. The trend might be difficult to see as the load factor follows an exponential distribution and higher values have very low probabilities of occurrence. For that reason, when higher values of load factor are assigned, it is possible to have other values for the rest of the variables that do no induce high load responses. However, it can be appreciated that the relevant shots of high torsion moment have all load factors above 1.8 g.

8.5. Worst case scenario

The ant-hill plots presented in the previous section allowed to identify the dependencies of the magnitude of study, in this case, the VTP torsion moment, with the input variables. They showed that the load response of that component is higher when a certain combination of inputs is given. Considering that combination it is possible to compute the worst-case scenario for the VTP torsion moment due to wake vortex encounter. The deterministic shot for the worst-case scenario will be useful in the comparison with the obtained results, its location with respect the reference loads and it will provide information about its probability of occurrence.

Regarding the input variables considered for the ant-hill studies, the values that induce higher responses are the following:

- Small distance to vortex tube, H1 = 0.75m.
- Maximum assumable yaw angle, Ψ = 20º/160º.
- Highest possible load factor, nz = 2.4.

After these inputs are set, in order to complete the deterministic worst-case shot, it is necessary to set the aircraft and flight parameters of the event. Considering the majority of the flight stages and analyzing the ones that involve heavier aircrafts, the critical flight stage for VTP torsion moment response was obtained. The heavy aircraft condition is due to the relationship between the aircraft weight and the circulation of the vortex tubes. The latter was proportional to the aircraft weight, and hence, flight stages with heavier aircraft will provide higher vortex circulation and higher excitation. The obtained flight stage was a climb segment for a short logistic mission where the aircraft has a significant weight with respect to the other stages. From the mission profiles distribution and the tables of the flight stages, the probability of occurrence for that particular segment can be derived.

With all, the worst conditions for the VTP torsion moment are established. Since the probability distributions for all the inputs are known, it is feasible to derive the probability of each one and after that, compute the final probability of occurrence for this worst case.

Table 8.5 Probability for VTP torsion moment worst-case

Condition	Probability
Mission and flight stage	$4.0 \cdot 10^{-2}$
nz = 2.4	$4.0 \cdot 10^{-4}$
H1 = 0.75 m	$2.5 \cdot 10^{-3}$
Yaw = 20º/160º	$1.3 \cdot 10^{-2}$
Roll, cruise and others	$2.875 \cdot 10^{-3}$
Final probability	**$1.5 \cdot 10^{-12}$**

As seen in table 8.5, the worst case for the VTP torsion moments has a lower probability that the one considered in the stochastic analysis, which is 10^{-7}. Once that is set, the next step is to represent that worst case along with the stochastic envelopes and assure that, as it is more unlikely, also produces a higher load response. To do so, the representation will show the stochastic envelopes combined in a total envelope (red line) that is the final envelope for the 10000 simulations of wake vortex encounters. The worst case, as it is a deterministic shot for a particular magnitude, is represented with a one-dimensional envelope as a grey line in the corresponding axis of the MZ. The total envelope will have a probability of occurrence of 10^{-7}, the reference loads a probability of 10^{-5}, and the worst case, the probability of 10^{-12} showed before.

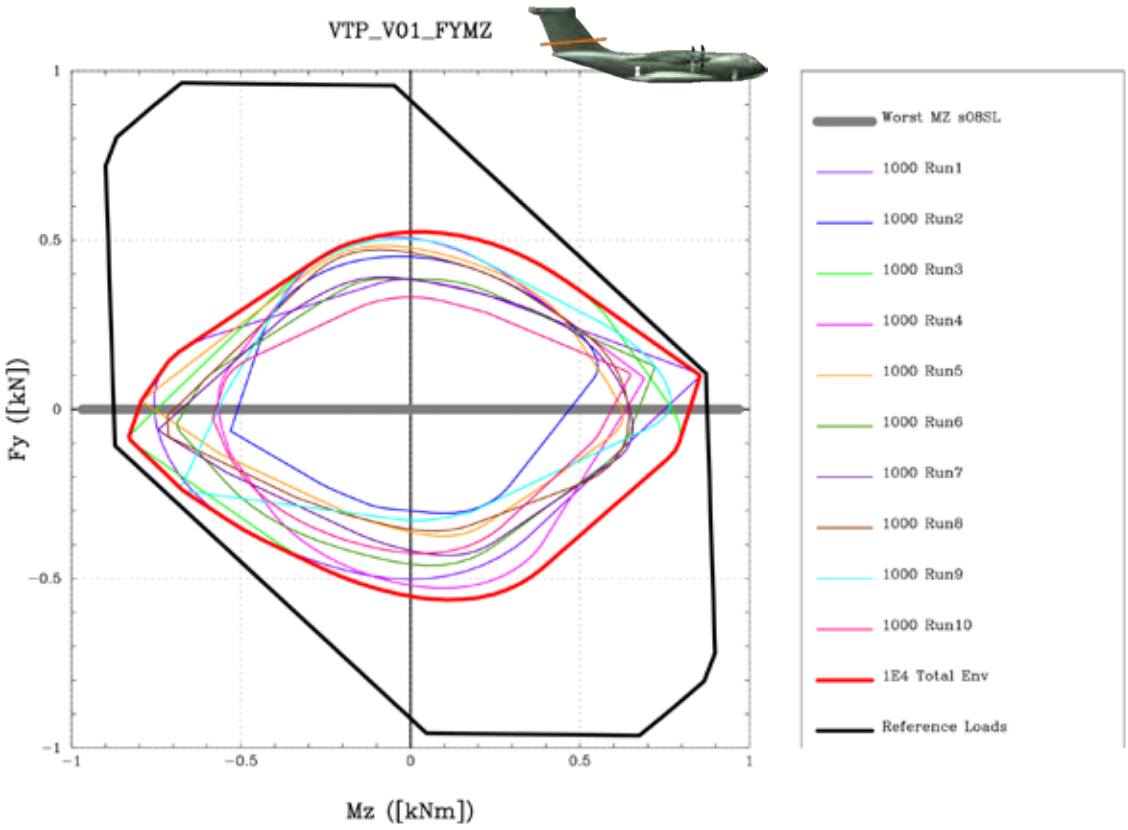

Figure 8.13 Total envelope for torsion moment (MZ) at VTP root

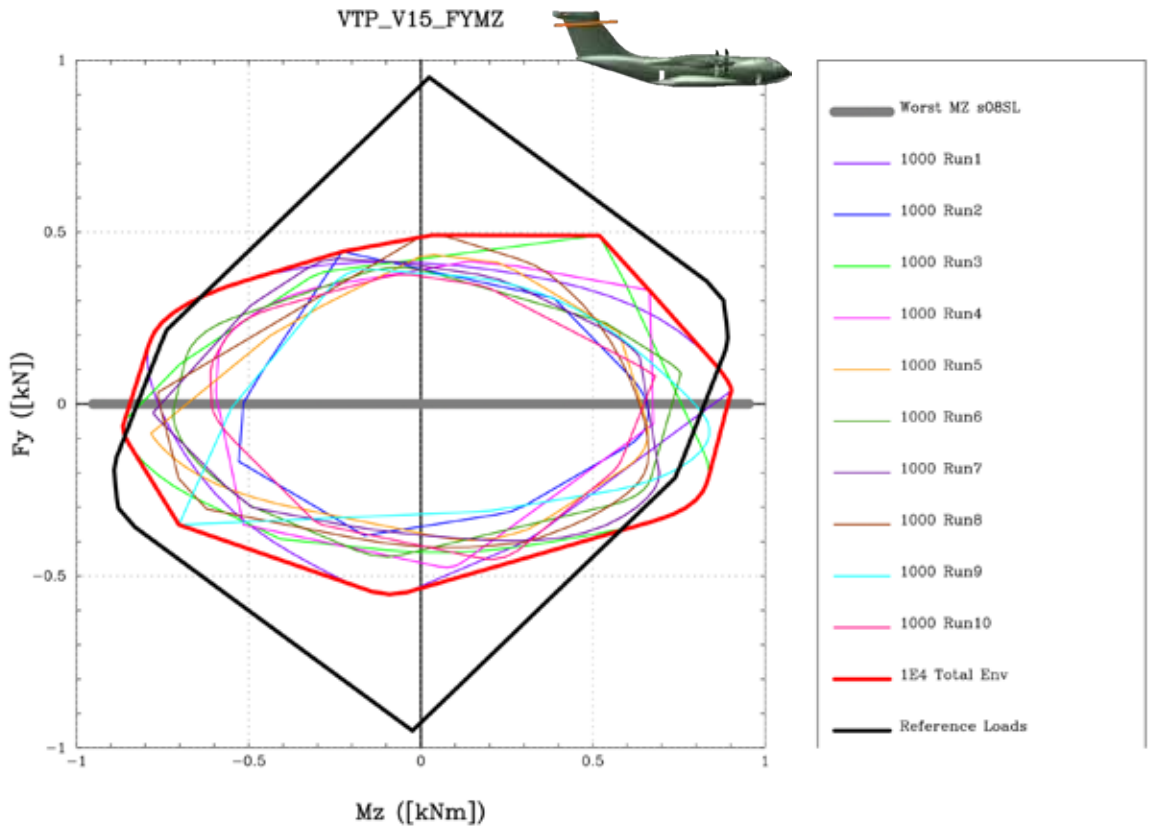

Figure 8.14 Total envelope for torsion moment (MZ) at VTP tip

The previous figures show the same behaviors as the initial envelopes presented for the same sections. For the case of the VTP root, figure 8.13, the total stochastic envelope in red, is inside the reference loads envelope, so there is not any exceed shot. In this same figure, the worst-case scenario gives higher values for the torsion moment, even more than the reference. Focusing on the relevant section of the VTP tip (figure 8.14), the total stochastic envelopes has some points outside the reference envelope due to the exceed shot of certain runs. The worst-case representation is again outside the reference and with maximum relative values higher than the stochastic results.

In this section, there has been taken an important step on the stochastic analysis, which is the total envelope of the 10 runs. From now on, there will be three main envelopes to be compared:

- The stochastic results
- The reference loads
- VTP torsion moment worst-case.

These three representations appear in the same plot but they reference different probabilities of occurrence. In the study of structural loads in service, as a common rule, the highest load values are also the ones with the lowest probability of occurrence. Returning to the figure 8.14, it could seem that there are some cases that could be important in terms of load responses for the aircraft. However, the probability of occurrence of those loads is also important. In order to be able to

compare those three envelopes using the same reference, it is necessary to apply safety factors given by the Airworthiness Authorities and Regulations of the aircraft loads.

8.6. Comparison of results

The last section about the computation and probabilities of the worst-case scenario for the torsion moment at the VTP leaves the idea that there are different envelopes referencing different load results and each one has its own probability of occurrence. In order to be able to compare the stochastic envelope with the reference one, it is necessary to apply the corresponding safety factors that should be apply to the loads depending on its probability.

These safety factors are based on aviation regulations. Specifically, it is the European Aviation Safety Agency (EASA) that determines them in the certification specification CS-25 for large airplanes [25]. In the appendix K about the interaction of systems and structure, the safety factors at the time of occurrence are defined. These factors are represented in figure 8.15, where the values are 1.5 for probabilities of 10^{-5} or greater and 1.25 for probabilities of 10^{-9} or less. The trend between both is linear in a logarithmic scale.

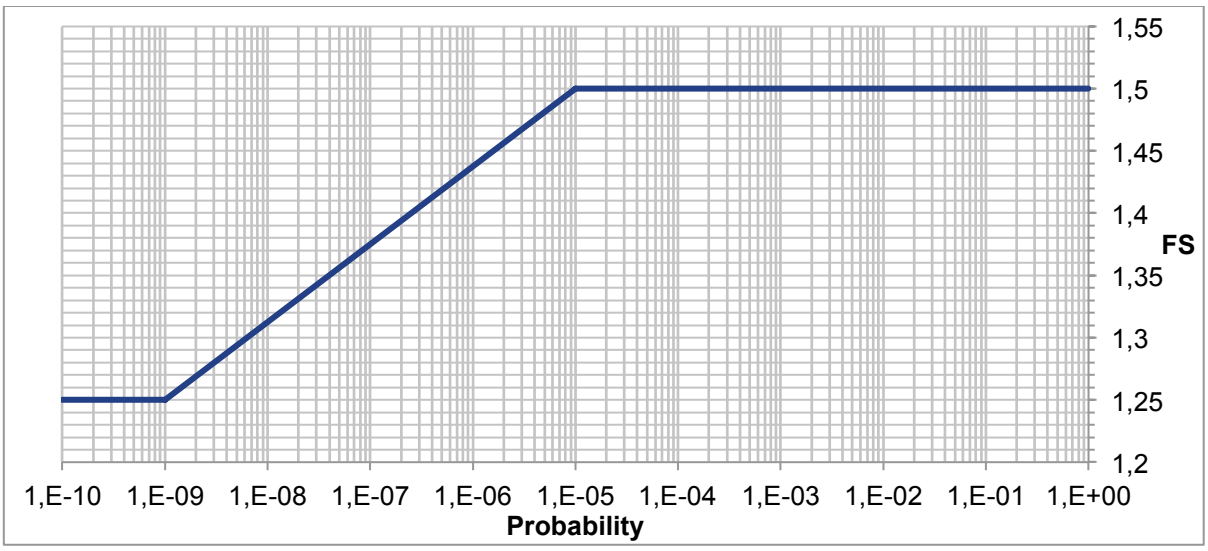

Figure 8.15 Safety Factors at the time of occurrence

Remembering the probabilities of each envelope considered, the safety factors to be applied to each one are as following:

- Reference loads = 10^{-5} → FS = 1.5
- Stochastic loads = 10^{-7} → FS = 1.375
- Worst case = 10^{-12} → FS = 1.25

Now, the procedure consists of applying the corresponding factor to each envelope. That means to multiply the load values of the envelopes for the obtained factor. For the worst case, it was presented before that it exceeds the reference loads. However,

now the safety factor is 16% lower than the one for the reference. Therefore, the corrected enveloped will be inside the reference loads after the application of the factors of safety. Thus, this will not be plotted in the final envelopes for the sake of clarity. These final results will only show the comparison between the stochastic loads of the wake vortex encounter (red line) against the reference loads of the A400M aircraft (black line). It was considered that the worst case was a very unlikely event and will not suppose a real thread in the normal operation of the aircraft. It was useful to consider the ultimate value of load response and have it as a limit for the stochastic loads, knowing how close they were.

There are two envelopes with different probabilities of occurrence, the reference and the stochastic loads. In order to be able to compare them in the same framework, each envelope should be multiplied by its corresponding factor. In that way, the reference loads should be multiplied by a factor of 1.5, while the stochastic envelope factorized by 1.375. Applying those safety factors, the following figures show the final load results. There have been focused on the VTP section closer to the HTP, VTP tip, and the junction between HTP and VTP because they were the sections with higher load values. It was shown in the initial envelopes presentation (figures 8.4 through 8.8) that the rest of the aircraft sections of study do not produce high load values and the stochastic results are lower than the reference loads.

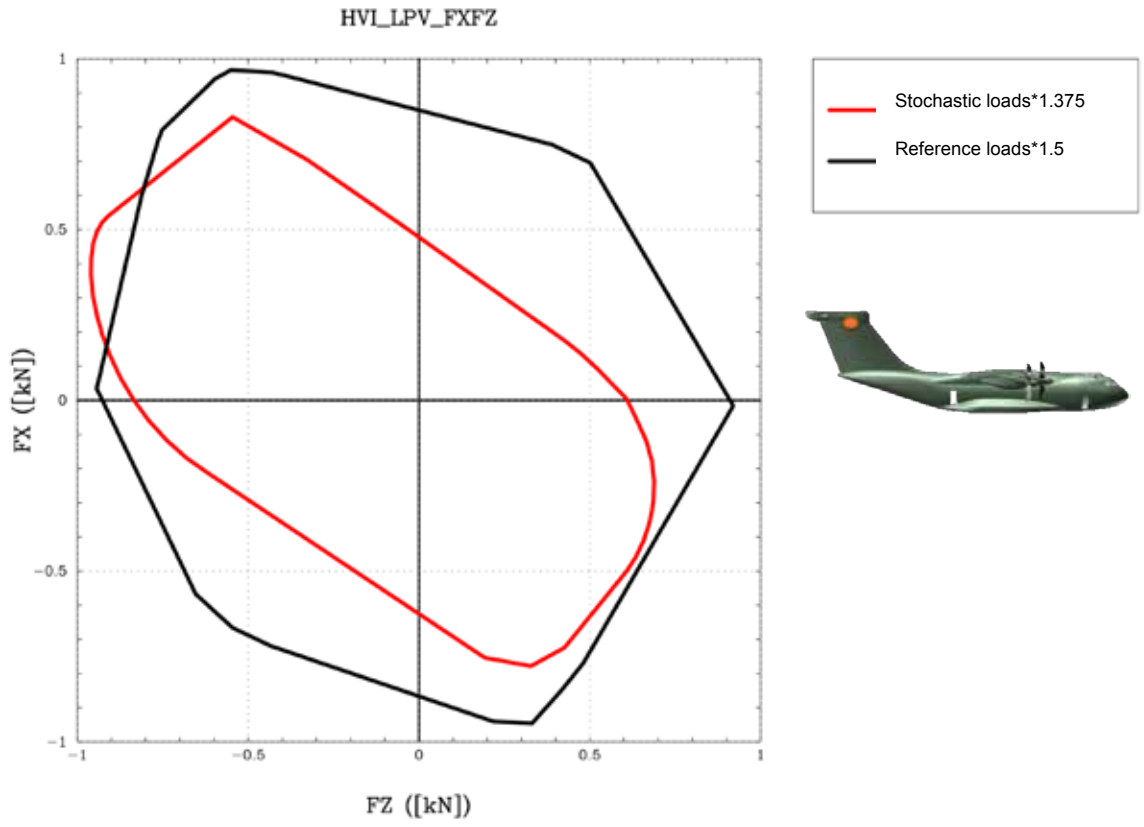

Figure 8.16 Final envelope for the left side of the HTP-VTP junction

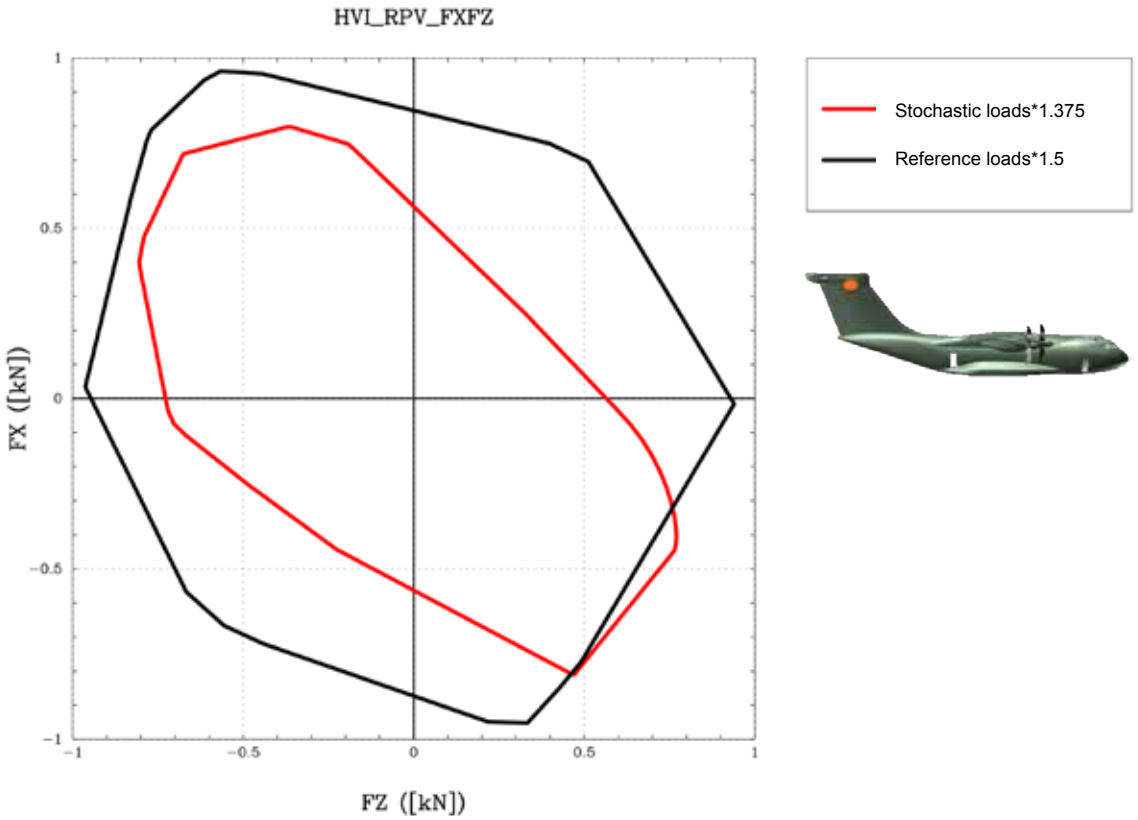

Figure 8.17 Final envelope for the right side of the HTP-VTP junction

The previous figures, 8.16 and 8.17, present the final results for the junction of the HTP and VTP. After the application of the safety factors to compare both envelopes, the previous exceeds are now slightly formal and probably they can be assumable for the aircraft structure. However, this is the area of interest of the study because it has been showed that the highest load values are obtained for this section and the VTP one closer to this point. In the other hand, figures 8.18 and 8.19 are the results obtained for the VTP tip section. They are focused on the two envelopes that involve torsion moment because it was the magnitude of interest. It can be seen that exceeds from the reference loads are slightly formal for this section too.

These results show that wake vortex encounter could induce high load values, especially for the torsion moment at the vertical tail plane. These high loads can be relevant at the junction between HTP and VTP. However, the probability of occurrence of those loads is low, so the safety factors applied to consider them wit the same framework reduce those exceeds. In conclusion, the loads generated in wake vortex encounters can be high for a certain combination of the encounter parameters but when they are translated to the normal life of the aircraft, they will not have significant importance.

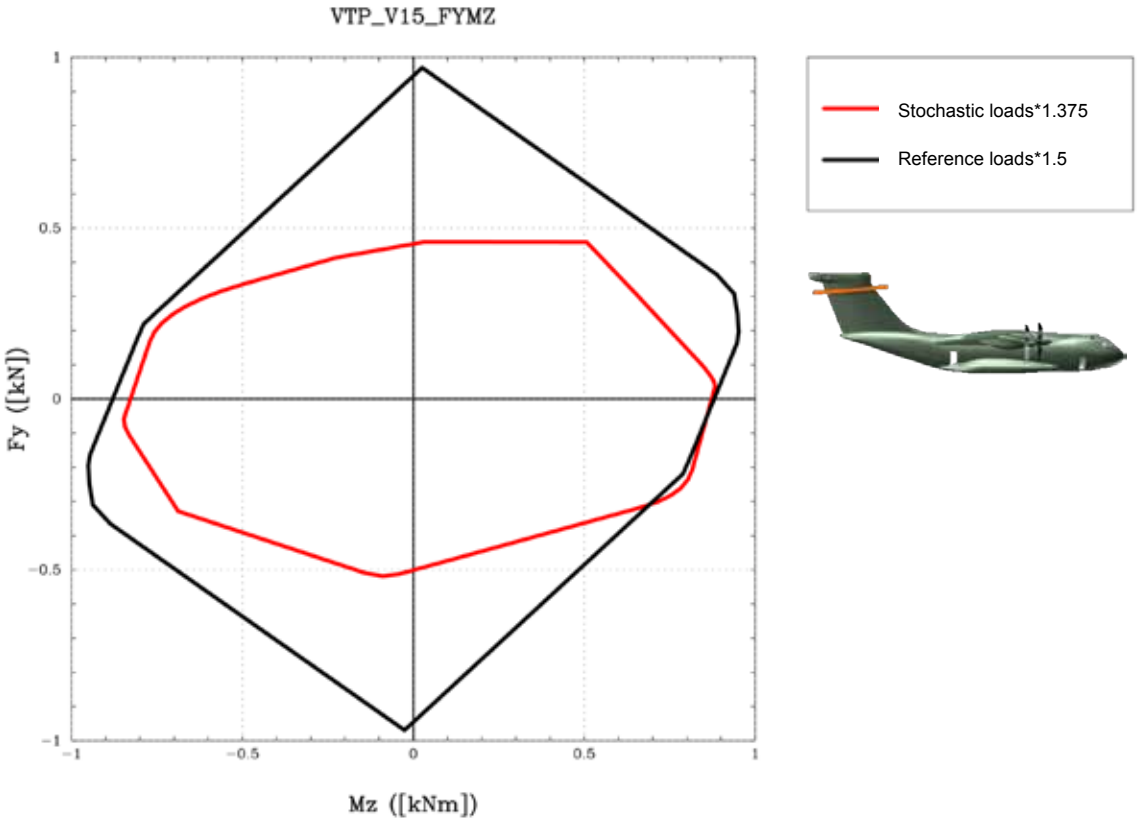

Figure 8.18 Shear force - torsion moment final envelope for the VTP tip section

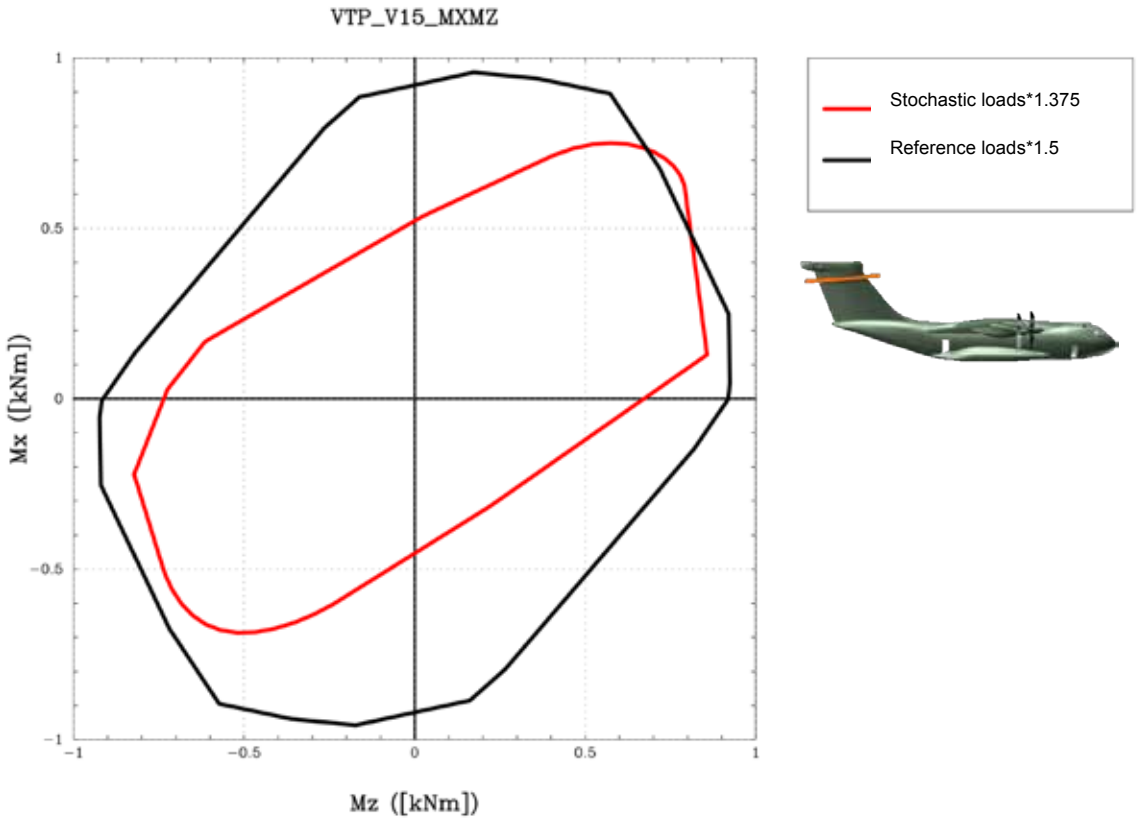

Figure 8.19 Bending - torsion moment final envelope for the VTP tip section

Chapter 9

CONCLUSIONS

9.1. Wake vortex encounter conclusions

After all the considerations mentioned in this study, some conclusions can be pointed out about the wake vortex encounter event. The first one is that this is a scenario worth studying. The airspace will become more and more overcrowded and aircraft will be operating closer to each other in the future. This trend is also applicable to military aircraft where the aerial navigation will be more complex with the introduction of new devices such as the unmanned aerial systems (UAS). This will increase considerably the probability for an aircraft to fly through the wake generated by another one or by itself. Therefore, the understanding of the physics and implications of wake vortex encounters is fundamental for the assurance of safety operations in the coming years. In that sense, this Master Thesis contributes to broaden the knowledge in this field by considering a relevant case of the problem that has been accompanied with flight tests.

The other important lesson learned from this work is that the model of the wake is one of the most important parts of the problem resolution. In its essence, wake vortex encounters are similar to other dynamic scenarios where the aircraft faces an excitation such as the case of discrete gusts. Thus, the better the model of that excitation, the more accurate the load results will be. It has been seen that the wake model depends on several factors, most of them related to atmospheric conditions. This is the main reason why it is difficult to obtain a good model for the disturbed velocity field generated by the wake vortex. The concept of two counter-rotating vortex tubes to represent the wake is significantly well established within the discipline. However, when considering the aging model, which is the evolution of the wake as time goes by, several issues arise. There are two different mechanisms that influence the wake evolution process. Those are the decay of the vortex circulation and the vortex diffusion and consequent growth of the vortex radius. There are studies about that aspect but still this is a field to be illuminated. In these pages, an aging model based on the vortex diffusion is presented. Nevertheless, it has not been proved to be useful to consider that aging mechanism by itself. Most likely, both aging effects are involved and they have a strong dependency on the atmospheric conditions. When the proposed model is compared to flight results, there is no way to determine the particular conditions of the atmosphere regarding turbulence and temperature stratification. Therefore, it is tough to derive an accurate model for the wake aging.

To sum up, those are the two main aspects to be pointed out after this analysis of wake vortex encounters. It can be considered a potential issue in the future for air navigation and the key to fully understand it is to derive a complete and descriptive method for the wake vortex generation and aging.

9.2. Stochastic analysis

Regarding the computation of loads through the stochastic analysis, these are the main lessons learned from that consideration. First, the approach of performing this kind of analysis can be useful for the cases where there is not very clear which is the representative case of the problem. Wake vortex encounter is a scenario that is not considered by any Airworthiness Authority or Regulation as a design specification. For that reason, there is not a characteristic case that the aircraft should pass successfully in order to determine its safe operation. Therefore, it seems reasonable to study the input variables involved in the problem, and then, simulate as much number of encounters as possible. In that way, a statistical base for the dynamic loads generated in the response can be obtained.

After the computation of a high number of numerical simulations, the first results showed that the loads obtained for wake vortex encounter might be significant for particular components in the tail area of the aircraft. In this case, the torsion moment of the vertical tail plane of the Airbus A400M. The rest of the components are contained within the reference loads. Thus, they are not relevant and the aircraft structure stands them with confidence. However, there is a certain combination of parameters of the encounter that produce slight formal exceedances of the reference loads. These high values have a very low probability of occurrence and they are completely assumable by the structure after the application of the corresponding safety factors determined by the Regulations. In conclusion, the results obtained are not a hazard for the normal operation of the aircraft or its structure.

With all, wake vortex encounter is an event that should be studied deeper as there are some conditions that induce high loads in the aircraft that crosses the wake. This could be an issue for the future where the increasingly air traffic can produce new and different conditions for the encounters that can lead to other high responses in other load magnitudes. It has become clear that the excitation that involves an event such as a wake vortex encounter is by no means negligible and it can produce relevant responses in the aircraft structure.

9.3. Future work

Once the conclusions of the study have been pointed out, some recommendations for possible continuations and future works can be presented. They are related to the tasks presented in these pages and can be classified into several categories.

The first one consists of continuing with the improvement of the wake model, especially the aging model. A relevant conclusion was that the wake model was the base for the proper calculation of the load response. Nowadays, there are few studies in the ambit of how the aging of the wake affects the loads generated in the aircraft. Most of the developments are theoretical and they do not take into account the implications in the aircraft that crosses the wake. For those reasons, it is necessary to improve the knowledge of the models of the aging mechanisms, both vortex circulation decay and vortex diffusion. The combination of the two effects could be the answer to a satisfactory wake aging model. Therefore, the next steps

could be focused on apply the different aging effects to real aircraft models such these and study the possibilities of each one. A better understanding of the relationship between the aging mechanisms with the atmospheric condition will also entail a considerable improvement in the computation of wake vortex encounters.

The second recommendation is to include real data in the problem consideration. It could be an interesting task to compare real data of wake vortex encounters with the results obtained in this study. This is not an easy task for the academic world or the people outside the aerospace companies. Those latter are the ones that have the resources to perform that tests and obtain the data. However, with collaboration agreements it could be possible to have data of real encounters that have already happened in aircraft operations and include them as reference in the study of wake vortex encounters.

Also, some aspects about the parameters of the encounter can be pointed out. In this study, the conditions were limited to lateral crosses of the wake vortex. This can be meaningful for a particular type of encounters but there is a wide range of possibilities not considered. For instance, one possible scenario can be wake vortex encounters were the crossing aircraft enters the wake in an almost parallel position. This could open the possibilities to wake crosses from behind the leader aircraft either from a below or above position. In order to achieve so, it is necessary to adapt the tools for obtaining the excitation of the disturbed velocity field for these conditions seen by the crossing aircraft. In this way, it would be expanded the casuistry of the problem and it would give a very useful approach for the most likely geometries for future wake vortex encounters.

The next issue is related with the possible benefits of wake vortex. Apart from being an excitation for other aircraft crossing it, it could be also used for obtaining fuel consumption savings due to certain flying formations. The velocity profile of wake vortex induces downwash velocities between the two vortex tubes. However, outside the wingspan of the generator aircraft, the aerodynamic effect is an upwash, which could lead to a lift increment zone. This aspect could be used to fly in certain formation such delta formation, where the each aircraft benefits from the wake generated by the one ahead of it. This effect could be helpful too in operation of air refueling where the two aircraft are close. Thus, there is also positive effects of wake vortex that could improve the performance of the aircraft flying near by.

Finally, the last remark is related to the proposal for a regulation scenario of wake vortex encounter. Works such this Master Thesis could be the base for starting to elaborate a proposal to Airworthiness Authorities in order to include this load case in the regulations. It could be a positive aspect for aircraft regulations to have a wider range of load scenarios. For that reason, it could be interesting to begin to elaborate the proposal for including wake vortex encounters in the standards.

REFERENCES

[1] Proctor, F. H., Hamilton, D. W., Switzer, G. F., “TASS Driven Algorithms for Wake Prediction”, *AAIA Aerospace Sciences Meeting and Exhibit*, Reno, Nevada, 2006.

[2] Liu, C., *Wake Vortex Encounter Analysis with Different Wake Vortex Models Using Vortex-Lattice Method*, Master of Science Thesis, Delft University of Technology, 2007.

[3] Brown, A. P., Bastian, M., “Wake Vortex Core Flowfield Dynamics and Encounter Loads In-situ Flight Measurements”, *AAIA Aerospace Sciences Meeting and Exhibit*, Reno, Nevada, 2008.

[4] Proctor, F. H., Hamilton, D. W., “Evaluation of Fast-Time Wake Vortex Prediction Models”, AIAA Aerospace Sciences Meeting and Exposition, Orlando, Florida, 2009.

[5] Schwarz, C. W., Hahn, K., Fischenberg, D., “Wake Encounter Severity Assessment Based on Validated Aerodynamic Interaction Models”, *AAIA Atmospheric and Space Environments Conference,* Toronto, Canada, 2010.

[6] Proctor, F. H., Ahmad, N. N., Switzer, G. S., Limon, F. M., “Three-Phased Wake Vortex Decay”, *AAIA Atmospheric and Space Environments Conference,* Toronto, Canada, 2010.

[7] AGARD Conference Proceedings 584, *The Characterization and Modification of Wakes from Lifting Vehicles in Fluids*, Trondheim, Norway, 1996.

[8] Saban, D., *Wake Vortex Modelling and Simulation for Air Vehicles in Close Formation Flight*, Ph. D. degree, Department of Aerospace Sciences, School of Engineering, Cranfield University, 2010.

[9] Karpel, M., “Increased-Order Modeling Framework for Nonlinear Aeroservoelastic Analysis”, Paper No. 2011-73, Proceedings of the International Forum on Aeroelasticity and Structural Dynamics, Paris, France, June 2011.

[10] Albano, E., and Rodden, W. P., “A Doublet Lattice Method for Calculating Lift Distributions on Oscillating Surfaces in Subsonic Flows”. AIAA Journal, Vol. 7, No. 2, Feb. 1969, pp. 279-285, and Vol. 7, No.11, Nov. 1969, p. 2192.

[11] Rodden, W.P., Giesing, J.P., and Kalman, T.P. “Refinement of the Nonplanar Aspects of the Subsonic Doublet-Lattice Lifting Surface Method,” Journal of Aircraft, Vol. 9, No. 1, Jan. 1972, pp. 69-73.

[12] Ginevsky, A. S., and Zhelannikov, A. I., “Vortex wake of aircrafts”, Springer 2009.

[13] Burnham, D.C., and Hallock, J.N., “Chicago monostatic acoustic vortex sensing system, volume IV: Vortex Decay”, DOT/FAA/RD-79-103 IV, July 1982.

[14] Devenport, W.J., Rife, M.C., Liapis, S.I., and Follin, G.J., "The structure and development of a wing-tip vortex", Journal of Aircraft 1996.

[15] Karpel, M. "DYNRESP-8: Dynamic Response of Aircraft Structures to Gusts, Manoeuvre Commands and Direct Forces - Theoretical Manual", KDC Report 2012-2, July 2010.

[16] Karpel, M., Shousterman, A., Reyes, M. and Climent, H. "Dynamic Response to Wake Encounter". 54th AIAA/ASME/ASCE/AHS/ASC Structures, Structural Dynamics, Materials Conference and Co-located Events, Boston, Massachusetts, 8-11 April 2013.

[17] Climent, H., Lindenau, O., Claverias, S., Viana, J.T., Oliver, M., Benitez, L., Pfeifer, D., and Jenaro-Rabadan, G., "Flight Test Validation of Wake Vortex Encounter Loads." Proceedings of the International Forum of Aeroelasticity and Structural Dynamics IFASD 2013. Bristol, 24-27 June 2013.

[18] Betz A, "Behaviour of vortex systems", Zeitschrift für angewandte Mathematik un Mechanik 12(3), June 1932

[19] Hageraats, W. A., Fluid Dynamic Simulations of Vortex-Jet Interaction, Master of Science Thesis, Delft University of Technology, 2006.

[20] Winckelmans, G., Duquesne, T., Treve, V., Desenfans, O., Bricteux, L., *Summary description of the models used in the Vortex Forecast System (VFS),* 2005.

[21] Viana, J.T., "A400M MSN1 crossing A400M MSN3 Wake Vortex Flight Tests Flight Tests Results and Numerical Simulations", AIRBUS MILITARY (MESY), April 2013.

[22] de Bruin, A.C. and Winckelmans, G., "Cross-flow kinetic energy and core size growth of analytically defined wake vortex pairs", NLR, NLR-CR-2005-412, 2005.

[23] Torralba, M.A. and Cerezo, J., "WESDE theoretical manual", AIRBUS MILITARY (MESY), May 2013.

[24] Cerezo, J. and Claverías, S., "A400M MSN1 Wake Vortex Encounter Tail Loads", AIRBUS MILITARY (MESY), April 2013.

[25] *Certification Specification CS-25 Large Aeroplanes*, Appendix K, European Aviation Safety Agency.

[26] Crow, S. C., *Stability theory for a pair of trailing vortices*, AIAA J., **8**, 2172-2179 (1970).

[27] Sarpkaya, T., "New Model for Vortex Decay in the Atmosphere," *Journal of Aircraft*, Vol. 37, No. 1, 2000, pp. 53-61.

[28] Holzäpfel, F., "Probabilistic Two-Phase Aircraft Wake-Vortex Model: Further Development and Assessment", *Journal of Aircraft*, vol. 43, No. 3, June 2006.

[29] Capart, R., Winckelmans, G., *Comparison between wind tunnel data (SWIM) and vortex simulations*, Aviator report, AW-UCL-111-007D, April 2003.

[30] Owen, P., *The decay of a turbulent trailing vortex (Turbulent trailing vortex decay calculated from circumferential velocity and eddy viscosity dependent on Reynolds number)*. Aeronautical Quaerterly, 21, 69–78, 1970.